HIERARCHICAL CONCEPT OF OPTIMIZATION BASED PATH PLANNING FOR AUTONOMOUS DRIVING

Dissertation

Zur Erlangung des akademischen Grades

Doktoringenieur

(Dr.-Ing.)

von M.Sc. Reza Dariani

geb. am 19.09.1984 in Teheran, Iran

genehmigt durch die Fakultät Maschinenbau
der Otto-von-Guericke-Universität Magdeburg

Gutachter:

Prof. Dr.-Ing. Roland Kasper

Junior-Prof. Dr.-Ing. Sebastian Zug

Verteidigt am: 14.07.2016

To my parents and my beautiful wife

DECLARATION

This dissertation is the result of my own work and includes nothing, which is the outcome of work done in collaboration except where specifically indicated in the text. It has not been previously submitted, in part or whole, to any university of institution for any degree or diploma.

Signed: _____

Date: _____

ABSTRACT

In this thesis, based on vehicle mathematic model which describes its dynamics, a hierarchical concept for autonomous driving is developed and explained. First level is path planning which finds a path between start point and end desired point. Then based on found path and a simple kinematic vehicle model initial inputs for next level of hierarchical concept is found which is path optimization. On path optimization level, based on a given objective function an optimal path is found. An optimal path is a trajectory for the vehicle with respect to different objectives such as energy consumption, comfort and safety. Then supposing sensors used in vehicle give us information about position, velocity and orientation of eventual obstacles on the road, path optimization level is updated in order to find a collision free path. Forasmuch as having an exact model which considers all uncertainty, external factors and disturbances is nearly impossible, a new level named path control is added which generates additional inputs to compensate the difference between optimal states and vehicle response to optimal inputs. Each of these levels of presented hierarchical concept of autonomous driving are explained with more details in this thesis. To show the correct functionality of the concept, they are modeled, implemented and simulated in different software such as Matlab and IPG-CarMaker and also implemented on a small size vehicle build at Otto-von-Guericke-University of Magdeburg named BugEE.

ACKNOWLEDGEMENTS

I would like to express my special appreciation and thanks to Professor Roland Kasper, my thesis advisor, who guided me, encouraged and motivated me all during this PhD thesis. Very special thanks to Junior Professor Stephan Schmidt who guided me and helped me through the project and also corrected my dissertation. Without his help on theoretical and experimental part of the project, realizing this project was impossible. I would like to thank Junior Professor Sebastian Zug who accepted to be my supervisor and for his comments and suggestion about work.

I would like to thank all the colleagues at chair of mechatronics, especially Mr. Martin Schünemann who helped me for experiments. Special thanks to Dr. Hans-Georg Baldauf for all his support on software level.

At the end I would like to thank my family who supported me all through my study, and very special thanks to my wife for all her support.

CONTENTS

LIST OF TABLES

LIST OF FIGURES

LIST OF ABBREVIATIONS AND ACRONYMS

Abbreviation	Meaning
2D	Two Dimensional
3D	Three Dimensional
ACC	Adaptive Cruise Control
AFS	Active Front Steering
ANV	Automotive Night Vision
AV	Autonomous Vehicle
BSM	Blind Spot Monitor
BugEE	Electric vehicle used for autonomous driving experiments
CAN	Controller Area Network
CC	Collision Cone
DARPA	Defense Advanced Research Projects Agency
DGPS	Differential Global Positioning System
DMS	Driver Monitoring System
ESC	Electronic Stability Control
GPS	Global Positioning System
IIHS	Insurance Institute of Highway Safety
LDW	Lane Departure Warning
LKS	Lane Keeping System
lrb	Lower Road Boundary
MHA	Moving Horizon Approach
NHTSA	National Highway Traffic Safety Administration

NLPQLP	SQP solver used for optimal control problem
OCP	Optimal Control Problem
ODE	Ordinary Differential Equation
RK4	Runge-Kutta 4th order
RPM	Probabilistic RoadMap
RRT	Rapidly-exploring Random Trees
RTZ	Restricted Traffic Zone
SQP	Sequential Quadratic Programming
Urb	Upper Road Boundary
VO	Velocity Obstacle

Index	**Meaning**
$(\dot{\cdot})$	First time derivative
$(\ddot{\cdot})$	Second time derivative
$\Delta(\cdot)$	Difference
$(\cdot)_{act}$	Actual vehicle quantity
$(\cdot)_{f}$	Quantity at front wheel in single track vehicle model
$(\cdot)_{fl}$	Quantity at front left wheel in double track vehicle model
$(\cdot)_{fr}$	Quantity at front right wheel in double track vehicle model
$(\cdot)_{l}$	Value of lower boundary
$(\cdot)_{\mathrm{opt}}$	Optimization quantity
$(\cdot)_{r}$	Quantity at rear wheel in single track vehicle model
$(\cdot)_{rl}$	Quantity at rear left wheel in double track vehicle model
$(\cdot)_{rr}$	Quantity at rear right wheel in double track vehicle model

$(\cdot)_u$	Value of upper boundary
$(\cdot)_{vhcl}$	Vehicle quantity

Symbol	**Meaning**	**Unit**
A^*	Shortest path algorithm	
a_x	Longitudinal acceleration	m/s^2
a_y	Lateral acceleration	m/s^2
B, C, D, E	Magic formula parameters	
b	Vehicle width	m
$bp()$	Backpointer in shortest path algorithm	
C	Center of gravity	
c_α	Lateral tire slip stiffness	N/rad
c_κ	Longitudinal tire slip stiffness	N/rad
$c(u)$	Cost function in shortest path algorithm	
d_l	Longitudinal error	m
d_s	Side (lateral) error	m
E	Set of edges	
F_D	Driving force	N
F_L	Load force	N
F_{Lx}	Load force in longitudinal direction	N
F_{Ly}	Load force in lateral direction	N
F_N	Force in normal direction	N
F_T	Force in tangential direction	N
F_x	Longitudinal force	N

F_y	Lateral force	N
F_z	Vertical force	N
$g(\underline{x},\underline{u})$	Nonlinear constraints function in OCP	
$g_e(\underline{p})$	Equality functions	
$g_i(\underline{p})$	Inequality functions	
$h(u)$	Heuristic function in shortest path algorithm	
J_z	Moment of inertia in z-axis	$kg.m^2$
k	Course angle	rad
K	Curvature	m^{-1}
l_f	Distance from vehicle center line to front wheel	m
l_r	Distance from vehicle center line to rear wheel	m
m	Mass	Kg
M_x	Roll moment	Nm
M_y	Pitch moment	Nm
M_z	Yaw moment	Nm
$\underline{p}$	Free variables in NLPQLP solver	
$\underline{R}$	Weight factor on objective function of OCP	
r_e	Effective rolling radius of tire	rad
T	Torque	Nm
t_0	Initial time	s
t_{calc}	Calculation time	s
t_p	Path planning horizon	s
$\underline{u}$	Input vector	
$\underline{U}$	Stack vector of inputs	

v	Velocity	m/s
v_x	Longitudinal (forward) velocity	m/s
v_y	Lateral velocity	m/s
V	Set of vertices	
x	x-coordinate	m
$\underline{x}$	State vector	
$\underline{X}$	Stack vector of states	
y	y-coordinate	m
$\underline{z}$	Noise	
Z_{forbid}	Forbidden zone in potential field strategy	
α	Tire side slip angle	rad
α_f	Front tire side slip angle	rad
α_r	Rear tire side slip angle	rad
β	Vehicle chassis side slip angle	rad
β_f	Vehicle side slip angle at front wheel	rad
β_r	Vehicle side slip angle at rear wheel	rad
δ	Steering angle	rad
δ_f	Steering angle at front wheel	rad
δ_r	Steering angle at rear wheel	rad
θ	Path parameter	m
κ	Longitudinal tire slip	
λ	Tangential line used for cone definition in velocity obstacle strategy	

μ	Friction coefficient	
ξ	Increment	s
τ	Horizon	s
ψ	Yaw angle	rad
ω	Angular velocity	rad/s
Ω_0	Angular speed of revolution of tire	rad/s

1 INTRODUCTION

Developing urban infrastructure and roads between cities made the transportation by automobile a dominant mode of travel. Increasing transportation by automobile consequence in rising carbon emissions, increasing congestion and also increase dramatically accident rates [1]. Traffic congestion wastes on average 111 hours of European and American time on grid lock annually [2] which is expected to increase 50% in 2030 comparing to 2013 which will be to $293.1 billion. In some mega cities such as Tehran in Iran, to reduce the congestion, a restricted traffic zone *RTZ*, is defined since 1981 [3] or to reduce the traffic and emission, a vehicle free zone only for pedestrian is implemented on the commercial heart "Bazaar". Converting gasoline-powered vehicles reduces emission problem but does little to reduce congestion or motor vehicle fatalities which is another major concern. Based on global status report on road safety [4] , 1.24 million people were killed on the world's road on 2010 which is unacceptably high. In general, road traffic injuries are the eight leading cause of death for young people aged 15-29 [5]. Only in USA motor vehicle crashes are the leading cause of death, claiming the lives of 18,266 Americans each year for those aged 5-34 [6]. In the most cases human error such as speed, seat-belt, drink driving, motorcycle helmets, etc. are the main reason of accident and sadly death [7].

Human factor such as age, fatigue and etc. has a big impact on traffic safety. For example, the incidence of traffic crashes increases sharply after age 55 [8]. Increasing the elderly population are expected to continue through the year 2030, at which point that for example the proportion of the US population aged 65 years and older will have increased to 21.8% [8]. Figure 1-1 shows the percentage of the population over 65 in Germany and figure 1-2 in the world. This simply means an increased number of older adults will be on the road.

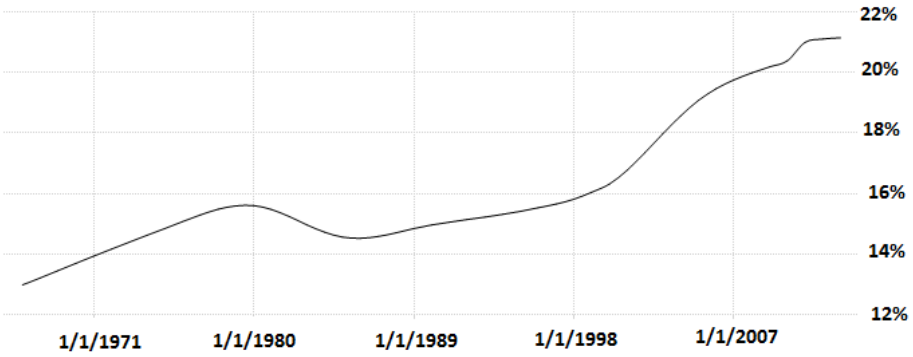

1-1: Population ages 65 and above (% of total) in Germany. Credit: Trading economics

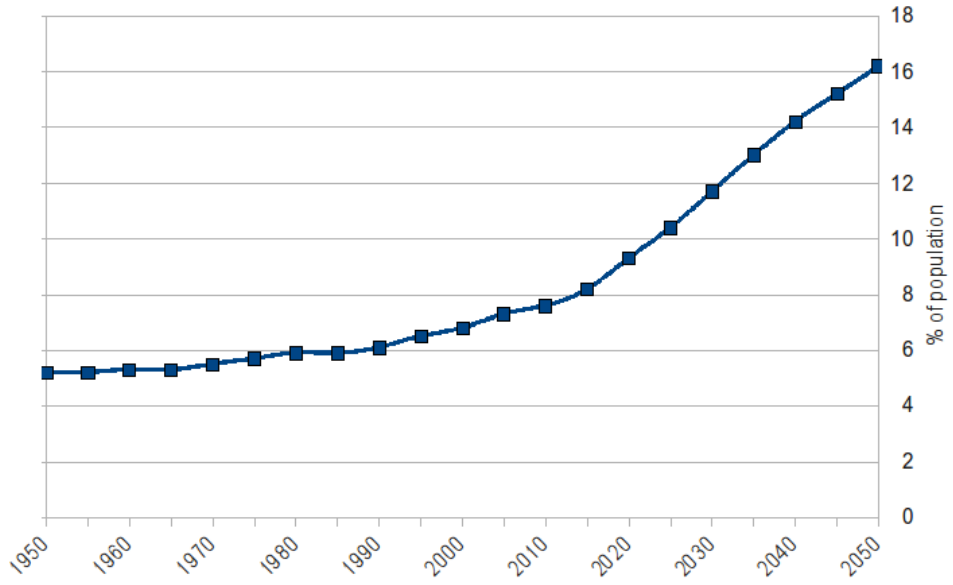

1-2: Population ages 65 and above (% of total) in the world. Credit: UN World Population Prospect

1.1 Driving assistance system Vs. Human error

To reduce driver error and assist driver in driving process, driving assistant system are developed. For example, focus level of driver may drop while driving due to fatigue or involving in second activity, or vision range can be limited or reduced in bad wheatear condition, then it is necessary to develop systems which warn or assist driver. Such systems by warning driver may help driver to react earlier in critical situation. If driver had reacted only half a second earlier in critical situations, approximately 60% of rear-end collisions and a third of frontal impacts could have been avoided [9]. Driving assistance systems not only increase driver safety but also reduce traffic and congestion cost. Such systems can warn the driver by beeping or vibration on steering wheel, or it can also take the control of the vehicle partially or completely to avoid any crash. Here some of these systems are explained briefly.

Driver focus level has big impact on safety, it can be reduced when driver is tired or when is involved in second activity. Driver Monitoring System *DMS*, is a system which monitors driver behavior and is able to detect if driver is not paying attention to the road by driver eye tracking. The system will warn the driver by flashing lights or warning sounds. Such system is presented by Toyota for first time in 2006 [10]. Also when driver is fully involved in driving, his/her vision is limited even in normal weather condition, for example the side view of the driver is limited especially in the zone which is called blind spot. A driving assistance system named Blind Spot Monitor *BSM*, can detect other vehicles located to the driver's side and rear and warn the driver [11]. Another assistant system in this type is Automotive Night Vision *ANV*, first introduced in 2000 by Cadillac which uses a thermographic camera to increase driver's perception and seeing distance in darkness or poor weather beyond the reach of the vehicle's headlights [12]. These systems were only a few examples of this kind in which the aim is only to warn driver as driver

remain the only controller of the vehicle. Another type of the driver assistant system, has ability to take partially the control of vehicle, for example Adaptive Cruise Control *ACC*, adjusts automatically the vehicle speed in order to keep safe distance from vehicle ahead, such system can be equipped with laser or radar sensor [13]. Another example is Lane Keeping System *LKS*, which not only warns the driver like Lane Departure Warning *LDW*, but it takes steps to ensure the vehicle stays in lane if no action is taken [14]. Another system which could be equipped with Adaptive Cruise Control is Collision Avoidance System in which in case of imminent crash, warns the driver or takes the control of the vehicle completely in the autonomous way by braking for low velocity and braking and steering for higher velocity [15]. Electronic Stability Control *ESC*, is a system that improves the vehicle stability by detecting and reducing loss of traction. When the loss of steering is detected, this system applies different brakes to the wheels individually in order to minimize loss of control. According to Insurance Institute for Highway Safety *IIHS*, and the U.S. National Highway Traffic Safety Administration *NHTSA*, one-third of fatal accidents could be prevented by the use of the technology [16] [17]. The driving assistance systems can reduce the accidents and fatalities dramatically but the main reason of the accident still remains which is driver, as he/she is the main vehicle controller. Another issue remain on traffic efficiency, air pollution and congestion cost.

1.2 Autonomous driving as a solution

The beginning of driving autonomous was not on the road but on the sea. Most likely the first self-propelled vehicles were sailboats and possibly the first to have some form of automated steering, the auto tiller [18]. This device uses ropes to connect something like a weathervane to the boat's tiller, so that the craft stays on course even with shifting winds. A decade after Wright brothers, airplanes got autopilot. In 1933, Wiley Post

became the first to fly solo around the world. The idea of autonomous vehicles has been with us almost as long as automobile [19].

AV technology is most easily conceptualized using a five-part continuum suggested by the National Highway Traffic Safety Administration *NHTSA*, [20], with different benefits of the technology realized at different levels of automation:

- Level 0 (no automation): All the primary vehicle functions such as throttle, brake and steering are controlled by driver and driver is solely responsible for monitoring the roadway and for safe vehicle operation.
- Level 1 (function-specific automation): Only one or more functions are automatic and in the case of multiple functions, they operate independently. Driver remain the main controller and responsible for operation but can choose to cede limited authority over a primary control (as in *ACC*); limited authority is assumed over a primary control like in *ESC* or additional control can be provided to help driver in some normal driving or crash-imminent situation like dynamic brake support in emergencies.
- Level 2 (combined-function automation): At this level at least two primary control functions work in unison to relieve the driver of controlling those functions. When driver gives authority in primary control in some limited driving situations, vehicle can use shared authority. Driver still remains the responsible for monitoring the road and safe operation and is assumed to be available at any time to take control of the vehicle as the system can gives back the control to the driver without any warning in advance.
- Level 3 (limited self-driving automation): At this level, driver is able to give full control to vehicle under certain traffic or environmental conditions and vehicle monitors for changes on the road. Driver is assumed to be available for occasional

control but with sufficiently comfortable transition time. The role of driver is change in this level, from controller to supervisor.

- Level 4 (full self-driving automation): Monitoring the roadway and all safety-critical driving functions are performed by vehicle. Role of driver is to provide destination or navigation input but is not expected to take the control of the vehicle at any time. This includes both occupied and unoccupied vehicles. By design, safe operation rests solely on the automated vehicle system.

AV technology level 4, can dramatically reduce the frequency of crashes as driver is not involved during driving process. AV technology level two and there, despite that driver is involved in driving process, can reduce the crashes as the vehicle is equipped with some automated functions. The Insurance Institute for Highway Safety *IIHS*, estimated that if all vehicles had forward collision and lane departure warning systems, side view (blind spot) assist, and adaptive headlights, nearly a third of crashes and fatalities could be prevented [21].

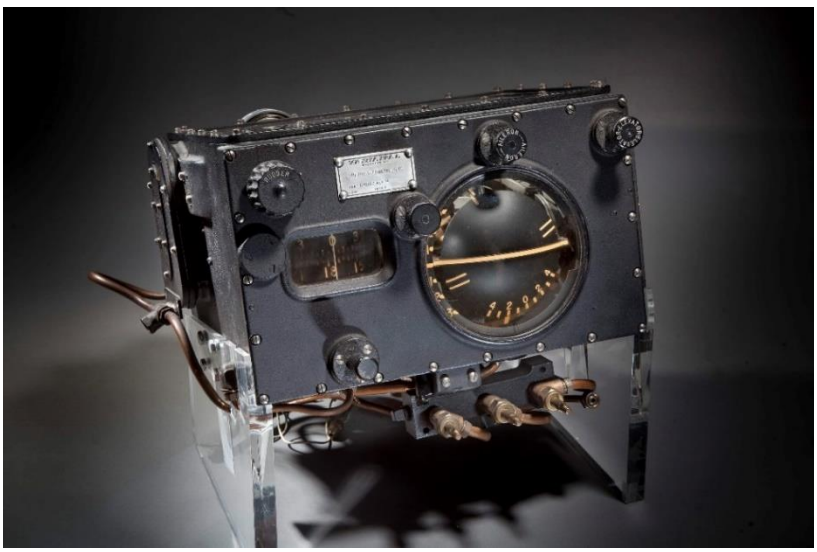

1-3: Sperry Gyroscope autopilot. Credit: Photo by Eric Long, National Air and Space Museum, Smithsonian Institution (NASM 2012-01350)

Another benefit of AV technology of level four is the possibility of mobility for those who are unable to drive like blind and disable persons and also unwilling person. As already noted, AV technology of Level 3 or above will likely decrease the cost of time in a car because the driver will be able to engage in alternative activities. As in AV technology the clean source of energy can be used, it has a positive impact on air pollution. In another hand when acceleration-deceleration is smoother as human driver, improves energy efficiency. As AV technology reduce the crashes, the vehicle and trucks can be made in lighter weight which reduce fuel consumption.

Research done in the field of autonomous driving can be divided into three phases based on [22]:

1. From approximately 1980 to 2003, researcher at universities worked on autonomous driving which can be categorized in two groups. The first who worked an automated highway system in which vehicle remain "dumb" as highway must guide it. And second group which worked on AVs which did not require special roads.
2. From 2003 to 2007, the U.S. Defense Advanced Research Projects Agency *DARPA*, held three "Grand Challenges" that markedly accelerated advancements in AV technology. The first two were held in rural environments, while the third took place in an urban environment. Each of these spurred university teams to develop the technology.
3. More recently, private companies have advanced AVs like Google's Driverless Car initiative has developed and tested a fleet of cars and initiated campaigns to demonstrate the applications of the technology.

In Germany as the birthplace of the automobile since Karl Benz and Nikolaus otto, the industries and universities focus on this filed. Some of universities projects are named bellow. The Autonomous Car team of Freie Universität Berlin has two projects on

autonomous driving, *MadeInGermany* and *e-Instein*. *MadeInGermany* is a modified Volkswagen Passat Variant 3c. Latest LIDAR/ RADAR sensor technology, as well as cameras, help to overview its surrounding area. A special GPS system gives precise information about the position. The car is also equipped with Drive-by-Wire technology, meaning that engine, brakes, steering and other actuating elements can be accessed directly via the CAN-BUS. *MadeInGermany* successfully drives autonomously in the streets of Berlin since 2011. *e_Instein* is a modified Mitsubishi *i-MiEV* is also Drive-by-Wire. Technical University of Braunschweig with *Stadpilot* project developed an autonomous Volkswagen Passat which operated successfully in 2010 its first automated drive along a preselected route through Braunschweig's urban traffic. Karlsruhe Institute of Technology cooperated with Daimler in 2013 to have a Mercedes drive autonomously. Universität der Bundeswehr of Munich develops *MuCAR-3* a modified Volkswagen Tourag by focusing on expectation-based perception and off-road navigation and driving. In Institute of Mobile System *IMS*, of Otto-von-Guericke-University of Magdeburg-Germany, a rebuild buggy car named *BugEE*, figure 1-4 is converted to electric by replacing internal combustion engine with four wheel hub motors. Steering system is replaced by Active-Front-Steering *AFS*, which offers the possibility to use this converted electric car also for autonomous driving. A differential GPS, *DGPS*, is used to know the exact position of vehicle which is used in control level and also to know position, velocity and orientation of obstacles. Approach used to drive this vehicle autonomously is explained briefly in the next section.

1.3 Hierarchical concept of Autonomous Driving

Classical approaches for path planning [23] are mainly rules and maneuvers based. However predefining and considering all the critical situations in path planning is not possible, this is why in this research work autonomous driving is based on mathematic

formulation which allows taking decision on unforeseen situations and restrictions related to the road and traffic situations in the case of obstacle or any collision, and also sudden changes on the road or existence of another vehicles.

Digital maps and navigation systems in these days are more than a way to find paths. They have the possibility to offer the high accuracy data about the road on real time and also inform driver about ahead road situation. In some maps, ex. Here by Nokia, the vehicle which use the map also helps to update by collecting the data of the actual road and send it to the map database and also alert other cars on the road about traffic obstacles or accidents in the vicinity. The data of the road, extracted from such system, can be used in path planning level in which road is considered without dynamics. Start and end point plus stationary obstacles which are known at this level are taken into consideration. Aim of this level, is to find a path from start point to end point without any collision with stationary obstacles. Based on the path found at path planning level and simple vehicle model initial solution for path optimization level is found.

1-4: Experimental vehicle, BugEE

In path optimization level, the dynamics of the vehicle is taken into consideration and aim is to find system inputs, driving force and steering angle velocity, which allow leading the vehicle alongside a calculated lane which could be optimal for different objectives such as energy consumption or comfort and etc. and allows taking into account some constraints such as limited velocity, width of the track, maximal lateral or longitudinal acceleration and etc.. Unlike path planning level, in path optimization level, both static and dynamic obstacles are taken into consideration and an obstacle avoidance strategy is implemented in this level to avoid any collision. When the optimal inputs found on path optimization level are implemented to the vehicle, there is no guarantee that vehicle behavior matches perfectly with the optimal solution due to the model uncertainty and environment disturbances such as different road friction and side wind. This error between optimal solution and vehicle behavior can be mapped on position level in longitudinal and lateral directions. To minimize these errors, path control level is added to the hierarchical concept [24] which generates additional inputs to compensate these errors.

The optimal control problem due to the big dimension of the system and length of course is numerically hard to solve and require much calculation time to find optimal solution. In another hand, optimal control problem must be updated in order to consider the dynamic behavior of road and traffic situation. To solve the problem in an easier way and make the system real-time capable, a "Moving-Horizon Approach" *MHA*, is used, in which global optimization problem is partitioned into sequence of local optimization problems with an adequate smaller horizon. Updating and solving the problem with small horizon offers the possibility to update road dynamics which is useful in the case of sudden changes, obstacles or other vehicles on the lane.

1.4 Thesis overview

As this work has a hierarchical concept, as is shown in figure 1-5, it can be explained level by level. Therefore at beginning vehicle and tire model must be presented which is done in chapter 2. In chapter 3 path planning is explained in two different levels, at first "route planning" is explained which is about to find a course from starting point to end point, then on next level which is "path planning", on that course, graphs are generated and shortest path on those graphs is found. Then by using a simple vehicle model which is presented in chapter 2, initial solution for path optimization level is found. Path optimization level is explained in chapter 4. At first optimal control problem *OCP*, is presented and converting this problem to the format of used solver, *NLPQLP*, is explained. Moving-Horizon approach, figure 1-6, and choice of its parameters is explained and justified in the same chapter. In chapter 5, two different strategies to avoid any collision are presented and compared.

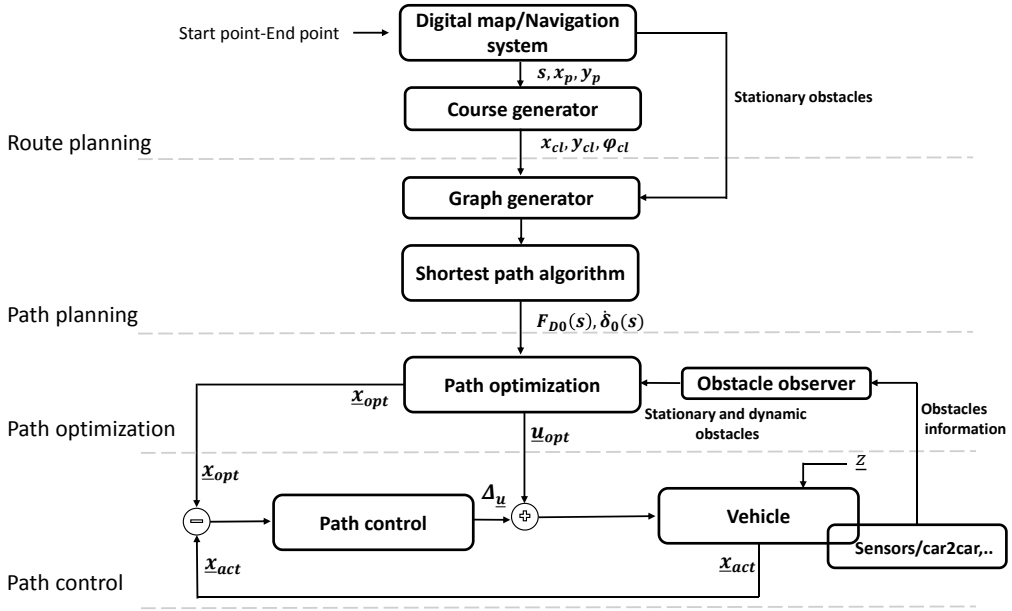

1-5: Hierarchical concept of autonomous driving

In chapter 6 path control level concept is presented and the functionality of the approach is proven with some simulation results done on *IPG-CarMaker*. In chapter 7 experimental setup is explained and the functionality of the approach is proven with experimental

results. And finality chapter 8 is conclusion of the project and suggested strategy for further development of the project.

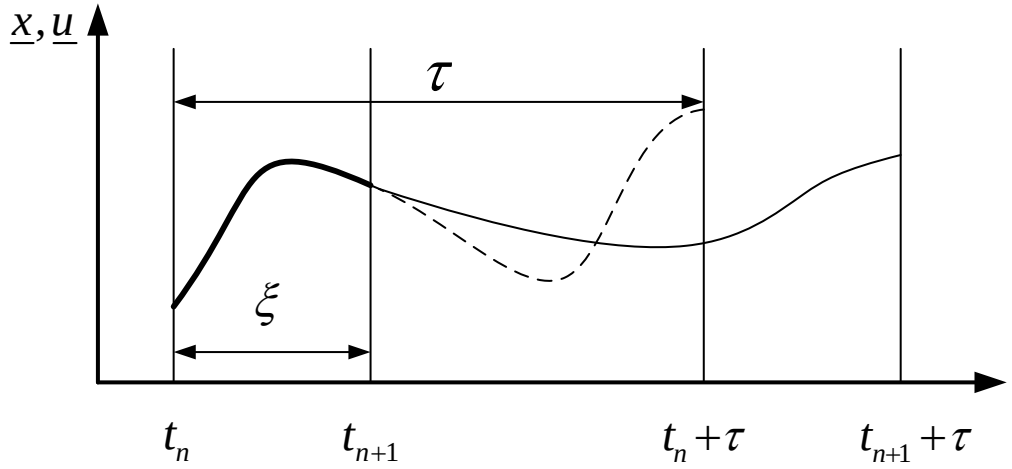

1-6: Moving horizon approach

2 TIRE AND VEHICLE DYNAMICS

2.1 Introduction

To describe the behavior of the vehicle, vehicle mathematic model is needed. Such model can be described without considering the forces that affect the motion and can be based purely on geometric relationships governing the system, such model is kinematic model. In spite such model does not give information about the relation and interaction between the forces, its simplicity can be useful to estimate and predict the behavior of another vehicles on the road, what can be considered as obstacles from our point of view. To describe the behavior of our vehicle, its dynamics is important, therefore a dynamic model is required. Dynamics of rigid vehicle may be considered as the motion of the rigid body with respect to a fixed global coordinate system. As dynamic model deal with forces and interaction between them, the forces acting on a system of connected rigid bodies must be considered. These forces can be divided into external and internal forces. Internal forces are acting between connected bodies, and external forces are acting from outside of the system. Example for internal force on the vehicle is driving forces on the wheels, F_D. An external force can be the traction force at the tireprint of a driving wheel, or a body force, such as the gravitational force on the vehicle's body. Tireprint is the contact area between a tire and the road [25]. Tires as the only mean of transfer the forces between the vehicle and the road, play very important role on vehicle dynamics. The force generated by tire influence longitudinal and lateral dynamics of the vehicle.

Between the models which describe the dynamics of the vehicle, single track model [26], received more attention between researchers and also in automobile industry [27] [28] [29]. This model despite its simplicity and without major modeling and parametrization effort, allows a physically plausible description of the driving behavior of the vehicle.
In this chapter, tire model is presented and its influence on the vehicle dynamics is discussed. Based on single track vehicle model, kinematic model is presented. To describe the dynamic behavior, single track dynamic model is developed and presented. Based on some assumption non-linear single track model is simplified by linearization of some parameters. And finally double track vehicle model as an extension of single track model is developed and presented.

2.2 Tire dynamics

Vehicle can maneuver by longitudinal, lateral and vertical force systems generated under the tires. To describe the forces and moments on the tire, a right-hand Cartesian coordinate frame at the center of tireprint is attached, figure 2-1 left. The x-axis is along the intersection of the ground with the plane made by narrowing the tire to a flat disk. The z-axis is perpendicular to the ground and y-axis makes the coordinate system right-hand. The force system that a tire receives from the ground can be decomposed along *x*, *y*, and *z* axis including a force and a torque on each axis [25]. These forces are assumed to be located at the center of the tireprint. Force along *x*-axis is longitudinal force F_x . Positive F_x results acceleration and negative value results breaking. Moment along x-axis, M_x is roll moment, which is also called bank moment or tilting torque. Force along z-axis is vertical force, it is also called wheel load. Moment along z-axis, M_z is yaw moment. $M_z > 0$ tends to turn the tire about the z-axis. Force along y-axis is lateral force which is tangent to the ground and orthogonal to both F_x and F_z.

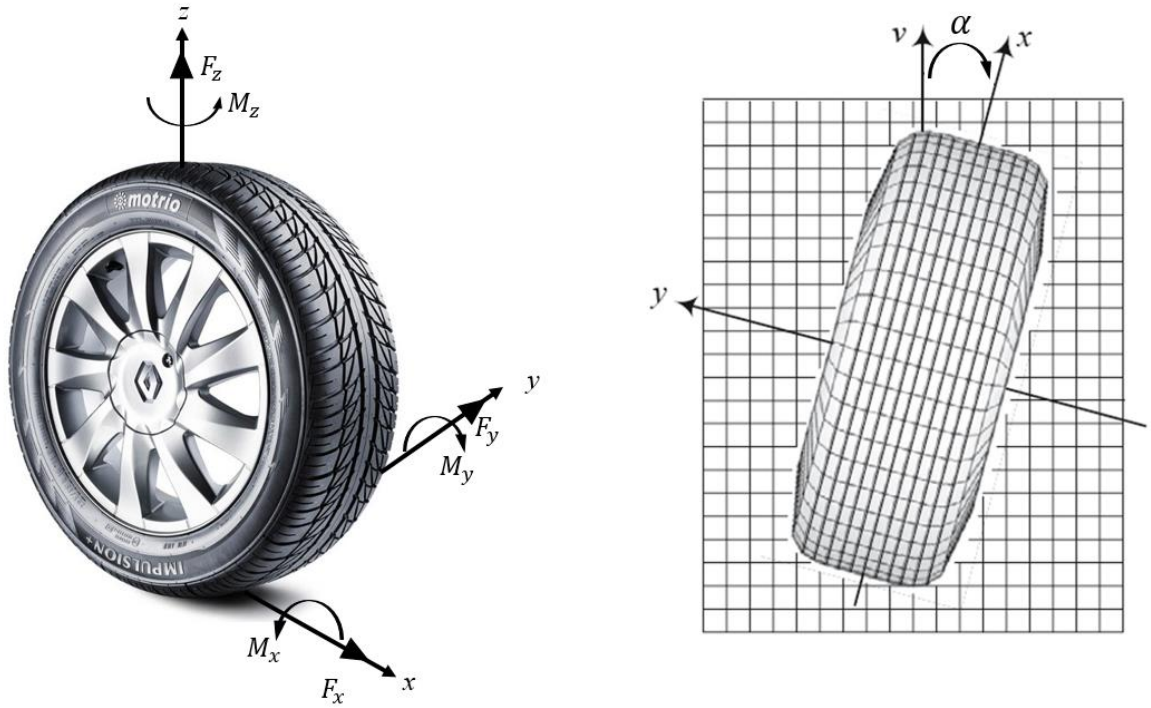

2-1: Left: Tire coordinate system. Right: Tire side slip angle

The resultant lateral force $F_y > 0$ if it is in the y-direction. Moment along y-axis, M_y is pitch moment. The pitch moment is also called rolling resistance torque [25].

As the tires are made with viscoelastic material they have deformation. When there is a pulling force on the tire, tire rolling resistance and side force occurs as a result of asymmetric structure of the tire [30]. In this case wheel may slip and possibly partial sliding in the contact patch can happen which generate horizontal forces. This effect has been seen by Reynolds in his experiment in 1876 [31]. In order to measure the longitudinal slip, the forward speed V_x and angular speed of revolution Ω_0 of a freely rolling wheel can be measured. Dividing these two quantities the effective rolling radius r_e is obtained.

$$r_e = \frac{V_x}{\Omega_0} \qquad 2\text{-}1$$

longitudinal slip κ, arises when the torque is applied about the wheel spin axis.

$$\kappa = -\frac{V_x - r_e\Omega_0}{V_x} \qquad 2\text{-}2$$

$\kappa = -1$ when the wheel is blocked ($v \neq 0, \omega = 0$) and $\kappa = 1$ for spinning wheel ($v = 0, \omega \neq 0$) . In acceleration and breaking phase the longitudinal slip has big value and it has small value in normal driving situation. During cornering maneuver, the tire contact pitch slips laterally while rolling such that its motion is no longer in the direction of the wheel plane. The deformation in tire carcass and tread results in sideslip angle,α, which is the angular difference between the direction that tire contact patch with the road is pointing and the direction of the wheel and can be defined as the ratio of the lateral and the forward velocity of the wheel.

$$tan\,\alpha = -\frac{V_y}{V_x} \qquad 2\text{-}3$$

For longitudinal and lateral tire slip angle, the sign is chosen such that the side force becomes positive at positive slip angle. The forces generated by the slip angles are the function of slip components and wheel load. The effect of camber angle is neglected here.

$$F_x = F_x(\kappa, \alpha, F_z) \qquad 2\text{-}4$$

$$F_y = F_y(\kappa, \alpha, F_z) \qquad 2\text{-}5$$

The force generated by sideslip angle is called side force and the force generated by longitudinal angle is named longitudinal force. Figure 2-2 from [30], shows the combined lateral and longitudinal slip characteristics. Figure 2-2 left shows the side force by adding different longitudinal slip. Same figure middle, shows the longitudinal force when different side angle is added. As it shown, the side force drops when longitudinal slip is added and vice versa. The same situation is for the longitudinal force.

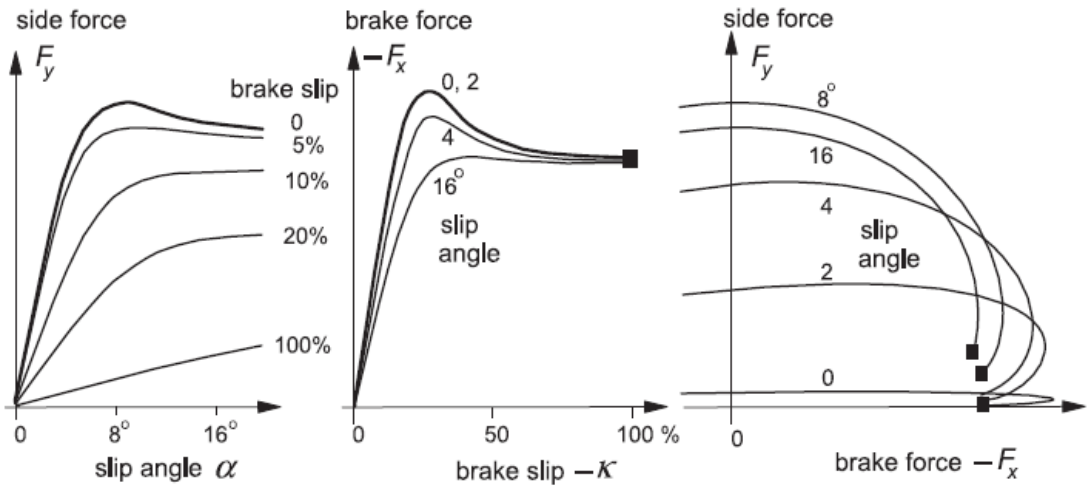

2-2: Combined side force and longitudinal (brake) force characteristics. Credit: H. Pacejka and I. Besselink, Tire and vehicle dynamics [30]

As both forces are the result of contact between tire and the ground, they are coupled. The coupling between them, figure 2-2 right, described by Kamm circle, figure 2-3.

$$\sqrt{{F_x}^2+{F_y}^2} \leq \mu \,.\, F_z \qquad 2\text{-}6$$

Equation 2-6 means, forces that act on the contact surface between the tire and the ground cannot exceed the product of the tire load F_z and the friction coefficient μ. During driving situation, both longitudinal and lateral force occur when accelerating or breaking is done while cornering. The slop of the slip curve is defined as slip stiffness.

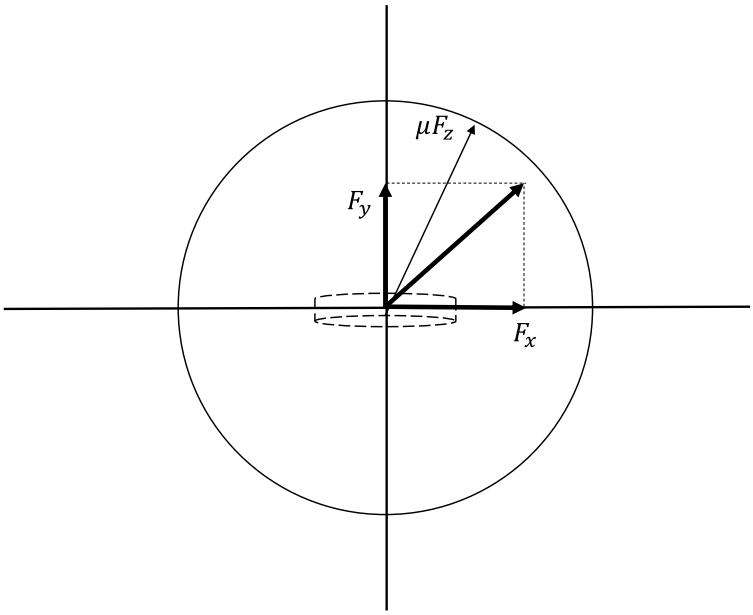

2-3: Kamm circle

The longitudinal slip stiffness is C_κ and lateral slip or cornering stiffness is C_α which play very important role in vehicle's handling and stability. At small levels of slip, the linearized forces can be represented by the following expressions:

$$F_x = C_\kappa . \kappa \quad \text{2-7}$$

$$F_y = C_\alpha . \alpha \quad \text{2-8}$$

At higher levels of slip, the forces remain constant or drop slightly when slip angles reach critical values. There are many different models to describe tire behavior, some of them are purely mathematic which describe physical characteristic of tire such as Magic formula tire model by Pacejka and Basselink [32] and some of them are physical model such as FE (Finite Element) model [33]. As the focus here is on the vehicle dynamics, the forces and torques occurring between tire and road is more important than deformation behavior itself, therefore a mathematic model is suitable. Magic formula by Pacejka and Basselink [32] doesn't have any particular physical basis for the structure of the equations but it is reasonably accurate. The general form of the magic formula for lateral tire force is:

$$F_y = D.sin[C.tan^{-1}(B.\alpha - E.[B.\alpha - tan^{-1}(B.\alpha)])] \quad \text{2-9}$$

The model parameter are as follows:

parameter	meaning
B	Stiffness factor
C	Shape factor
D	Peak value
E	Curvature factor

Table 2-1: Magic formula parameters

In normal driving situation when the slip angle does not reach its critical value, a simple linear formulation with saturation can be used as equation 2-10.

$$F_y = \begin{cases} -C_\alpha . \alpha, & |\alpha| \leq \alpha_{max} \\ \pm F_{ymax}, & |\alpha| > \alpha_{max} \end{cases} \qquad 2\text{-}10$$

Figure 2-4 compares the lateral force F_y in Magic formula and linear formulation with saturation. As mentioned in normal driving situation in which there is no high acceleration or braking, the value of longitudinal slip and consequently the value of longitudinal tire force is low. In another hand lateral side slip and force has bigger influence on vehicle lateral dynamics. Hence to describe the dynamic of the vehicle, only lateral slip angle and lateral force are taken into account.

2.3 Vehicle dynamics

The lateral dynamics of the vehicle are represented here by single track model also named as bicycle model. This model is a standard representation in the area of ground vehicle dynamics. In single track model the rear wheels and front wheels are summarized to one each, see figure 2-5. The vehicle chassis is modeled as rigid body which can move in x, y direction and rotate ψ about vertical axis. In figure 2-5, point C is the center of gravity of vehicle body, v is the vehicle velocity at its center of gravity, ψ is yaw angle which is from x-axis to the longitudinal axis of the vehicle body AB.

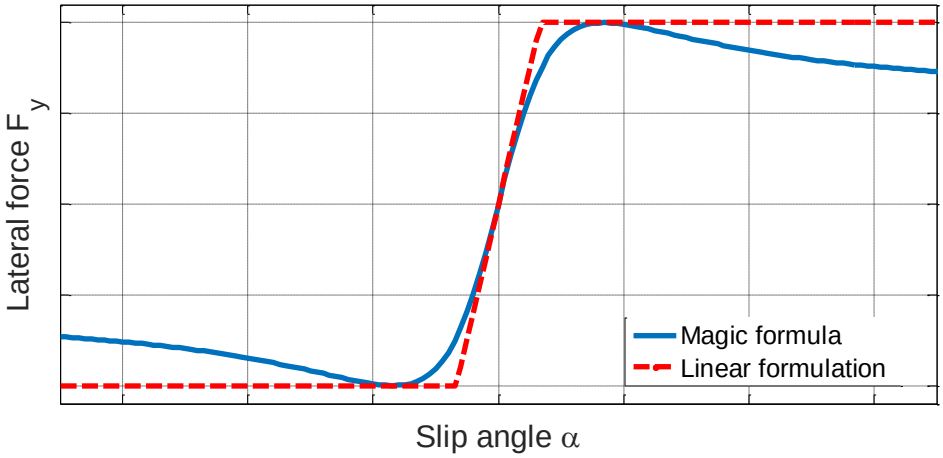

2-4: Lateral force F_y using Magic formula and linear formula for a sample tire

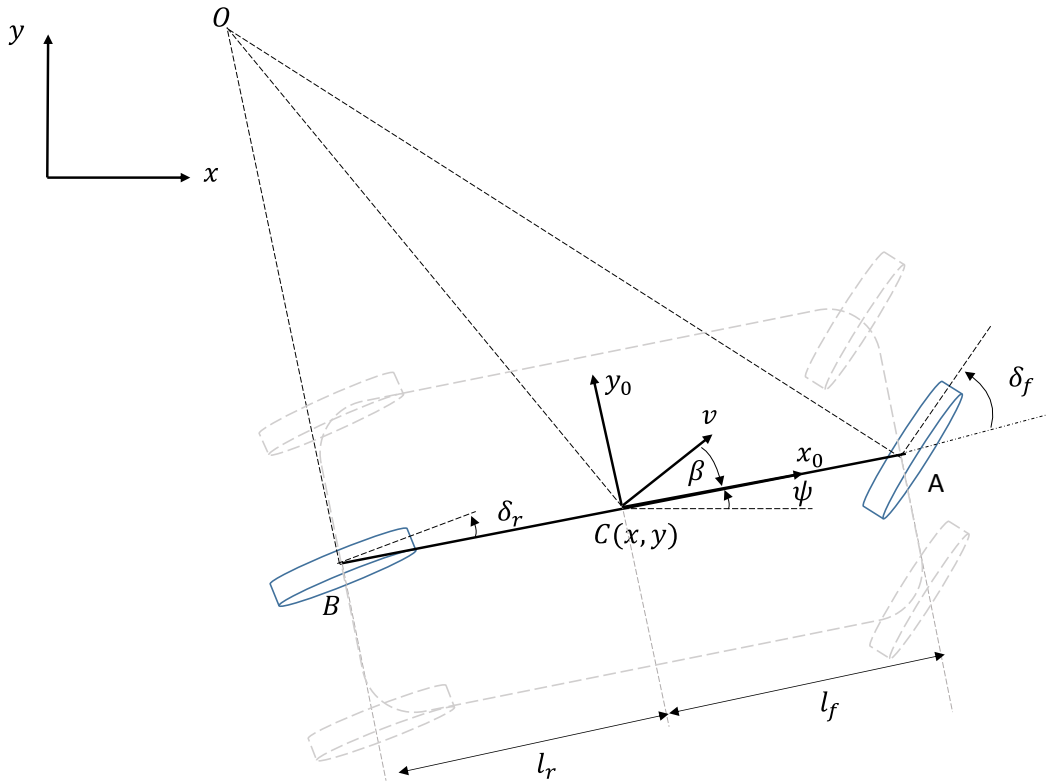

2-5 : Single track model at low velocity

Yaw angle describes the orientation of the vehicle. Side slip angle β, is the angle from the longitudinal axis of the vehicle body AB to the direction of the vehicle velocity, v. Single track model is derived assuming both front and rear wheel can steer. Front and rear steering wheel angle are presented by δ_f and δ_r respectively. Distance from vehicle center line to the front wheel is l_f, and distance from vehicle center line to rear wheel is l_r. In single track model all lifting, rolling and pitching angles are neglected. These assumptions hold well for most typical driving situations.

2.3.1 Kinematic model of single track

In kinematic model of the vehicle, equations of motion are based on geometric relationships governing the system without considering the forces that affect the motion. The simplicity of this model is useful to describe the behavior of another vehicles on the road when information about vehicle states such as position, velocity and orientation can

be updated. The main assumption used to develop the kinematic model is that velocity vector at the front wheel make an angle of δ_f with the longitudinal axis of the vehicle. This is equivalent of assuming that the slip angle of both wheels are zero. This assumption is only valid when the vehicle velocity is low, for example less than 5 $^{m}/_{s}$. At low velocity the lateral force generated by tire is small. Kinematic model of vehicle can be expressed as follows:

$$\dot{x} = v.cos(\psi - \beta)$$

$$\dot{y} = v.sin(\psi - \beta) \qquad 2\text{-}11$$

$$\dot{\psi} = \frac{v.cos(\beta).tan(\delta_f)}{l_f + l_r}$$

Where β is

$$\beta = arctan\left(\frac{l_r.tan\,\delta_f}{l_f + l_r}\right) \qquad 2\text{-}12$$

2.3.2 Dynamic model of single track

At higher vehicle velocity, velocity at each wheel is not anymore in the direction of the wheel. This is why the kinematic model is not valid at high velocity and instead dynamic model must be used. To develop a dynamic model, motional actions necessary for moving vehicle and its resulting forces under consideration of the natural laws must be taken into account. In this model driving force is presented by F_D and resistance force or load force presented by F_L. This force in longitudinal direction F_{Lx} , can be due to friction and in lateral direction F_{Ly}, can present the disturbances such as side wind. In this model vehicle slip angle β_f and β_r are also defined for each wheel as the angle from the longitudinal axis of the vehicle body AB to the direction of the wheel velocity, v_f and v_r, which are different from tire slip angle which is the angle from the longitudinal axis of the wheel to direction of wheel velocity.

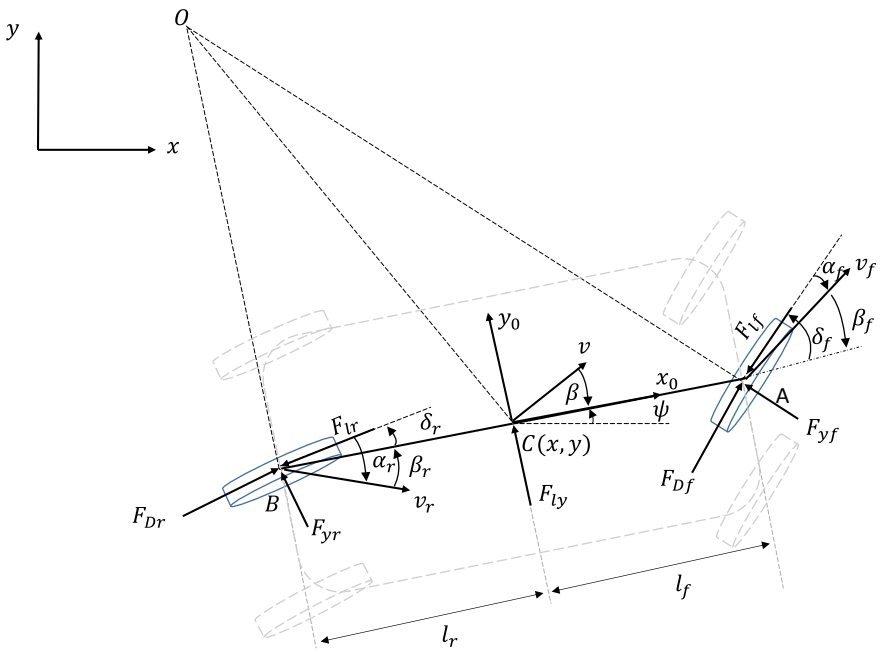

2-6: Single track model at high velocity

At first, second Newton's law along tangential axis which is the direction of course angle is applied to extract the longitudinal motion,

$$m.a_x = \sum F_T \qquad 2\text{-}13$$

Applying Newton's second law for motion along normal axis which is perpendicular to tangential line or course angle of vehicle, extract the lateral motion,

$$m.a_y = \sum F_N \qquad 2\text{-}14$$

In which $\sum F_N$ is the sum of forces in normal axis and a_y is the centripetal acceleration. a_y is related to the angular velocity and the road radius.

$$a_y = \omega^2.r \qquad 2\text{-}15$$

And angular velocity can be written as:

$$\omega = \frac{v}{r} \qquad 2\text{-}16$$

Angular velocity can also be written as the derivative of heading angle or course angle k, which is the angle between vehicle's direction of motion and x-axis.

$$k = \psi - \beta \tag{2-17}$$

$$\omega = \frac{dk}{dt} = \frac{d(\psi - \beta)}{dt} \tag{2-18}$$

From equations 2-15, 2-16 and 2-18

$$a_y = v.(\dot{\psi} - \dot{\beta}) \tag{2-19}$$

From equation 2-14 and 2-19

$$\dot{\beta} = \dot{\psi} - \frac{1}{m.v}.\sum F_N \tag{2-20}$$

Applying the Newton's second law for rotation about z-axis describe the yaw motion

$$J_z.\ddot{\psi} = \sum T \tag{2-21}$$

Where J_z is the moment of inertia and $\sum T$ is the sum of torques. The sum of forces in tangential and normal directions and also rotary torques about z-axis are:

$$\sum F_T = (F_{Dr} - F_{lr}).cos(\delta_r + \beta_r) - F_{yr}.sin(\delta_r + \beta_r) - F_{ly}.sin\beta + (F_{Df} - F_{lf}).cos(\delta_f + \beta_f) - F_{yf}.sin(\delta_f + \beta_f)$$

$$\sum F_N = (F_{Dr} - F_{lr}).sin(\delta_r + \beta_r) + F_{yr}.cos(\delta_r + \beta_r) + F_{ly}.cos\beta + (F_{Df} - F_{lf}).sin(\delta_f + \beta_f) + F_{yf}.cos(\delta_f + \beta_f) \tag{2-22}$$

$$\sum T = F_{yf}.cos(\delta_f).l_f - F_{yr}.cos(\delta_r).l_r$$

By implementing the forces from equation 2-22 to the equations 2-13, 2-20 and 2-21, the differential equation of vehicle dynamics can be described as equations 2-23.

$$\dot{\beta} = \dot{\psi} - \frac{1}{m.v}.((F_{Dr} - F_{lr}).sin(\delta_r + \beta_r) + F_{yr}.cos(\delta_r + \beta_r) + F_{ly}.cos\beta + (F_{Df} - F_{lf}).sin(\delta_f + \beta_f) + F_{yf}.cos(\delta_f + \beta_f))$$

$$\dot{\psi} = \omega$$

$$\dot{\omega} = \frac{1}{J_z}.(F_{yf}.cos(\delta_f).l_f - F_{yr}.cos(\delta_r).l_r) \tag{2-23}$$

$$\dot{v} = \frac{1}{m}.((F_{Dr} - F_{lr}).cos(\delta_r + \beta_r) - F_{yr}.sin(\delta_r + \beta_r) - F_{ly}.sin\beta + (F_{Df} - F_{lf}).cos(\delta_f + \beta_f) - F_{yf}.sin(\delta_f + \beta_f))$$

$$\dot{x} = v.cos(\psi - \beta)$$

$$\dot{y} = v.sin(\psi - \beta)$$

The vehicle behavior is influenced by driving force F_D and steering angle δ impose by driver. As explained in tire model section, lateral force generated on tire it depends on tire characteristic and tire slip angle, α. This force can be calculated by using linear formulation or Magic formula. In order to obtain the tire sideslip angles α_f and α_r, the velocity components perpendicular to the center line is extracted. Index *f* and *r* mean front and rear respectively.

$$v_f . \sin\beta_f = l_f . \dot{\psi} - v . \sin\beta \qquad 2\text{-}24$$

$$v_r . \sin\beta_r = l_r . \dot{\psi} + v . \sin\beta \qquad 2\text{-}25$$

The velocity components in the direction of the longitudinal center line of the vehicle must be equal since the car body does not expand or shrink, which means:

$$v_r . \cos\beta_r = v_f . \cos\beta_f = v . \cos\beta \qquad 2\text{-}26$$

The velocity term in equation 2-24 and 2-25 is eliminated by division by corresponding terms from 2-26. Then

$$\tan\beta_f = \frac{l_f . \dot{\psi} - v . \sin\beta}{v . \cos\beta} = \frac{l_f . \dot{\psi}}{v . \cos\beta} - \tan\beta \qquad 2\text{-}27$$

$$\tan\beta_r = \frac{l_r . \dot{\psi} + v . \sin\beta}{v . \cos\beta} = \frac{l_r . \dot{\psi}}{v . \cos\beta} + \tan\beta \qquad 2\text{-}28$$

As it is shown in figure 2-6, tire slip angles is:

$$\alpha_f = \delta_f - \beta_f = \delta_f - arctan\left(\frac{l_f . \dot{\psi} - v . \sin\beta}{v . \cos\beta}\right) \qquad 2\text{-}29$$

$$\alpha_r = \delta_r - \beta_r = \delta_r - arctan\left(\frac{l_r . \dot{\psi} + v . \sin\beta}{v . \cos\beta}\right) \qquad 2\text{-}30$$

2.3.3 Linearization of single track model for small angles

As differential equation of the motion shows, equation 2-23, this model is non-linear. This non-linearity makes the system complex. Based on some assumption the vehicle

model presented in equation 2-23 can be linearized. Tire side slip angle α, which has unneglectable value in normal driving situation, makes the most important non-linearity on tire model. Therefore as described in tire model section, lateral force on tire, as a function of tire slip angle can be linearized, equation 2-10. The vehicle dynamics equation of motion shows that the non-linearity remains for $\dot{\beta}$ and ω. The chassis and wheels side slip angles β, β_f and β_r and steering angle δ_f and δ_r are small angle, therefor $\cos(\beta, \delta) = 1$ and $\sin(\beta, \delta) = \beta, \delta$. In our case, the modeled vehicle can steer only by front wheel, therefore $\delta_r = 0$. The load force is assumed to have effect only in longitudinal direction, which makes $F_{ly} = 0$ and the driving force is only implemented on the rear wheel, therefore $F_{Df} = 0$. These assumption make the equations of motion as below:

$$\dot{\beta} = \dot{\psi} - \frac{1}{m.v} . ((F_{Dr} - F_{lr}).\beta_r + F_{yr} + F_{yf})$$

$$\dot{\psi} = \omega$$

$$\dot{\omega} = \frac{1}{J_z}.(F_{yf}.l_f - F_{yr}.l_r) \qquad 2\text{-}31$$

$$\dot{v} = \frac{1}{m}.((F_{Dr} - F_{lr}) - F_{yr}.\beta_r - F_{yf}.(\delta_f + \beta_f))$$

$$\dot{x} = v.cos(\psi - \beta)$$

$$\dot{y} = v.sin(\psi - \beta)$$

And slip angle on wheel can be rewritten as:

$$\beta_f = \frac{l_f.\dot{\psi}}{v} - \beta \qquad 2\text{-}32$$

$$\beta_r = \frac{l_r.\dot{\psi}}{v} + \beta \qquad 2\text{-}33$$

As it is shown in figure 2-6, tire slip angles are:

$$\alpha_f = \delta_f - \beta + \frac{l_f.\dot{\psi}}{v} \qquad 2\text{-}34$$

$$\alpha_r = \beta + \frac{l_r.\dot{\psi}}{v} \qquad 2\text{-}35$$

2.3.4 Double track model

As electric vehicles have the possibility to be equipped with four different motors such as wheel hub motors, offer the opportunity to take into account four independently adjustable driving forces. The main advantage of this model is to control the yaw rate and lateral motion of the vehicle more accurate especially while cornering [34] by separating the forces on each wheel.

$$\underline{F_D} = [F_{Dfr}, F_{Dfl}, F_{Drr}, F_{Drl}] \qquad 2\text{-}36$$

Indexes fr,fl,rr and rl refer to front right, front left, rear right and rear left respectively. Equations of motion can be written as:

$$\dot{\beta} = \dot{\psi} - \frac{1}{m.v}.\Big(\big((F_{Drr} - F_{lrr}).sin(\beta_{rr}) + (F_{Drl} - F_{lrl}).sin(\beta_{rl}) + F_{yrr}.cos(\beta_{rr}) + F_{yrl}.cos(\beta_{rl}) + F_{ly}.cos(\beta) + (F_{Dfr} - F_{lfr}\big).sin\big(\delta_f + \beta_{fr}\big) + (F_{Dfl} - F_{lfl}).sin\big(\delta_f + \beta_{fl}\big) + F_{yfr}.cos\big(\delta_f + \beta_{fr}\big) + F_{yfl}.cos(\delta_f + \beta_{fl})\Big)$$

$$\dot{\psi} = \omega$$

$$\dot{\omega} = \frac{1}{J_z}.\Big(\big(F_{yfr} + F_{yfl}\big).cos\big(\delta_f\big).l_f + \big(F_{Dfr} + F_{Dfl}\big).sin\big(\delta_f\big).l_f - \big(F_{yrl} + F_{yrr}\big).l_r - F_{Drl}.b_{rl} + F_{Drr}.b_{rr} - F_{Dfl}.b_{fl}.cos\big(\delta_f\big) + F_{Dfr}.b_{fr}.cos\big(\delta_f\big) + F_{yfl}.b_{fl}.sin\,\big(\delta_f\big) - F_{yfr}.b_{fr}.sin\,\big(\delta_f\big)\ \Big) \qquad 2\text{-}37$$

$$\dot{v} = \frac{1}{m}.\Big(\big(F_{Drr} - F_{lrr}\big).cos(\beta_{rr}) + (F_{Drl} - F_{lrl}).cos(\beta_{rl}) - F_{yrr}.sin(\beta_{rr}) - F_{yrl}.sin(\beta_{rl}) - F_{ly}.sin(\beta) + (F_{Dfr} - F_{lfr}).cos\big(\delta_f + \beta_{fr}\big) + \big(F_{Dfl} - F_{lfl}\big).cos\big(\delta_f + \beta_{fl}\big) - F_{yfr}.sin\big(\delta_f + \beta_{fr}\big) - F_{yfl}.sin\big(\delta_f + \beta_{fl}\big)\Big)$$

$$\dot{x} = v.cos(\psi - \beta)$$

$$\dot{y} = v.sin(\psi - \beta)$$

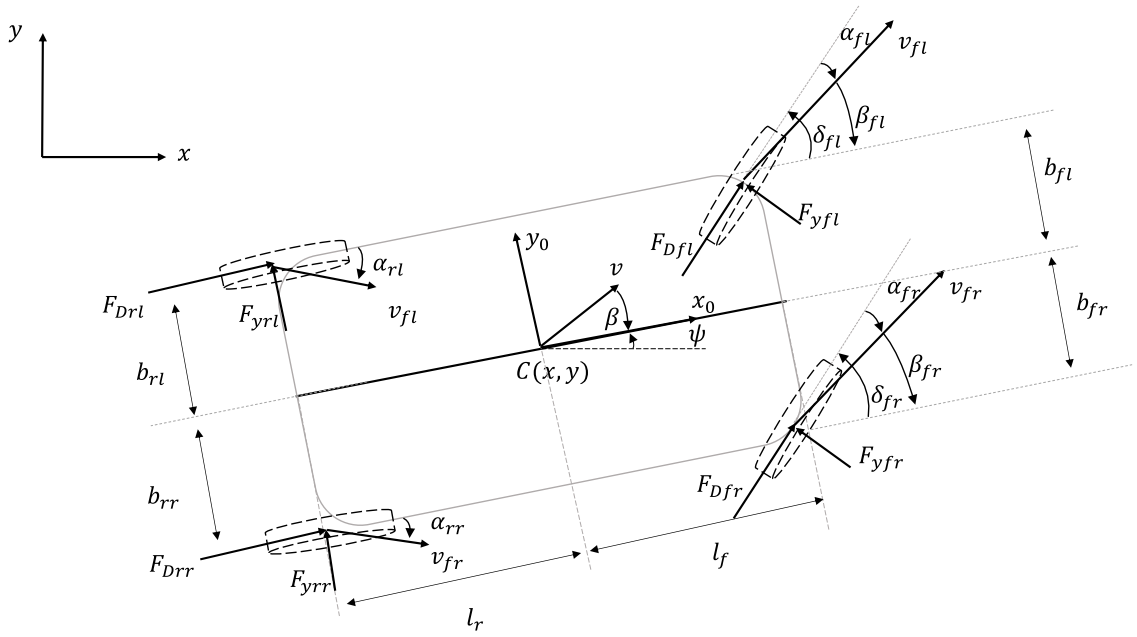

2-7: Double track vehicle model

Steering angle for front left and front right are equal and has the value of δ_f.

As the four wheels are considered, therefore the width of the vehicle also play a role on vehicle dynamics, see figure 2-7. In order to found tire slip angle the velocity components perpendicular to the center line is extracted.

$$v_{fr}\,.\,sin\,\beta_{fr} = l_f.\dot{\psi} - v\,.\,sin\,\beta$$

$$v_{fl}.\,sin\,\beta_{fl} = l_f.\dot{\psi} - v\,.\,sin\,\beta \qquad \text{2-38}$$

$$v_{rr}\,.\,sin\,\beta_{rr} = l_r.\dot{\psi} + v\,.\,sin\,\beta$$

$$v_{rl}.\,sin\,\beta_{rl} = l_r.\dot{\psi} + v.\,sin\,\beta$$

The velocity components in the direction of the longitudinal center line of the vehicle are:

$$v_{fr}\,.\,cos\,\beta_{fr} = v\,.\,cos\,\beta + \dot{\psi}.\,b_{fr}$$

$$v_{fl}.\,cos\,\beta_{fl} = v.\,cos\,\beta - \dot{\psi}.\,b_{fl} \qquad \text{2-39}$$

$$v_{rr}\,.\,cos\,\beta_{rr} = v\,.\,cos\,\beta + \dot{\psi}.\,b_{rr}$$

$$v_{rl}\,.\,cos\,\beta_{rl} = v.\,cos\,\beta - \dot{\psi}.\,b_{rl}$$

Dividing related terms from equation 2-38 by 2-39

$$tan\,\beta_{fr} = \frac{l_f.\dot{\psi} - v\,.sin\,\beta}{v\,.cos\,\beta + \psi.b_{fr}}$$

$$tan\,\beta_{fl} = \frac{l_f.\dot{\psi} - v.sin\,\beta}{v.cos\,\beta - \dot{\psi}.b_{fl}} \quad (2\text{-}40)$$

$$tan\,\beta_{rr} = \frac{l_r.\dot{\psi} + v\,.sin\,\beta}{v.cos\,\beta + \dot{\psi}.b_{rr}}$$

$$tan\,\beta_{rl} = \frac{l_r.\dot{\psi} + v\,.sin\,\beta}{v.cos\,\beta - \dot{\psi}.b_{rl}}$$

As it is shown in figure 2-7, tire slip angles are:

$$\alpha_{fr} = \delta_f - \beta_{fr} = \delta_f - arctan\left(\frac{l_f.\dot{\psi} - v\,.sin\,\beta}{v\,.cos\,\beta + \dot{\psi}.b_{fr}}\right)$$

$$\alpha_{fl} = \delta_f - \beta_{fl} = \delta_f - arctan\left(\frac{l_f.\dot{\psi} - v\,.sin\,\beta}{v\,.cos\,\beta - \dot{\psi}.b_{fl}}\right) \quad (2\text{-}41)$$

$$\alpha_{rr} = \delta_r - \beta_{rr} = -arctan\left(\frac{l_r.\dot{\psi} + v.sin\,\beta}{v\,.cos\,\beta + \dot{\psi}.b_{rr}}\right)$$

$$\alpha_{rl} = \delta_r - \beta_{rl} = -arctan\left(\frac{l_r.\dot{\psi} + v\,.sin\,\beta}{v\,.cos\,\beta - \dot{\psi}.b_{rl}}\right)$$

2.4 Conclusion

In this chapter different vehicle models such as kinematic model and dynamic models are explained. Single track model and its linearization and also double track model is explained. As the equation of motion in kinematic model shows, vehicle and tire characteristic parameter such as mass and length of the vehicle or tire stiffness do not have any impact on the model. Hence this model is not precise to define the behavior of the vehicle, but its simplicity could be used to estimate and predict the behavior of another vehicles when their position, velocity and orientation information can be delivered and

updated for example with Car2Car communication. This model will be used in chapter 5 to estimate the obstacle behavior and a simpler kinematic model will be used in chapter 3 to find the initial inputs of the optimal control problem. Single and double track dynamic model both consider motional forces on the vehicle body and on the wheels. Double Track model has the advantage of having four different adjustable forces which increase controllability of the yaw rate and lateral motion of the vehicle especially while cornering. Simplicity of the single track model is beneficial in calculation time point of view as it has less complexity and nonlinearity comparing to double track model. In chapter 4 both models are implemented as dynamic system in optimal control problem and the advantage and disadvantage of each model is explained with more details.

3 PATH PLANNING STRATEGY

3.1 Introduction

In previous chapter dynamic model of the vehicle is presented which will be used later in optimization level in order to find optimal control inputs based on a given objective function for autonomous driving. In order to find optimal solution an initial solution is required and as the dynamic vehicle model is nonlinear the quality of the optimal solution depends on the quality of the initial solution. Driving force F_D, and steering angle velocity $\dot{\delta}$, are the inputs of the vehicle dynamic models, therefore when the start point and end point of the course are defined, initial solution is the driving force F_D, and steering angle velocity $\dot{\delta}$, which lead vehicle through this course. When start point and end point is known, a course between them can be generated with the help of navigation system or digital map, this level is called *route planning*. After that the course is generated, a path on this course is found as the base of initial solution, this level is called *path planning*. For example let's consider the case of driving from point A to the given point B. The streets or roads which connect these two points are the course and the center line of the course can be considered as a suitable path on this course. However as digital maps have live traffic update, information about some stationary obstacles such as blocking part on the course due to construction or an accident can be known [35] [36]. In this case they can be considered in *path planning* level and a path which avoid these obstacles can be found. This last improves the quality of initial solution.

Path planning in simple terms is finding a free path from start point to end point. Path planning as an important and vast field of research has many application in industries, like finding a path for a manipulator robot in 3D environment [37], in order to reach the

goal and also avoid any collision with another manipulator robot and also itself. In robotic path planning is used to find a path for robot [38], or it is used in computer games, where game character must be moved in game environment without any collision with game defined obstacles such as mountains or opponent army. Path planning is more challenging when it deals with dynamic environment. Dynamic environment means the space in which path must be found has a dynamic behavior, like the dynamics objects which moves in this space. In this case, aim in not only to find a path, but also a collision free path by considering both stationary and dynamic obstacles.

Path planning for autonomous driving unlike the path planning for a manipulator has the advantage of having 2D environment which makes the path planning easier. In case of autonomous driving, as the infrastructure of the streets and roads are normally well defined, the path planning can be done based on the information delivered via digital maps or a navigation systems. When live traffic update is available aim is to find a path between start point and end point by avoiding all the known stationary obstacles like a partly blocked road due to road construction. The dynamic objects, like another vehicles, pedestrians or cyclists, are not considered in this level. While the vehicle moves on the road, sensors used in the vehicle and car2car communication, gather the information about the road and update the road situations. Dynamic obstacles and stationary objects which are not considered in *path planning* level, will be avoided directly in the path optimization level, see chapter 4.

In order to find the path, the given environment in which the vehicle must move, course, also called workspace can be defined as a set of connected graph in order to find the suitable path. There are several methods such as Dijkstra or A* which find the shortest path in this set of graphs. In the next part, course generation is explained.

3.2 Course generating

When the start and end point is known, a course can be generated with the help of a navigation system or a digital map. In this case some discrete points (x_p, y_p) between start and end point are generated. Then based on these points a discrete path parameter s, can be introduced which describe the travelled distance on the course from start to the end point. These discrete points are used in order to find the road geometrical approximation with cubic spline interpolation formulation. As the interpolation with the points is done piecewise, the travelled distance through the points can be calculated as follows by knowing the x-y coordinates of the discrete points x_p and y_p .

$$s_0 = 0 \tag{3-1}$$

$$s_{k+1} = s_k + \sqrt{(x_{p_k} - x_{p_{k-1}})^2 + (y_{p_k} - y_{p_{k-1}})^2}$$

By using the discrete point x_p and y_p the yaw angle of the course can be defined as:

$$\varphi_k = tan^{-1}\left(\frac{\Delta y_{p_k}}{\Delta x_{p_k}}\right) \tag{3-2}$$

Therefore the center line of the course can be describe with the help of s parameter in the form of cubic spline interpolation as:

$$S_{xp}(s) = x_{cl}(s) = a_x.(s - s_k)^3 + b_x.(s - s_k)^2 + c_x.(s - s_k) + d_x$$

$$S_{yp}(s) = y_{cl}(s) = a_y.(s - s_k)^3 + b_y.(s - s_k)^2 + c_y.(s - s_k) + d_y \tag{3-3}$$

$$S_{\varphi}(s) = \varphi_{cl}(s) = a_{\varphi}.(s - s_k)^3 + b_{\varphi}.(s - s_k)^2 + c_{\varphi}.(s - s_k) + d_{\varphi}$$

In which index cl refers to center line and a, b, c and d are cubic spline interpolation coefficients. Now the equations of the center line of the course are defined which helps to generate graphs on the course which will be used to find the shortest path in path planning level.

3.3 Graph generating

In previous section the course between start to end point is generated. In order to find a valid path on the course there are different methods often used such as *Rapidly-exploring Random Trees* (RRTs) [39] or *Probabilistic RoadMap* (PRM) [40] [41]. In RRTs methods often two trees of valid paths are growing rooted in start and end point by random sampling till they meet in the middle. The direction of the growth can be considered also from start to the end [42] [43]. Another method is *Probabilistic roadmap* which constructs the roadmap by iteratively sampling the workspace randomly. If the sampled point belongs to the free configuration, a node is added. Free configuration is part of workspace, here the course, in which there is no obstacle and forbidden configuration is a part of workspace with obstacle. The generated nodes connect to the existed nodes. A region of connectivity can be defined in which only the nodes situated in a certain distance are connected which helps to save time [44]. If two nodes are connected an edge between the two associated nodes is added to the roadmap. For each individual node, the connection condition for all the present node is checked and this process is repeated after adding a new node. The process of adding node continues till satisfying some stop criteria that usually is when a predefined set of query configuration are inner-connected via roadmap. Figure 3-1 shows the example of *Probabilistic roadmap* in a given workspace. The red points are the nodes and the dotted blue lines are vertices between connected nodes. The black circle shows the connectivity distance for a given node. The PRM and RRT are the efficient methods to find the path in unconstructed environment but this advantage can be a disadvantage for autonomous driving as both of methods develop their vertices and trees in a random way and the probable path between start point to end point may not be desirable for autonomous driving.

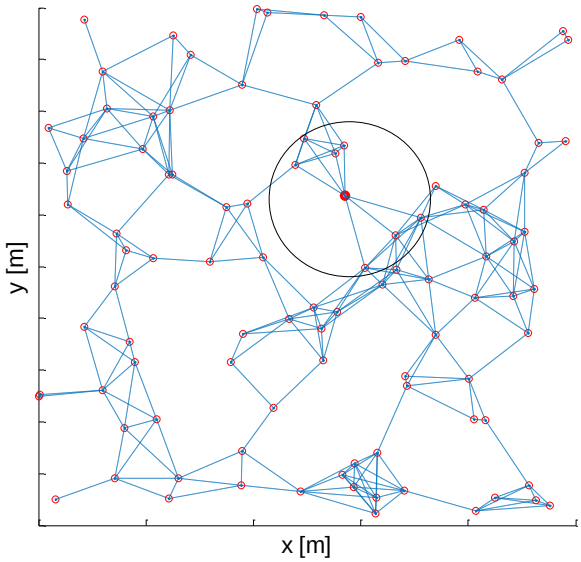

3-1: Probabilistic roadmap

In another hand, there is no guaranty that all the workspace will be covered uniformly. Another important factor which must be considered is to find a path which satisfy also driving fashion. For example an oscillatory path, or a path which is near road boundary when the center line is free is not desirable but they might be valid. As the width of the workspace in the case of autonomous driving is limited to the width of the road in which vehicle must drive, the definition of the nodes can be predefined instead of probabilistic, which also has the advantage of considering all the workspace in a uniform way. Using *Predefined roadmap* instead of *Probabilistic roadmap* offers the possibility to find the path by considering all the workspace uniformly. Choosing a reasonable distance between the nodes helps to generate a smooth path. *Predefined roadmap* has the same generality as *Probabilistic roadmap*, the only difference is that node generation is not random. Generality of both algorithm is explained in the table below.

Figure 3-2 shows the result of *Probabilistic roadmap* and *Predefine roadmap* for a given course of $10m$ and width of $4m$ with the same number of nodes 55, and same connectivity region of $3m$. As it is shown, for this example of *Probabilistic roadmap*, some part of the road are over covered by so many nodes and vertices and some area are not well covered,

as the generation of the nodes are random, unlike the case of *Predefined roadmap* in which all the course area is covered uniformly.

3.4 Shortest Path algorithms

After defining the course in the form of graphs, a shortest path algorithm can be used to find a path. Dijkstra Algorithm is able to find the shortest path from a given node u_{start} to all vertices. In this order for a given graph $G = (V, E)$ consisting of a set of vertices V and a set of edges $E \subset V \times V$, and for each edge $(u, v) \in E$ an associated nonnegative cost $c(u, v)$ which is often the distance of the motion. Dijkstra's algorithm based on [44] definition, works by maintaining for each vertex u the shortest path distance $g(u)$ from the start vertex.

Probabilistic roadmap algorithm	**Predefined roadmap algorithm**

repeat
$\boldsymbol{c} \leftarrow$ a random configuration in $\boldsymbol{\mathcal{C}}$
If $\boldsymbol{c} \in \boldsymbol{\mathcal{C}_{free}}$ **then**
$\boldsymbol{V} \leftarrow \boldsymbol{V} \cup \{\boldsymbol{c}\}$
$\boldsymbol{N} \leftarrow$ a subset of $\boldsymbol{V}$ containing nodes neighboring $\boldsymbol{c}$
for all $\boldsymbol{c'} \in$ N **do**
if $\boldsymbol{dist_{c-c'}} <$ connectivity distance
$\boldsymbol{E} \leftarrow \boldsymbol{E} \cup (\boldsymbol{c}, \boldsymbol{c'})$
until stop criterion is satisfied
	for x =StartPoint **:**Resolution **:** EndPoint
	{
	for y =LowerBoundary**:**Resolution**:**UpperBoundary
	{
	$c(x, y)$
	If $c \in \mathcal{C}_{free}$ **then**
	$V \leftarrow V \cup \{c\}$
	$N \leftarrow$a subset of V containing nodes neighboring c
	for all $c' \in$ N **do**
	if $dist_{c-c'} <$ connectivity distance
	$E \leftarrow E \cup (c, c')$
	}}

Table 3-1: *Probabilistic roadmap* algorithm and *Predefined roadmap* algorithm

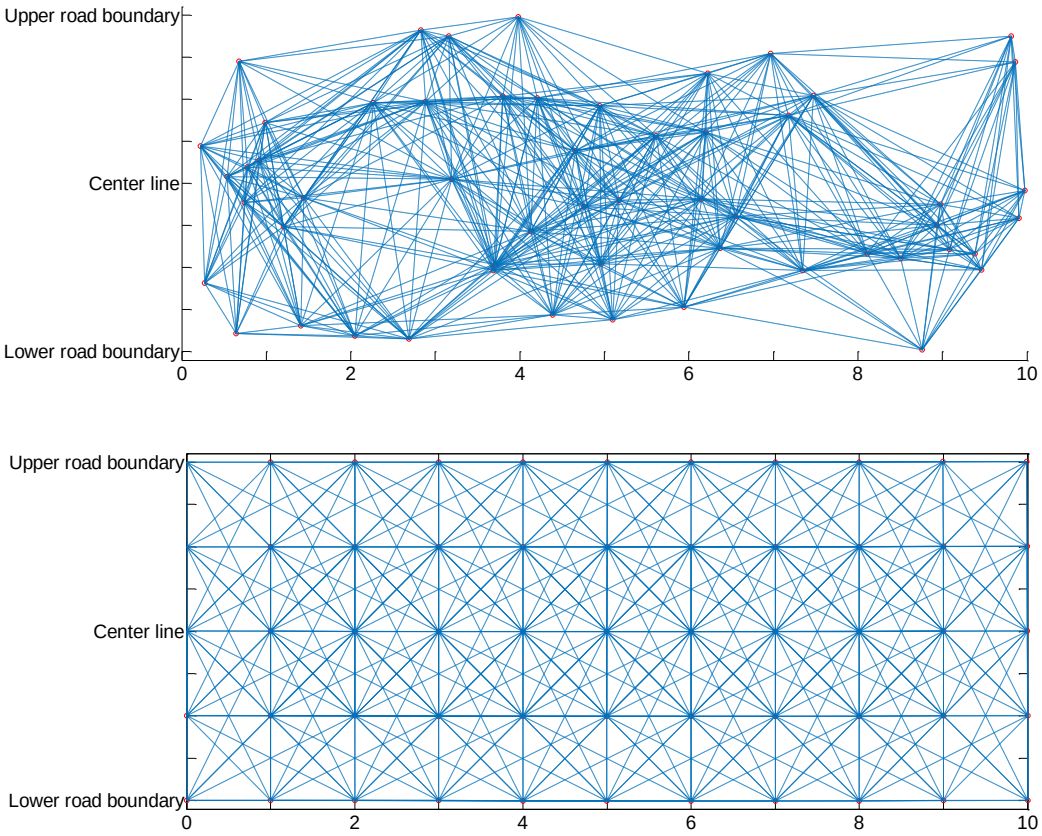

3-2: Probabilistic roadmap (up) vs. Predefined roadmap (down)

Further, a backpointer $bp(u)$ is maintained for each vertex indicating from which neighboring vertex the shortest path from the start comes. Hence, a shortest path to some vertex can be read out by following the backpointers back to the start vertex. Initially, of all vertices the shortest path distance is set to infinity, except for the start vertex whose distance is set zero. From the start vertex, the shortest path distances are propagated through the graph until all vertices have received their actual shortest path distance. To this end, the start vertex is inserted into a priority queue, with a key equal to its shortest path distance (zero in this case). In each iteration of the algorithm, the minimal element u is popped from the priority queue, and of all neighbors of u it is checked whether their shortest path distance can be decreased by changing their backpointer to u. If the distance of some vertex is decreased, it is inserted (or updated) in the priority queue, as it may enable other vertices to decrease their distances. When the priority queue becomes empty,

all vertices are guaranteed to have their actual shortest path distance and correct backpointer associated with it [44].

Another important algorithm is A* which is an extension of Dijkstra algorithm that tries to reduce the total number of edges explored by incorporating a heuristic estimate of the cost to get to the goal point. Therefore instead of finding the shortest path to all the vertices in the graph, it is only interested in a shortest path to a specific goal vertex u_{goal}. In that event a heuristic value $h(u)$ is added to $g(u)$ which is the distance from vertex u to the goal vertex. Both algorithm are explained in the next table.

Dijkstra algorithm	A* algorithm
for all $\boldsymbol{u} \in \boldsymbol{V}$ do	**for all** $u \in V$ do
$\boldsymbol{g(u) \leftarrow \infty}$	$g(u) \leftarrow \infty$
$\boldsymbol{g(u_{start}) \leftarrow 0}$	$h(u) \leftarrow$ distance between u and u_{goal}
Insert $\boldsymbol{u_{start}}$ **into** $\boldsymbol{Q}$	$g(u_{start}) \leftarrow 0$
repeat	**Insert** u_{start} **into** Q
$\boldsymbol{u} \leftarrow$element from $\boldsymbol{Q}$ with minimal $\boldsymbol{g(u)}$	**repeat**
Remove $\boldsymbol{u}$ from $\boldsymbol{Q}$	$u \leftarrow$element from Q with minimal $g(u) + h(u)$
for all neighbors $\boldsymbol{v}$ of $\boldsymbol{u}$ **do**	**Remove** u from Q
if $\boldsymbol{g(u) + c(u,v) < g(v)}$ **then**	**for all** neighbors v of u **do**
$\boldsymbol{g(v) \leftarrow g(u) + c(u,v)}$	**if** $g(u) + c(u,v) < g(v)$ **then**
$\boldsymbol{bp(v) \leftarrow u}$	$g(v) \leftarrow g(u) + c(u,v)$
Insert or **update** $\boldsymbol{v}$ in $\boldsymbol{Q}$	$bp(v) \leftarrow u$
until $\boldsymbol{Q = \emptyset}$	**Insert** or **update** v in Q
	until $u = u_{goal}$ or $Q = \emptyset$

Table 3-2: Dijkstra and A* algorithm

3.5 Path planning results

As in autonomous driving aim is to reach a destination, A* seems to be more permissible algorithm as it finds the path to the goal vertex u_{goal}. Another important factor to take into consideration is drive fashion as not all paths are suitable for autonomous driving although if they reach destination. For example let's consider the case of a stationary obstacle on the middle of the way. A* algorithm will avoid the obstacle by overtaking and after continue till the goal point and it will not return back to center line in order to keep the path as short as possible. This solution is not desirable as the center line is free but in another hand the previous solution is also valid. Figure 3-3 illustrates this situation in which the aim is to travel from start point to the goal and there is a stationary obstacle on the center line as it is shown with black rectangle. The path to avoid this obstacle is found by overtaking the obstacle from right side and it keeps the same trajectory and just before reaching the goal it returns back to center line, which is not desirable because returning back to center line could happen just after overtaking the obstacle. In the figure the path is shown with black line and red dotted line is spline interpolated path in order to make it smooth.

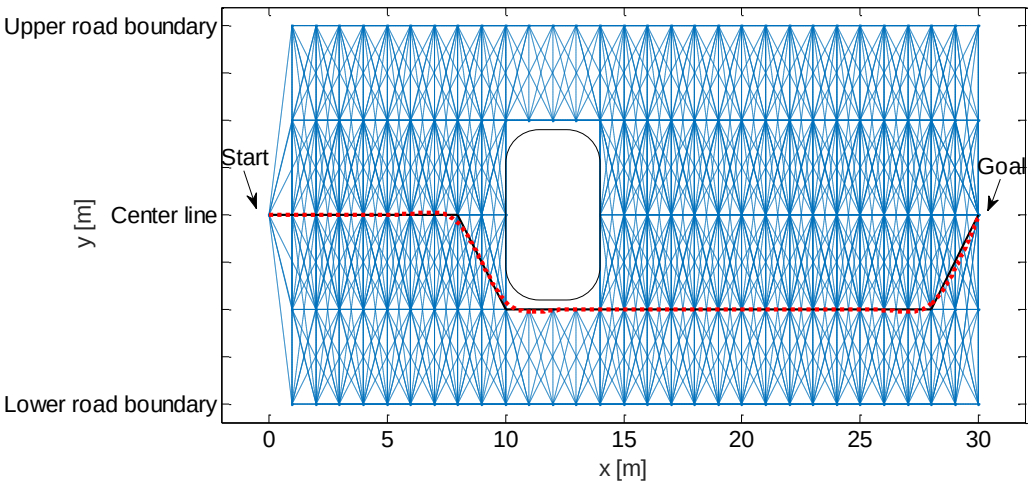

3-3: Path planning with stationary obstacle , A*

In order to solve this problem, another heuristic cost function which is the distance of each node to the center line can be added to the algorithm which solves the previous problem. By adding this last, the nodes which are closer to the center line are preferred. In another hand the shortest path is the path which connect the start node to the goal node by travelling through center line. If the center line is blocked, like previous case, after overtaking the obstacle, the path returns back to the center line. Another advantage of adding the center line heuristic cost to the algorithm is the possibility of multiplying the cost of the nodes which are situated in the lower part of the center line by a factor bigger than one. This multiplication makes the center line heuristic cost asymmetric for the nodes upper and lower of the center line. This multiplication makes the cost of the nodes of the lower part higher, therefore overtaking path is preferred from upper side of the lane which satisfies the urban rules and driving fashion. Figure **3-4** shows the previous problem in which center line heuristic cost is added to the algorithm. As it is shown, the path avoids the stationary obstacle from upper part of the road and after overtaking the obstacle, it returns back to the center line.

Another critical situation which could happen in urban situation is when multiple obstacles exist on the road, for example case of road construction in which the both sides of the road are blocked and a narrow course exists between them.

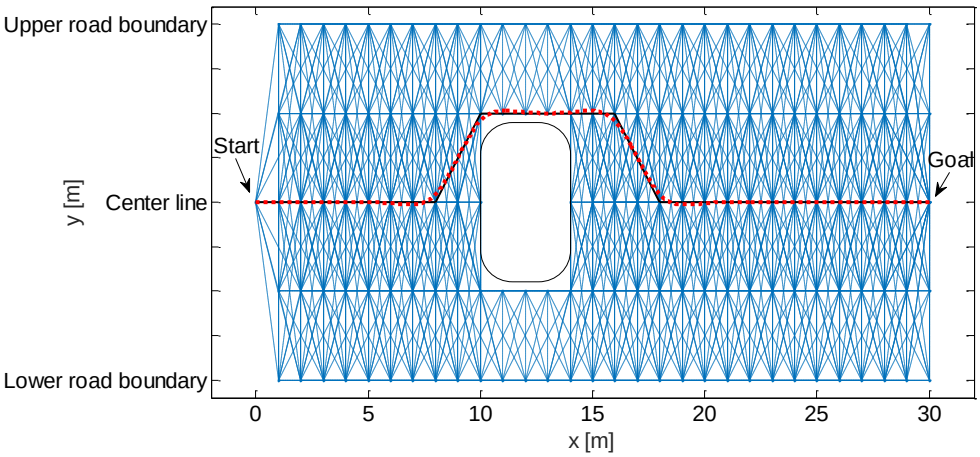

3-4: Path planning with heurisitic center line cost

This situation becomes more critical when it occurs while cornering. Figure 3-5 illustrates this situation in which at beginning of the road there is a stationary obstacle on the straight part of the road which is over taken by left maneuver and after entering the right turn there are two stationary obstacles and narrow space between them is used to overtake both obstacles. After over taking each obstacle the path return backs to the center line. Calculation time of shortest path algorithms depend on the number of nodes and vertices. A big workspace with thousands of nodes and vertices only need few millisecond. For example simulating scenario of figure 3-4 with 150 nodes and more than 2000 vertices required only $5ms$.

3.6 Initial solution for path optimization level

As explained in the introduction of this chapter, the aim of path planning level is to generate an initial solution for path optimization level as the quality of the optimization result depends on the initial solution. Based on the results of the path planning and a simple kinematic vehicle model, required steering angle velocity $\dot{\delta}$, can be found. In this model the effect of slip angle is ignored which is suitable for simple courses but when the course is more complicated due to vehicle dynamics the effect of slip angle is significant, but the solution based on simple kinematic model can be used as a rough initial solution.

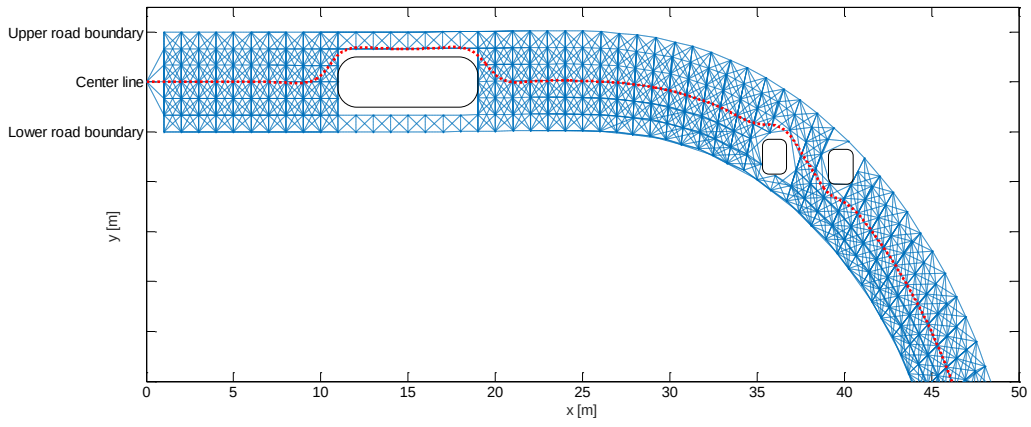

3-5: Path planning in a complicated senario

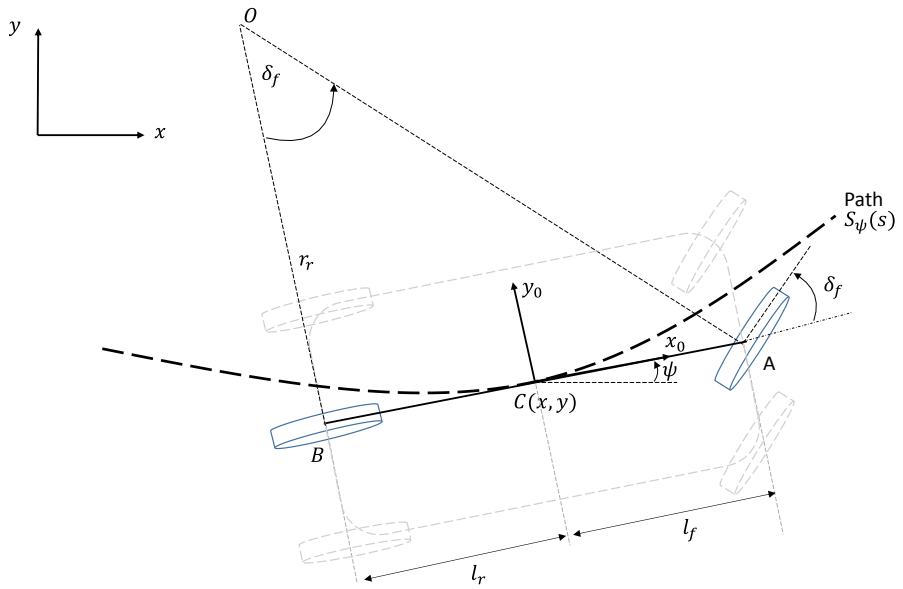

3-6: Simple kinematic vehicle model used to find initial solution

As it shown in figure 3-6 a given constant steering angle δ_f leads the vehicle along a circular path with radius r_r around the point o. By using the geometry calculation the corresponding steering angle velocity can be found as [45]:

$$\delta_f(s) = tan^{-1}\left(\frac{l_f + l_r}{r_r(s)}\right) \qquad 3\text{-}4$$

The inverse radius of the curve, called also curvature K is defined as:

$$\frac{1}{r_r(s)} = K(s) = \frac{\partial\psi(s)}{\partial s} \qquad 3\text{-}5$$

As the path is defined, the path yaw angle can be used to calculate corresponding steering angle as:

$$\delta_f = tan^{-1}\left(\left(l_f + l_r\right).\acute{S}_\psi(s)\right) \qquad 3\text{-}6$$

in which $\acute{S}_\psi(s) = \frac{\partial s_\psi(s)}{\partial(s)}$.

As the valid velocity for the given course can be known via digital map or navigation system, the initial solution for the driving force can be conducted based on this velocity for known load of the vehicle in the form of:

$$F_D(s) = F_L(s, v_0) \qquad 3\text{-}7$$

3.7 Conclusion

The concept of the path planning level explained in this chapter can be illustrated by figure 3-7 in two different levels. The first level called *route planning* provides the information about the center line of the course from starting point to the goal. As the information about the stationary obstacle such as any blockage on the road due to the road construction may be available via digital map or navigation system, a second level called *path planning* is added which first generates graphs on the road and by considering the stationary obstacles finds the shortest path from start point to the goal by avoiding the obstacles by using shortest path algorithm like A*.

Based on the path found in *path planning* level and by using a simple vehicle kinematic model corresponding steering angle velocity and driving force of the path is calculated which will be used as an initial solution in the path optimization level which will be explained in the next chapter.

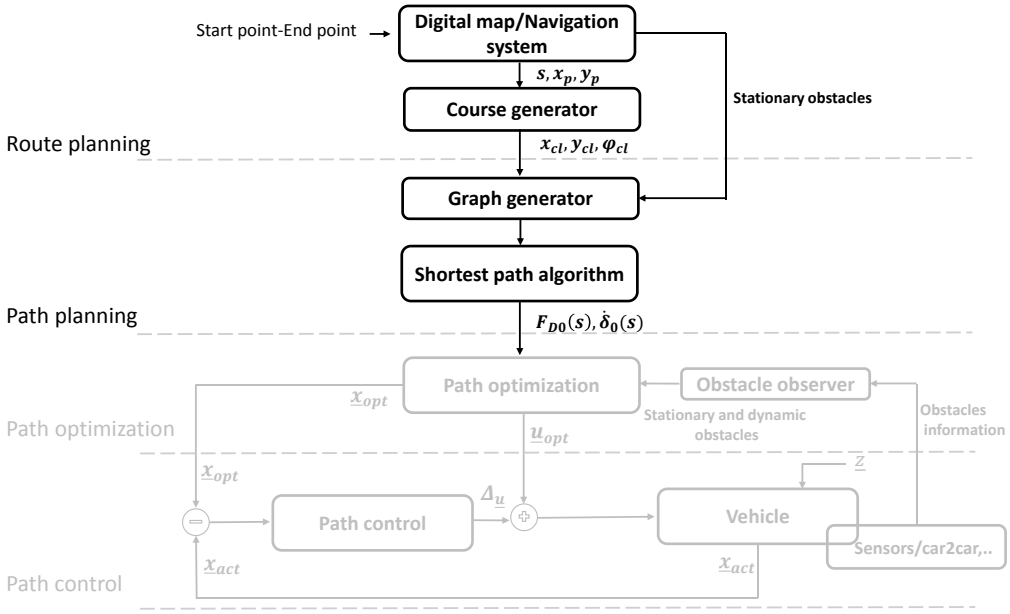

3-7: Path planning general concept

4 PATH OPTIMIZATION LEVEL

4.1 Introduction

In previous chapter path planning level is explained, on that level the shortest path connecting the start point to the end point by considering some criteria's such as collision avoidance with static obstacles is found and based on a simple kinematic vehicle model the inputs of the system based on this path are found. These inputs will be used in the path optimization level as the initial solution of the system. The goal of this level is to find a path which is optimal for different objectives such as energy consumption or comfort by considering the vehicle dynamics. In that event an optimal control problem *OCP*, based on vehicle dynamic model is designed. An optimal control problem includes a cost function J, which is a function of states, control variables or both. The optimal control problem is solved with a Sequential Quadratic Programming *SQP*, solver. In this chapter the construction of the optimal control problem, definition of the objective function and moving horizon approach and its effect is explained.

4.2 Optimal control problem

In chapter 2, dynamic model of vehicle is described with ordinary differential equations, *ODE*. As explained, driving force F_D, and steering angle velocity $\dot{\delta}$, are inputs of the system. The aim of path optimization is to find these parameters which allow leading vehicle on an optimal path. In order to find these parameters, an optimal control problem *OCP*, must be solved in which, driver is modeled as a penalty function and the vehicle as the dynamic model. In that event, as the vehicle model is nonlinear, Sequential Quadratic

Programming *SQP*, as one of the most effective methods for nonlinear constrained optimization is used [46]. NLPQLP solver, solves the nonlinear programming problems by a *SQP* algorithm. This solver is developed by K.Schittkowski [47] which is a Fortran implementation. The transformation and reformulation of the optimal control problem to the NLPQLP format is explained in Schmidt [48] but as it is the base of the path optimization level, the main part are repeated here briefly.

The optimization problem is given as:

$$\min_{\underline{x},\underline{u}} J(\underline{x}(t_f), \underline{u}(t_f)) \tag{4-1}$$

with dynamic system and nonlinear constraints:

$$\dot{\underline{x}} = f(\underline{x}, \underline{u}) \tag{4-2}$$

$$g_l \leq g(\underline{x}, \underline{u}) \leq g_u \tag{4-3}$$

as well as states and inputs restrictions:

$$\underline{X_l} \leq \underline{x} \leq \underline{X_u} \tag{4-4}$$

$$\underline{U_l} \leq \underline{u} \leq \underline{U_u} \tag{4-5}$$

The equation 4-2 represents the dynamic of the system, in our case vehicle model of equation 2-31 or 2-37 can be used. Index l and u in equations 4-3, 4-4 and 4-5 refer to lower and upper value respectively. As the equation 4-1 shows the objective function consider the states and inputs at the end of time interval t_f. Therefore to deal with the objective function with the integration part, the objective function can be rewritten as:

$$J(\underline{x}, \underline{u}) = J\left(\underline{x}(t_f), \underline{u}(t_f)\right) + \int_{t_0}^{t_f} f_J\,(\underline{x}(t), \underline{u}(t))dt \tag{4-6}$$

in which the additional integral part can be added as a state of the system as:

$$\dot{x}_J = f_J\,(\underline{x}(t), \underline{u}(t)) \tag{4-7}$$

Optimization problem is formulated in NLPQLP as:

$$\min_{\underline{p}} J(\underline{p}) \tag{4-8}$$

with equality and inequality constraints as:

$$\underline{g}_e(\underline{p}) = 0 \tag{4-9}$$

$$\underline{g}_i(\underline{p}) \geq 0 \tag{4-10}$$

as well as parameter limitation as:

$$\underline{p}_l \leq \underline{p} \leq \underline{p}_u \tag{4-11}$$

$J(p)$ is objective function with the vector p that is the free parameter vector. These parameters can be limited, equation 4-11, in the range of $\underline{p}_l$ and $\underline{p}_u$ which represent lower and upper limitation boundaries. Set of equality and inequality equations can be defined in the form of equations 4-9 and 4-10. To solve the ordinary differential equations, *ODEs* of the optimal control problem numerically, an explicit Runge-Kutta method is used, in which the states of the system at future time is calculated from the states of the system at current time, therefore the states of the system can be defined as follows:

$$\begin{aligned} \underline{x}_1 &= f_{RK}(\underline{x}_0, \underline{u}_0) \\ \underline{x}_2 &= f_{RK}(f_{RK}(\underline{x}_0, \underline{u}_0), \underline{u}_1) \\ &\vdots \\ \underline{x}_n &= f_{RK}(f_{RK} \dots f_{RK}(\underline{x}_0, \underline{u}_0), \underline{u}_1, \dots, \underline{u}_{n-1}) \end{aligned} \tag{4-12}$$

In equation 4-12 the current states are a result of previous states and inputs and f_{RK} refer to the Runge-Kutta function. Now the stack vector for the states $\underline{x}$ and inputs $\underline{u}$ can be defined as follows:

$$\underline{X} = \begin{bmatrix} \underline{x}_0 \\ \underline{x}_1 \\ \vdots \\ \underline{x}_n \end{bmatrix}; \quad \underline{U} = \begin{bmatrix} \underline{u}_0 \\ \underline{u}_1 \\ \vdots \\ \underline{u}_{n-1} \end{bmatrix} \tag{4-13}$$

Nonlinear system of equation can be written as:

$$\underline{X} = F(\underline{U}) \tag{4-14}$$

This means, with known initial states, all system states can be described as a function of the input variables. So the resulting free variables $\underline{p}$ are just the system inputs $\underline{U}$. Knowing that ($\underline{U} \equiv \underline{p}$) we can start transforming the problem.

$$J\left(\underline{x}(t_f), \underline{u}(t_f)\right) = J(\underline{X}, \underline{U}) = J(F(\underline{U}), \underline{U}) = J(\underline{U}) = J(\underline{p}) \qquad 4\text{-}15$$

The restriction of input variables is already considered in equation 4-11, to consider the restriction of the states as equation 4-16,

$$\underline{X}_l \leq \underline{X} \leq \underline{X}_u \qquad 4\text{-}16$$

Equation 4-16 can be written in the form of inequality of 4-10 as:

$$-F(\underline{U}) + \underline{X}_u \geq 0$$
$$F(\underline{U}) - \underline{X}_l \geq 0 \qquad 4\text{-}17$$

In the same way, we can handle the additional nonlinear constraints as:

$$-G(F(\underline{U}), \underline{U}) + \underline{G}_u \geq 0$$
$$G(F(\underline{U}), \underline{U}) - \underline{G}_l \geq 0 \qquad 4\text{-}18$$

The formulation of 4-17 and 4-18 offer the possibility to consider the inequalities as the equation 4-10 inside optimal control problem. Considering inequalities in this form in the optimal control problem has the advantage to be checked in each iteration in order to find the control values which satisfy the inequality. In another hand the parameters considered in these inequalities form must be exact in each iteration. As the formulation of the inequalities shows, the validity is only when the inequalities is satisfied, otherwise the solution is invalid and a new solution which satisfies the inequalities must be found. This kind of inequality constraints are called *hard constraints*. The disadvantages of these kinds is when the solution of the optimal control problem results in the border of validity-invalidity. The solution in this case may be again near the border of validity-invalidity which is not suitable as it require more iterations. Let's imagine the case of a vehicle which drives in a course with a given road width. In this case a solution near street width

border is valid but is not desirable. A way to solve this kind of problem is to present a new type of the constraint named *soft constraints*. In this form, the optimal control problem is formulated without any nonlinear constraints, instead the constraints are added to the objective function in form of penalty functions. The advantage of the *soft constraint* is that the optimal solution of the objective function also satisfies the nonlinear inequality constraints. Another advantage of the *soft constraints* is that the border of validity-invalidity is not sharp as *hard constraints* and a security margin can be considered. Let's consider a parameter that must be restricted in a given boundary as:

$$lower\ boundary \leq x \leq upper\ boundary \qquad 4\text{-}19$$

Soft constraint for this parameter can be presented as a simple quadratic form as it shown in figure 4-1 with blue dashed line. The *hard constraint* is shown with black line for the given boundaries. The problem of the quadratic kind of *soft constraint* is that results to center of allowed range. As an example, if the road width boundary is presented by quadratic *soft constraint*, it results to keep the vehicle in the center line as moving far from the center line increases the cost of penalty function. Another way to present the soft constraints is to define a margin of the constraint, and the penalty function grows in a quadratic form after this margin as it is shown in figure 4-1 with orange dotted line.

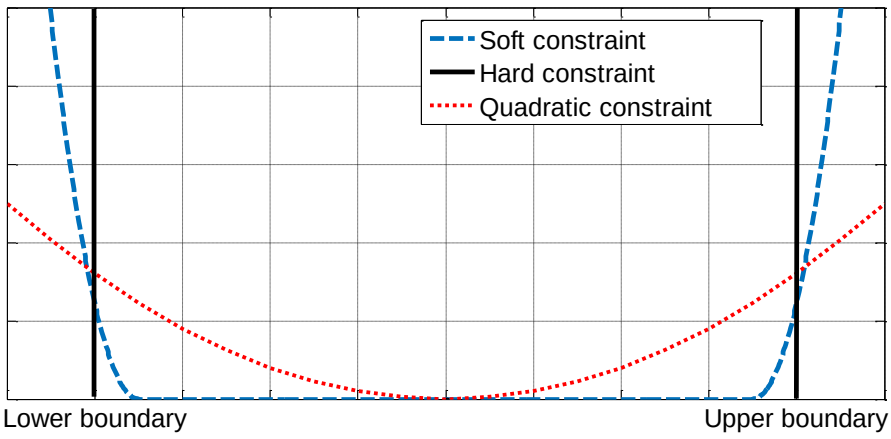

4-1: Hard constraint vs. Soft constraint

Restriction and limitation of autonomous driving must be taken into account in optimal control problem. The restrictions are mostly imposed by vehicle construction and vehicle dynamics. As the final aim is to validate the results with a rebuild buggy car, figure 1-4 , the restrictions such as maximum-minimum applicable steering angle and control inputs restriction such as the maximum torque applicable on vehicle motors and maximum steering angle velocity must be taken into account based on the restriction on the vehicle. Respecting the road width in order to keep the vehicle inside the permissible road width is another important constraint which depends on the road geometry. Urban rules and driving fashion impose another sort of restrictions, such as left side overtaking, respecting forehead distance, urban/highway velocity limitation and much more. All of this restriction can be added to the objective function in the form of soft constraints. But increasing the number of *soft-constraints* in the form of penalty function in objective function can influence the main objective function, therefore taking into consideration of each soft constraint with a given weight as impact factor is critical.

Figure 4-2 shows the interaction between optimal control of *ODE* and the optimal solver NLPQLP. As it is shown at top level the nonlinear optimal control and restriction and limitation are defined. Then the objective function, the actual solution of the constraint equations and the gradient of objective function and the constraints are passed to the NLPQLP solver. These gradient values will make the Jacobian matrixes of the Lagrangian function. The calculation of the Hessian of the Lagrangian is done inside the NLPQLP. Based on these information the first iterative solution is generated. This solution will be used to reproduce the new objective function value, the new constraints value and their gradients which will be used to find the next iterative solution. This process will be repeated till that one of the ending conditions will be satisfied such as finding the optimal solution or reaching the maximum number of iteration. In the first case the output will be the solution and in the second case the corresponding error code.

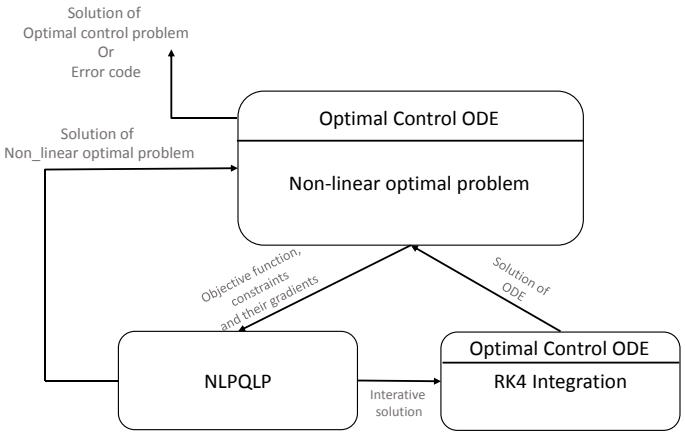

4-2: Interaction between OCODE and NLPQLP solver

The native optimal solver of NLPQLP is a Fortran implementation which was used in the first stage of the work, see [48], but to make it more compatible with another software platform such as communication part, the code was converted in C and the optimal control problem is developed as a C++ platform.

4.3 Moving-Horizon approach

Complicated structure and also high length of the course make the optimal control problem numerically difficult to solve and also require high computational time. A possibility to deal with this problem is using Moving-Horizon approach, *MHA* [49]. In this approach, the global optimization problem covering the complete driving task is portioned into several local optimal sub-problems of τ second named horizon, which are comparatively easier to solve. Local optimal control problem structure is similar to global problem just that not the whole course is considered. Also in real driving scenario, the driver has a limited information about all the road and knows only about ahead road. Moving-horizon approach also update the optimal control problem by saving the solution for a part of problem, ξ ,named increment as a portion of horizon, and used it as the

starting point for the next optimal sub-problem. This last offers the possibility to update the control problem and taking into consideration outside influences such as other vehicles and obstacles promptly in the optimization problem, equation 4-8. Figure 4-3 shows the general concept of moving horizon approach in which the optimal control problem is solved for a horizon τ whch is from t_n to $t_n + \tau$. Then a part of this solution, is saved, the optimal control problem is updated and a new problem from t_{n+1} to $t_{n+1} + \tau$ will be solved. In the figure the time step which is used to solve the *ODE* is shown as Δt. The time step Δt defined as a portion of the horizon τ.

$$\Delta t = \frac{\tau}{n} \qquad 4\text{-}20$$

As it explained above, updating the problem offers the possibility to consider external events such as existence of another vehicle on the road or an obstacle but the number of optimal control sub-problems which must be solved to drive the given course also increase which means more calculation time. Therefore choice of a suitable horizon and increment is critical to have the advantage of being real-time and fast rate of update. The choice of these parameters is explained in section 4.4.2.

4.4 Path optimization for autonomous driving

Single track model 2-31 or double track model 2-37 with the linear tire model 2-10 can be used to describe the dynamic system inside optimal control problem 4-2. The vehicle is controlled by steering angle velocity $\dot{\delta}$ and driving force F_D. As the driver is considered as a penalty function, the definition of the objective function defines the covered path. The definition of the objective function plays very important role on the vehicle behavior. Hence the objective function definition is a crucial step.

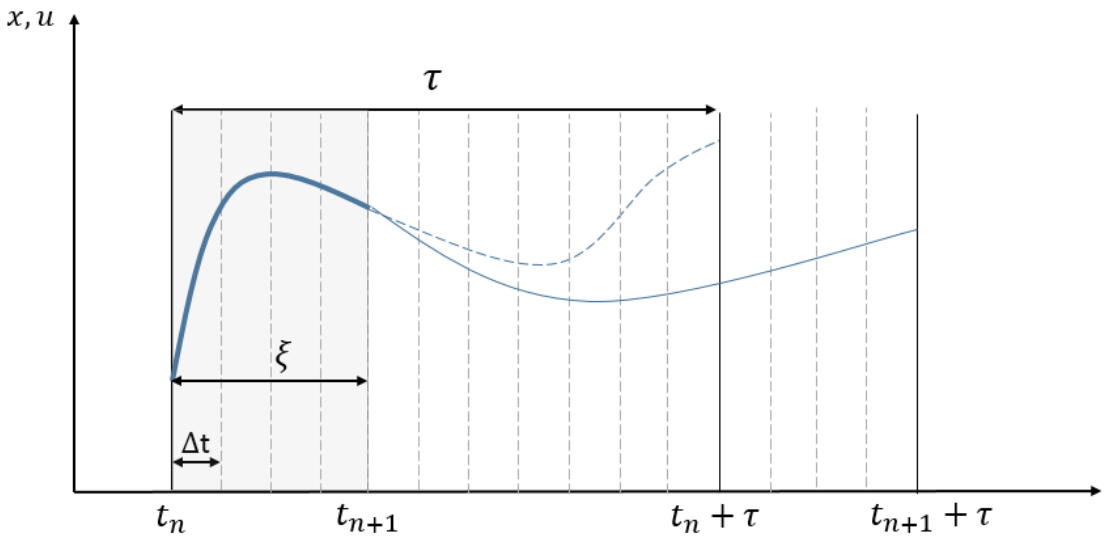

4-3 : Moving Horizon Approach concept

Travelling from start point to the goal point is the main task in autonomous driving. In that event, the optimal control inputs must be found in this order. Minimizing the distance from starting point to the goal point may result in high acceleration and high velocity which is not always desirable. In another hand it can be dominant part of the objective function and reduce the effect of another parts. As the travelled distance based on the center line of the track is already known (see chapter 3), can be concluded that in order to minimize the distance to goal, the subtraction of vehicle travelled distance at the end of horizon from the travelled distance at beginning of the horizon can be used.

$$J(\underline{x}, \underline{u}) = -R_S.\,[s(t_n + \tau) - s(t_n)] \qquad 4\text{-}21$$

Another important constraint to take into consideration is the road width boundary in order to keep the vehicle inside the road permissible width. To apply this constraint in the optimal control problem the distance of the vehicle from course center line must be calculated. Introducing a path parameter θ as the travelled distance of the vehicle which is an extension of the nonlinear state space model of the vehicle 2-31 allows to describe the road with the help of splines when the road geometry is known in dependence of θ (see section 3.2) and gives an easy way to introduce the problem of compliance with the

road width boundaries restriction to the optimization problem as a soft constraint penalty function.

$$\theta = \int_{t_0}^{t_f} v \, dt \tag{4-22}$$

With a given centerline of the track:

$$x_{cl} = f_x(\theta) \tag{4-23}$$

$$y_{cl} = f_y(\theta) \tag{4-24}$$

$$\varphi_{cl} = f_\varphi(\theta) \tag{4-25}$$

Index cl means center line. Equations 4-23, 4-24 and 4-25 present the position and orientation of the center line of the track in the global coordinate system for vehicle given position. In order to keep the vehicle in road permissible width, it is important to calculate the actual lateral distance $a(\underline{x}, \theta)$ of the vehicle from the tracks center line as follows:

$$a(\underline{x}, \theta) = -sin(\varphi_{cl}(\theta)) . (x_{cl}(\theta) - x_{vhcl}) + cos(\varphi_{cl}(\theta)) . (y_{cl}(\theta) - y_{vhcl}) \tag{4-26}$$

The index $vhcl$ refers to vehicle. The restriction to keep the vehicle inside the permissible road width can be formulated as a nonlinear state constraint as:

$$lrb(\theta) < a(\underline{x}, \theta) < urb(\theta) \tag{4-27}$$

urb and lrb mean upper and lower road width boundary respectively. Penalty function based on equation 4-27 keeps the vehicle in the road boundary but having a deviation on the upper part or lower part of the track is possible which is not desirable. In real driving scenario keeping the center line is preferable by having the freedom to move within the lane for example while avoiding an obstacle. Another important factor as a traffic rule about road is to consider that the overtaking maneuver must be done from left side. Hence reducing the cost on the left side of the road on the penalty function results in not symmetric penalty cost on the left side and the right side of the lane, therefore overtaking from left cost less. Road boundary penalty function can be written as:

$$J_{RB}(\underline{x},\underline{u}) = \int_{t_n}^{t_n+\tau} R_{RB}.f_{RB}\left(a(\underline{x},\theta),urb(\theta),lrb(\theta)\right) + \int_{t_n}^{t_n+\tau} R_{CL}.\ a(\underline{x},\theta)^2 d_t$$
$$+ R_{LP}.f_{LP}\left(a(\underline{x},\theta),urb(\theta),lrb(\theta)\right) \qquad 4\text{-}28$$

In which R_{RB}, $R_{CL}$and R_{LP} are the weight factor of the function to keep the vehicle inside the road width boundary, function to keep the vehicle in the center line and function of left side maneuver priority respectively. To consider the effect of each function properly the weights factor must be chosen in this order:

$$R_{RB} \gg R_{LP} \gg R_{CL} \qquad 4\text{-}29$$

Figure 4-4 shows the road boundary penalty functions, in which center line penalty function is shown with dotted blue line, road width boundary penalty function is shown with dashed red line, left side maneuver priority penalty function is shown with dash-dot orange line and global road boundary penalty function is shown with black line.

The vehicle behavior also by considering the restriction and limitation could be not desirable in comfort matter by passenger. Lateral and longitudinal high acceleration may result in passenger discomfort. Therefore to increase the comfort they must be minimized, here comfort is more considered as point of lateral acceleration, hence longitudinal acceleration can be considered in the same way.

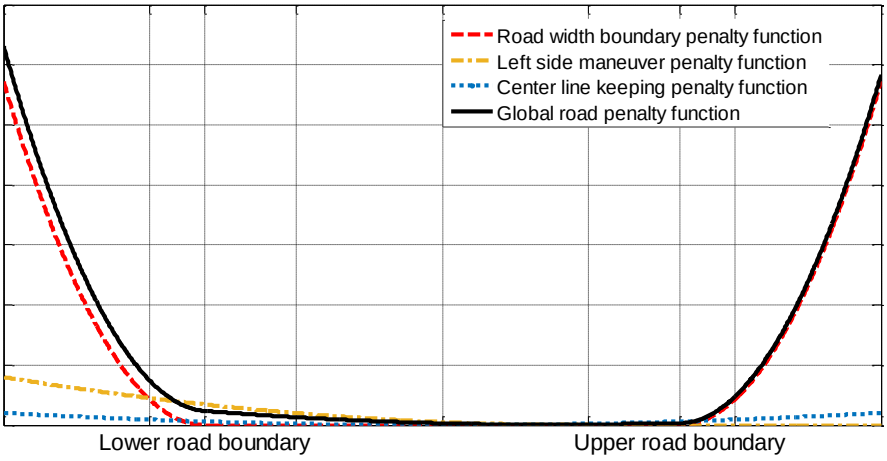

4-4: Road boundary penalty functions

As it is explained in introduction, one of the reason to focus on autonomous driving is energy efficiency. Reducing congestion cost can be considered as the main issue, but travelling in an efficient way by minimizing the energy consumption is an important issue too. Hence the choice of the objective function $J(\underline{x},\underline{u})$ must satisfy this last. Driving Force F_D as a measurement of consumed energy can be used in order to make the energy use efficient.

$$J(\underline{x},\underline{u}) = \int_{t_0}^{t_f} \underline{F_D}^T . R_F . \underline{F_D} + \int_{t_0}^{t_f} a_y . R_{ay} . a_y \qquad 4\text{-}30$$

R_F and R_{ay} are weight matrixes of force penalty function and lateral acceleration penalty function respectively. Equation 4-31 results in maximum travelled distance with minimum force and lateral acceleration by keeping the vehicle within the permissible road boundary.

$$J(\underline{x},\underline{u}) = -R_S.[s(t_n+\tau) - s(t_n)] + \int_{t_0}^{t_f} \underline{F_D}^T . R_F . \underline{F_D} + \int_{t_0}^{t_f} a_y . R_{ay} . a_y + J_{RB}(\underline{x},\underline{u}) \qquad 4\text{-}31$$

Another restrictions such as minimizing the longitudinal acceleration, or minimizing steering angle or steering angle velocity or limitation on velocity can be added to the objective function in the form of penalty functions.

4.4.1 Choice of vehicle model

In chapter 2, two different vehicle dynamic models are explained, single track model and double track model with four different motors. As the equations of the motion 2-31 and 2-37 show, linear single track model has less complexity due to linearization comparing to the double track model. As the dynamic model in single track model is linearized for small wheel slip angle α and steering angle δ, it can be expected that this model does not fit for bigger value of α and δ with double track model. Therefore in this case double

track model is more reliable. Another fact to consider is the complexity of double track model due to the high number of inputs and also nonlinearity of the model, hence more calculation time for this model is expected. In order to choose one of these models for further development of the project, both are implemented in optimal control problem, equation 4-8, and results of both models are shown for a simple turn maneuver. In both, objective function definition is to respect the road width boundary, keeping velocity 5.8 $^{m}/_{s}$, minimizing driving force and maximizing travelled distance. Figure 4-5 illustrates the vehicle position for both model for the given objective function. As it is shown in the same figure and figure 4-6 due to the lateral forces as the result of tire slip angles, double track model needs more forces while cornering comparing to single track model to compensate the effect lateral force and keep the velocity. Tire slip angles for both models are shown in 4-6 and as it is shown due to different tire slip angles in each wheel, double track model generates different forces.

Another important fact to consider is calculation time needed to find the optimal solution for both model. For the given scenario double track model needs around 6 times more calculation time as it has bigger *ODE* system which require more integration time and also nonlinearity of the system makes the optimal control problem more complicated. Linearization done on single track model results on not accurate value for lateral forces which can be seen while cornering in previous scenario. In another hand double track model due its nonlinearity requires more calculation time comparing to single track model. As being real-time is critical in autonomous driving, single track model satisfy time criteria as it is faster than double track model. And to compensate the lack of accuracy and also compensate the external disturbances a path control level will be added which will be explained in chapter 6.

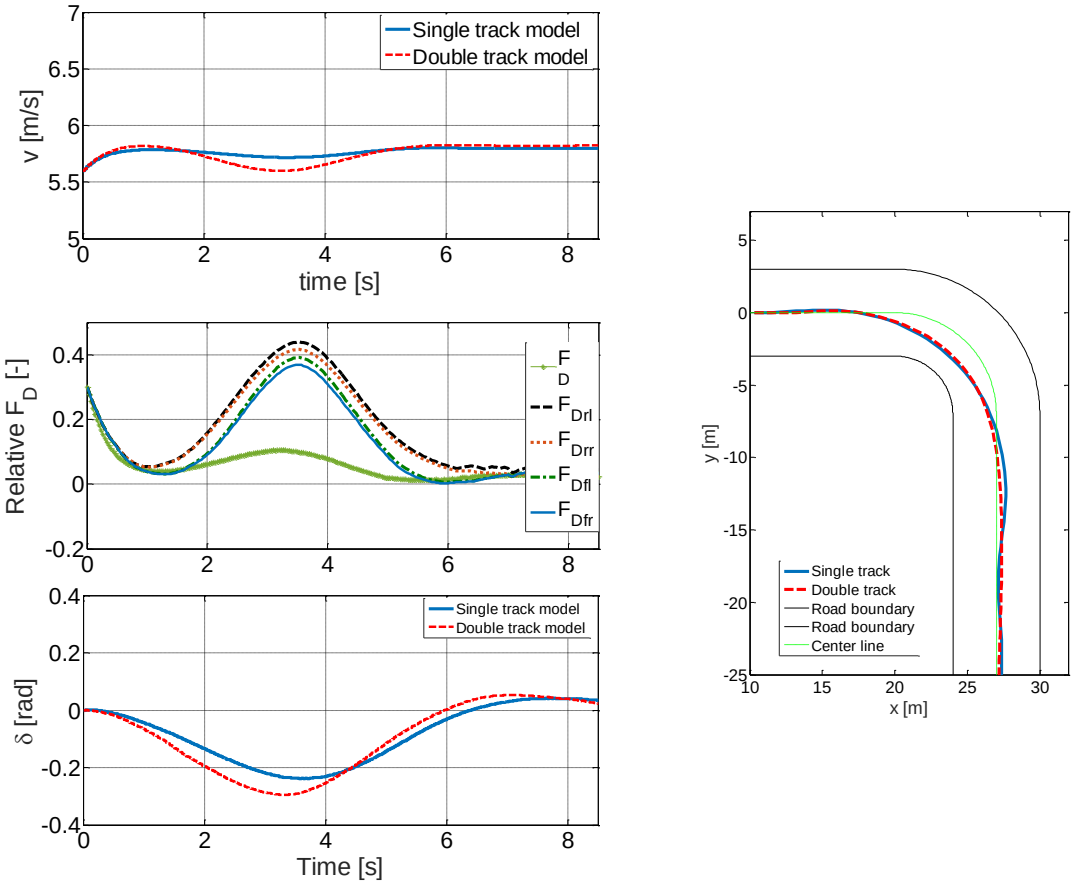

4-5: Single track model vs. Double track model. Left up: velocity. Left middle: Relative driving force. Left down: Steering angle. Right: Vehicle position

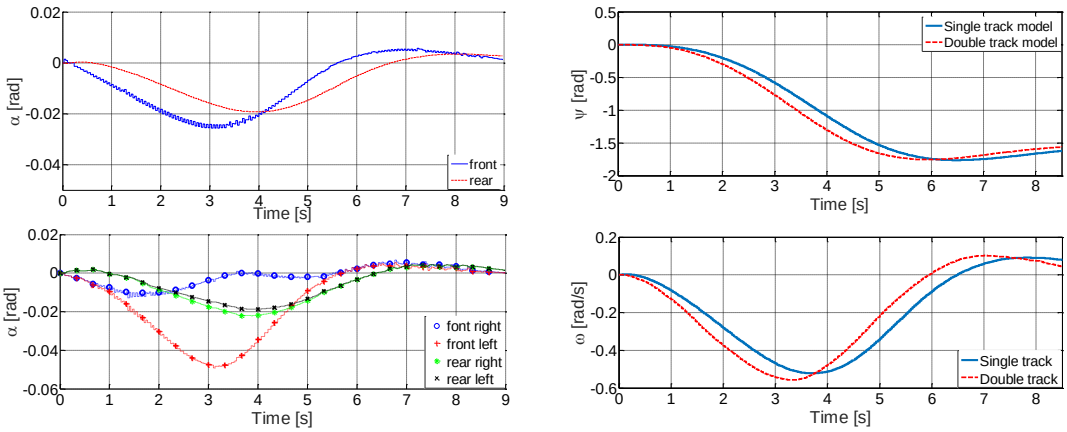

4-6: Single track model vs. Double track model. Left up: Tire slip angles for single track model. Left down: Tire slip angles for double track model. Right up: Yaw angle. Right down: Yaw angle velocity

4.4.2 Moving-Horizon parameters

Before showing the result of path optimization, the choice of moving horizon parameters, τ and ξ, must be justified. In that event, based on the simple straight line driving scenario, the effect of each parameter is explained in figure 4-7. In this scenario aim is to travel 100 m with the fix velocity of 6.5$^{m}/_{s}$. The figure shows the effect horizon τ and increment ξ on calculation time. The different horizon are shown on the *x*-axis and the relative calculation time on *y*-axis. The same experiment is repeated for different increments ξ. Integration time Δt for each experiments is $\frac{1}{20}$ of the horizon τ. Although the increment as a part of horizon is time portion, but here to make it more readable and avoid floating point, is shown as a percentage of the horizon. As it is also clear in the figure, the higher value of increment means higher rate of update and result in more calculation time as more optimization problem must be solved. In another hand slow rate of update is not desirable as the road dynamics must be taken into account. Horizon as the "range of view" must not have a small value in order to consider the forehead events. To consider the forehead events, and be able to consider the dynamics of the road inside the optimization problem a big horizon value and small increment must be chosen. Another important issue to take into consideration is being real-time. Therefore the parameters must be selected in the way that also satisfy this last. In figure 4-7, the required time to drive the given scenario based on the length of the course and vehicle velocity is shown with dashed black line hence all the combination of the horizon and increment which are above this line result in a real-time calculation.

Calculation time, based on the computer in which the optimal control problem is solved and the way in which the problem is implemented can be changed. Therefore in figure 4-7 aim is only to show the general effect of moving horizon parameter on calculation time of a given problem.

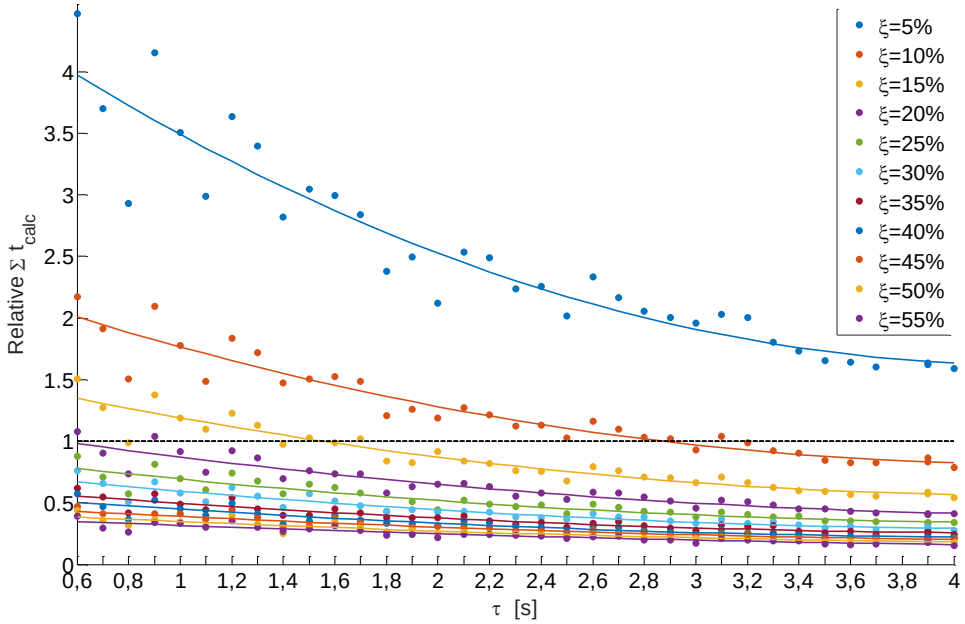

4-7: Relative calculation time for different horizon τ and increment ξ

More efficient implementation of the problem by using parallelization reduce dramatically calculation time. With parallelization of the code and implementation on 3.50 GHz CPU, a horizon of $5s$ and increment of $\xi = 10\%$ can be solved in the range of 50 to 100 ms based on the complexity of the problem which satisfy real time criteria.

4.4.3 Path optimization results

To show the results of path optimization, different test course can be used [50] [51] [34] but in order to make it more realistic, an urban situation with straight line driving, square turning and a sharp turning is chosen as it is shown in figure 4-8. The aim is to drive from starting point and reach maximum urban velocity of 14 $^{m}/_{s}$ and keep the lateral acceleration small in order to increase comfort. All the constraints such as road width boundary, maximum velocity and lateral acceleration are introduced to the optimal control problem in the form of soft constraints. Blue line in figure 4-8 shows the position of the vehicle, as it shown in figure 4-9 down-right, the velocity of the vehicle before square and left turning is reduced in order to keep the lateral acceleration small and after

it increases again to the given velocity, see 4-9 down-left. Up-left and up-right show the vehicle slip angle β, and steering angle δ, respectively.

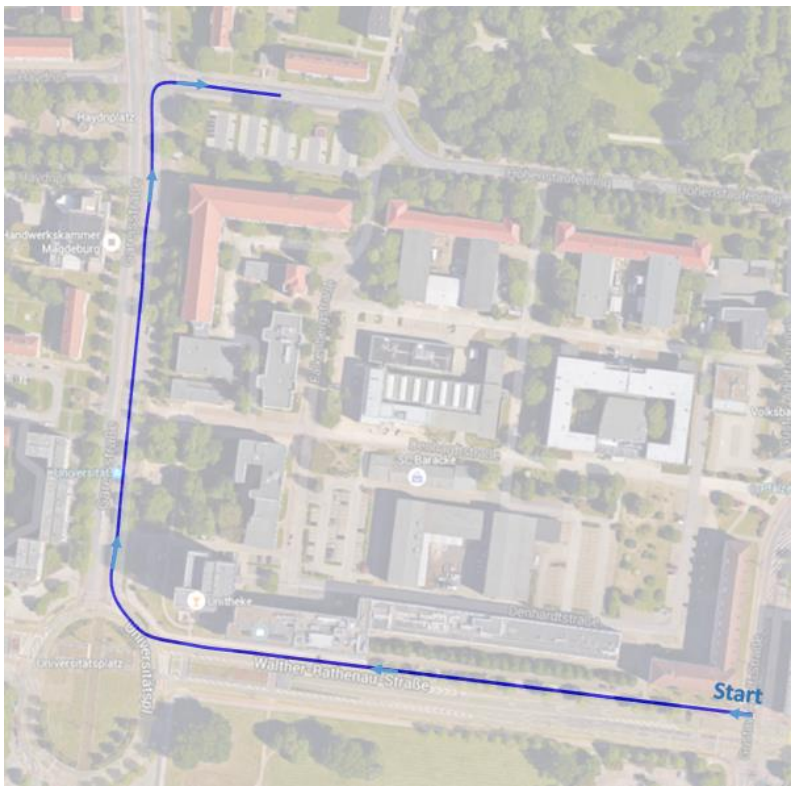

4-8 : Urban scenario test course for path optimization

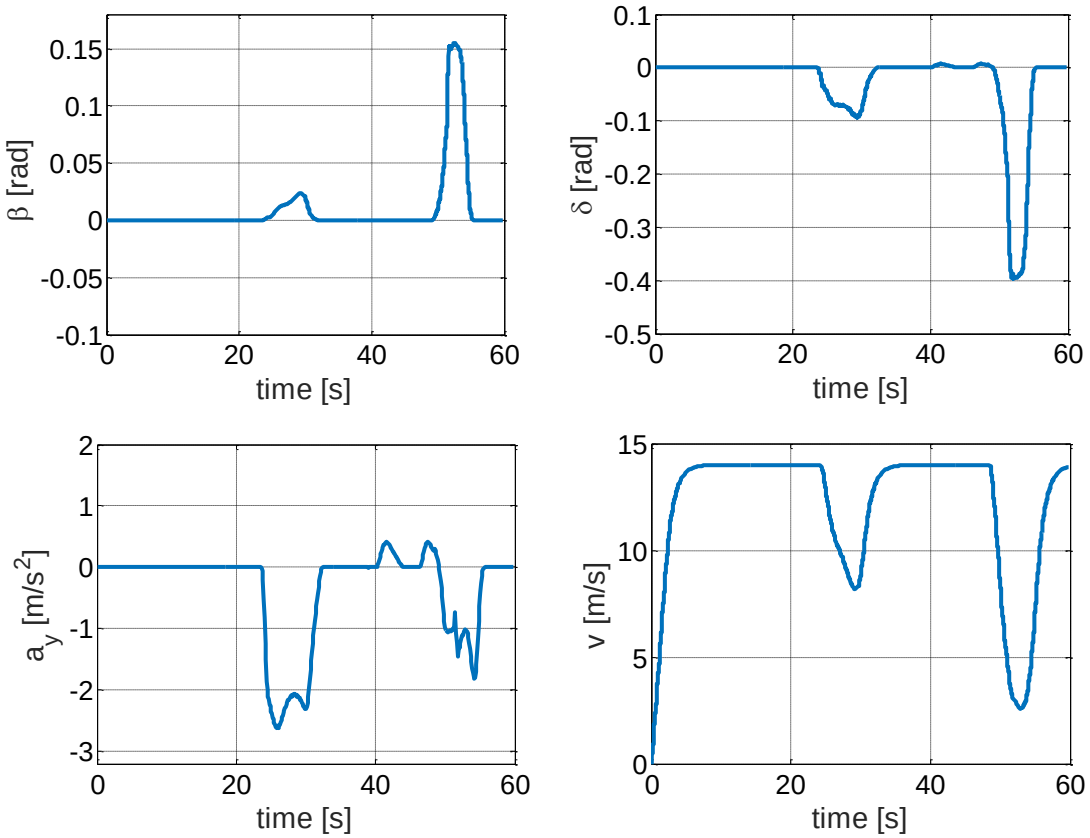

4-9: Vehicle slip angle β, steering angle δ, lateral acceleration a_y and velocity v

4.5 Conclusion

In this chapter based on the vehicle dynamic model an optimal control problem is designed. A Sequential Quadratic Programming *SQP*, solver named NLPQLP is used to solve the optimal control problem. The transformation of the optimal control problem to NLPQLP optimizer format is explained. The problem of using the nonlinear constraints as the inequality equations is explained and *soft constraints* as a solution is proposed and used. Due to the high length of course, and complexity of the problem, Moving-Horizon approach *MHA*, by portioning the global optimal control problem to the local sub-problems is presented and the choice of the *MHA* parameters are justified. The path optimization level is validated by simulation results based on a realistic urban scenario. As there are many different vehicle on the road, considering them in order to avoid any collision is critical. Hence different strategy to avoid any obstacle and collision will be presented in the next chapter.

5 OBSTACLE AVOIDANCE

5.1 Introduction

In previous chapter based on a given objective function an optimal solution which leads the vehicle through an ideal trajectory is found. But as far as we are not the only vehicle in traffic network and also fast changes in traffic structure, collision free driving is highly important. To avoid collision there are several strategies to find a possible collision free path. In the classical approaches [52] i.e. the configuration space, obstacle avoidance is considered as a planning problem and the focus is on path planning problem which provides the low level control with a collision free path, therefore the path must be precisely specified. In this strategies an inaccurate model or a slight error in the motion may result in a collision as the path is based on the vertices on the edge of the robot and obstacles [52]. In another hand the control level implemented is generally several orders of magnitude slower than the response time of the robot (vehicle) which limits its capabilities for interactive operations [37]. A solution to this problem was to make better use of low level control capabilities by using artificial potential field. The main idea of artificial potential field is that the robot/vehicle moves in a field of forces. The position to be reached is an attractive pole and obstacles are repulsive surfaces for the robot/vehicle parts. Another approach to avoid obstacles is neural network approach in which an initial phase of learning is required which can be based on human driving behavior data [53]. In [54] a method is proposed in which the prelearning phase in not required. In this method the target globally attract the robot in whole workspace through the neural activity propagation, while the obstacle have only local effect to avoid

collision. Another method used in motion planning and robotics to avoid the obstacles is velocity obstacle [55]. The main idea behind this method is to choose the velocity vector of the robot/vehicle in a way that results in a collision free path with another moving obstacles at some moment in time, assuming that the other obstacles keep their current velocity.

To avoid any collision on path planning level, graphs generated in chapter 3 can be extended to dynamic path planning by adding time dimension in the configuration space. In another hand building such graphs during preprocessing is not useful due to the transitory nature of configuration space as the obstacles motion are not assumed to be periodic. Solution to this problem is proposed in [44] in which the near-time-optimal path in the graphs-time space between start point and goal point is searched without collision with moving obstacles. As in our work, autonomous driving is based on optimization, therefore aim is to combine obstacle avoidance with path optimization level. This combination has the advantage to consider the dynamic parameters of the vehicle while any obstacle avoidance. For example in autonomous driving, if it is possible, a collision avoidance by strong deceleration or strong lateral acceleration is not preferable as they do not satisfy the comfort criteria's. And more important all the maneuver of the vehicle in order to avoid any collision must fulfill the vehicle dynamics. Hence velocity obstacle and a simple form of potential field are chosen as obstacle avoidance strategies as they can simply be added to the path optimization level.

Unlike most of robotic cases, in autonomous vehicles, how to avoid an obstacle is also important. For example avoiding maneuver which is used to avoid a vehicle must be different from avoidance maneuver of a pedestrian or a cyclist. In the case of pedestrian or cyclist a better avoidance is done by complete stop as pedestrian/cyclist has the priority. Therefore the nature of the obstacle also must be taken into consideration.

5.2 Obstacle classification

As mentioned before, the nature of obstacle must have influence on how it must be avoided. Avoiding pedestrian and a vehicle in the same way is not suitable as it raises danger for pedestrian. Obstacle recognition can be done with the help of different sensors such as radar, LIDAR or a camera. There are several study on the obstacle and object recognition [56] [57] but in this work the focus is not on the obstacle detection or recognition but only on avoidance. Therefore we suppose that the type of the obstacle is already known. Obstacles on the traffic network can be classified as stationary obstacles, dynamic obstacles and Pedestrian/cyclist obstacles. Example of stationary obstacle can be a parked car on the road or a blockage on the road. Any stationary obstacle can be presented by its position and its size. Any other type of the vehicle which moves is considered as dynamic obstacles and can be presented by its size, actual position, velocity, and orientation by assuming that it keeps its velocity during a horizon τ and these information can be updated at each increment ξ. Another group of obstacles are cyclist and pedestrian. By the nature of the movement they belong to one of the stationary or dynamic obstacle groups but as the way to avoid them is different from both of stated groups, due to security and traffic priority they are classified as a separate group. The simple kinematic vehicle model is used to model the dynamic obstacles and also pedestrian and cyclist.

5.3 Obstacle avoidance strategies

As mentioned in the introduction of this chapter, the velocity obstacle and a simple form of potential field are chosen as obstacle avoidance strategies. In both strategies the shape of the vehicle and obstacle is defined as a convex polygon and is assumed that the position, velocity and orientation of the obstacles are known or measurable.

5.3.1 Velocity obstacle

The main concept of velocity obstacle is generally explained based on the circular robot and circular obstacles [58] or between virtual agents [59]. As the main obstacle avoidance strategies are developed for the robotic application, the word robot is used in the most cases but the strategies can be extended to other applications. To make the shape definition for vehicle and obstacle more precise than circle, another shape definition will be proposed later which match better with the vehicle structure, but to explain the generality of the strategy, circular shape is preferred. Consider the vehicle A and another vehicle which is considered as obstacle B, as it is shown in figure 5-1 left, at time t_0 with their velocities v_A and v_B respectively. The vehicle A can be considered as point at its geometric center $\hat{A}$ when its radius is added to the obstacle B, shows as $\hat{B}$, figure5-1 right. The state of each moving object is represented by its position and a velocity vector attached to its center. A collision cone $CC_{A,B}$ for A and B as a set of colliding relative velocity is defined as:

$$CC_{A,B} = \{v_{A,B} \mid \lambda_{A,B} \cap \hat{B} \neq 0\} \qquad 5\text{-}1$$

In which $v_{A,B}$ is the relative velocity of $\hat{A}$ respect to $\hat{B}$ which is defined as $v_{A,B} = v_A - v_B$ and $\lambda_{A,B}$ is the line of $v_{A,B}$. λ_f and λ_r are the tangential lines of the cone in front and rear respectively. Any relative velocity which lies between these tangential lines when obstacle $\hat{B}$ keeps its velocity results in collision. To find the velocity vector which results in collision free, the cone can be translated by velocity vector of the obstacle, figure 5-2 left. In this figure velocity vector of B, is added to A and from that point, the collision cone is defined. This last offers the possibility to extend the approach for multiple obstacles as it is shown in figure 5-2 right. Hence the velocity obstacle, *VO*, is defined as:

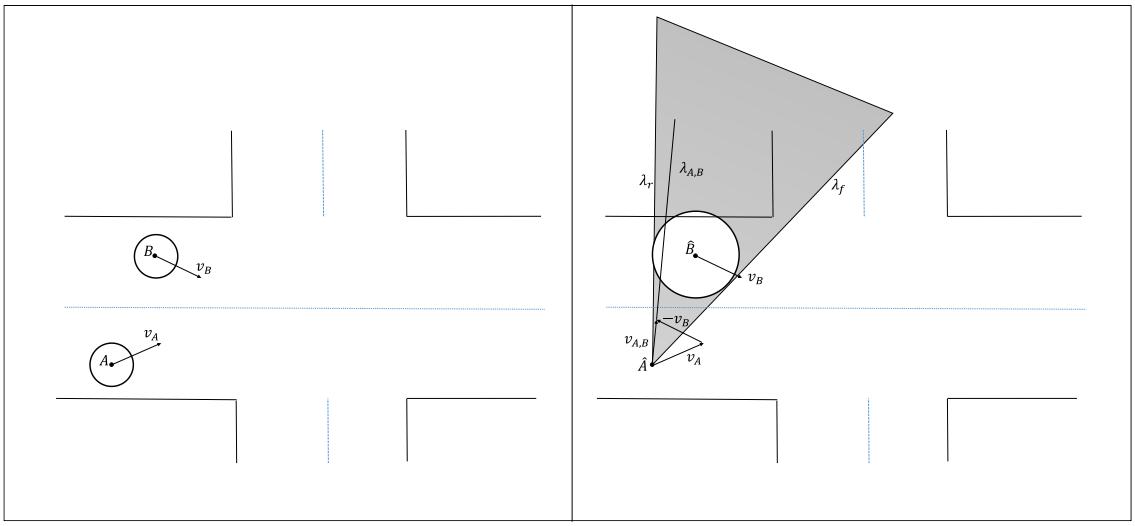

5-1 : Left: Vehicle A and obstacle B. Right: Avoidance cone

$$VO = CC_{A,B} \oplus v_B \tag{5-2}$$

where $\oplus$ is Minkowski sum operator. Therefore, the avoiding velocities partitions is when v_A is outside of VO.

$$A(t) \cap B(t) = \emptyset \; if \; v_A(t) \notin VO(t) \tag{5-3}$$

The velocity obstacle for multiple obstacles is written as follows:

$$VO = \cup_{i=1}^{m} VO_{B_i} \tag{5-4}$$

In which m is the number of obstacles. For more detailed explanation about velocity obstacle strategy see [58].

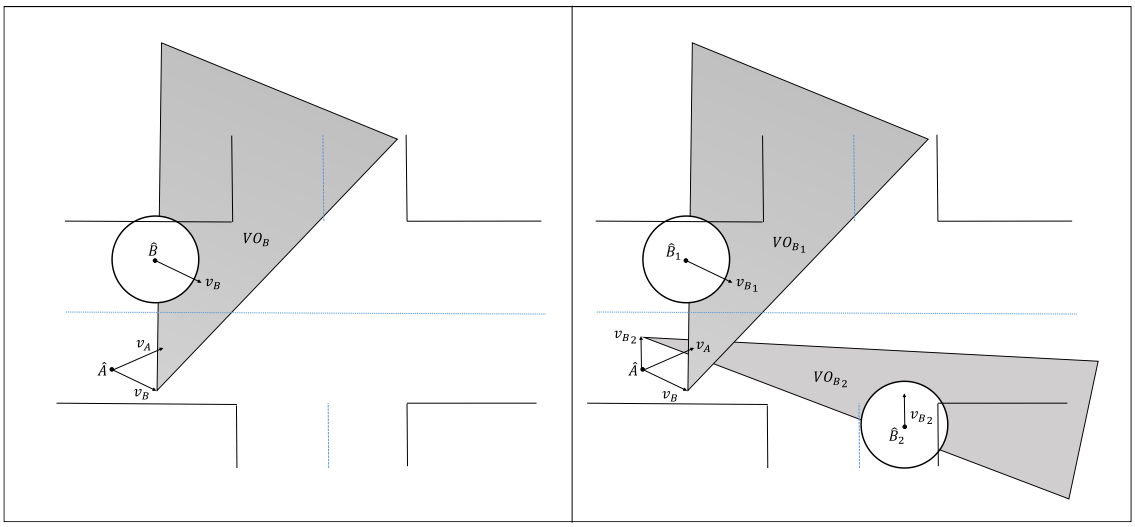

5-2: Obstacle velocity approach. Left: single obstacle. Right: multiple obstacles

5.3.2 Potential field

Another approach which can be easily added to the path optimization level is potential field which is defined on position level [60] [61]. The main idea of potential field approach is that the robot/vehicle moves in a field of forces in which destination is an attractive force and obstacles are repulsive surfaces. Definition of attractive force for destination is not necessary in this level as it is defined before in the objective function, see equation 4-21. To define repulsive surfaces, geometry definition of the obstacle which is considered as convex polygon, is used. Therefore at first step, vehicle and obstacles can be considered as circular objects. Like obstacle velocity strategy, size of vehicle is added to size of obstacles and the vehicle can be considered as a point at its geometric center. The area in which obstacle is situated which has also the size of vehicle in addition, is defined as forbidden zone, Z_{forbid}. Any vehicle position, $P_{vehicle}$ outside this zone result in collision free avoidance.

$$P_{vehicle}(t) \cap Z_{forbid}(t) = \emptyset \qquad 5\text{-}5$$

In order to find a collision free path, the calculated trajectory for time horizon τ must satisfy equation 5-5 in which it is assumed that obstacle keeps its velocity. Required information to use this strategy is obstacle geometry, velocity, position and orientation. Equation **5-5** can be introduced to optimization problem as a penalty function in which aim is to maximized the distance of the vehicle and forbidden zone, Z_{forbid}, when the equation **5-5** is not satisfied. The distance from vehicle center to the forbidden zone is calculated based on the line which connect vehicle center to the center of the forbidden zone circle. But for any other obstacle/vehicle shape except circle more precise formulation must be used in order to calculate the distance between vehicle center and forbidden zone, which will be explained later.

To show the functionality of both avoidance strategies a simple urban scenario is considered. Aim is to overtake a small fix obstacle on the middle of the road. Road has two lanes and each lane has width of $3m$, vehicle has length of $2.56m$ and width of $1.8m$ and velocity of 5.6 $^{m}/_{s}$, and on the center line of right lane there is a traffic cone with width and length of $30cm$ which must be avoided. In both approaches the obstacle and vehicle are considered as circumscribed circle. Blue line is position of the vehicle geometry center and red point is traffic cone. In both approaches obstacle is overtaken from left and after vehicle is returned back to the center line.

Figure 5-4 shows the result for a situation that obstacle moves with velocity of 2 $^{m}/_{s}$ and vehicle keeps its velocity which is 5.6 $^{m}/_{s}$. Figure 5-4 up shows avoiding maneuver by using obstacle velocity approach and down is the result for potential field approach. Blue line is the position of the center of the gravity of the vehicle. Blue points show the position of the vehicle and red points show the position of the obstacle for different time. t_0 is the starting time which shows the initial position of the vehicle and obstacle and points are sampled each second. In both strategies obstacle is avoided by left maneuver and after overtaking the obstacle, vehicle returns back to the center line of its initial lane. The slight difference between two paths is due to different nature of both strategies.

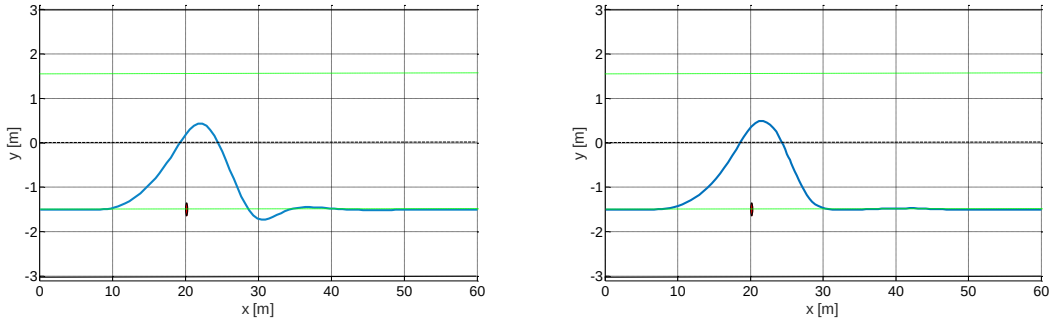

5-3: Static obstacle avoidance. Left: Potential field strategy. Right: Obstacle velocity strategy

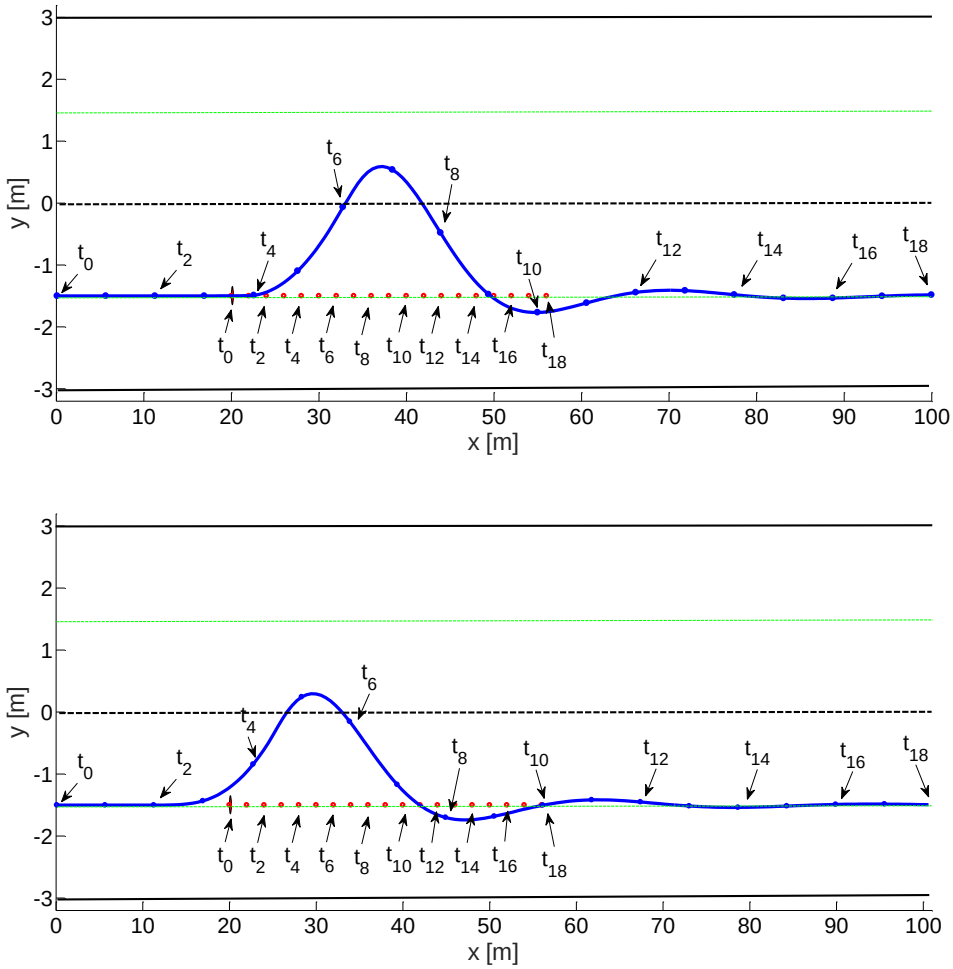

5-4: Dynamic obstacle avoidance. Up: Obstacle velocity strategy. Down: Potential field strategy

5.4 Geometry definition problem

As the exact geometry of the obstacles is not known, defining a circumscribed shape for obstacle is critical. In most cases circumscribed circle is used which has simple formulation and works fine in most robotic cases. But for autonomous driving more precise geometry definition is decisive. In this sector advantages and disadvantage of each proposed shape is explained.

5.4.1 Circumscribed circle

Using circle to define forbidden zone, Z_{forbid} has the advantage of simple circle equation and fix distance around this zone which is radian of the circle. This definition in velocity obstacle approach requires only two tangential lines to define velocity obstacle cone. The main disadvantage of this approach is when the obstacle has big size. Let's assume that a car must avoid another car, figure 5-5, therefor the size of the vehicle must be considered circular which is a circle with at least a diameter equal to the length of vehicle to cover the vehicle. By considering the same situation for the obstacle, in potential field strategy the diameter of the forbidden zone, Z_{forbid}, is diameter of obstacle circle plus diameter of vehicle circle which is big and can block the trajectory. This big circle in velocity obstacle,VO results in a wide forbidden cone. Figure 5-5 illustrates this situation, in which vehicle A drivivng with velocity v_A and has width and length of w_A and l_A. Aim is to overtake vehicle B which has velocity v_B and width and length of w_B and l_B. As figure shows road is unidirectional with two lanes, therefore over taking by left maneuver is possible. Figure 5-6 shows the forbidden zone,Z_{forbid} and velocity obstacle cone for this scenario.As it is shown, in both strategies there is no way to avoid the obstacle by respecting road width boundary. In potential field the size of forbidden zone,Z_{forbid} cover all the road.

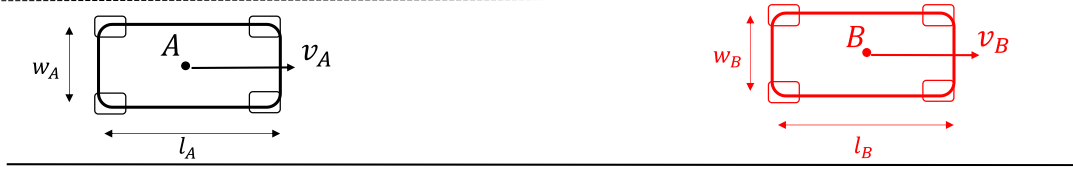

5-5: Urban scenario, vehicle avoidance

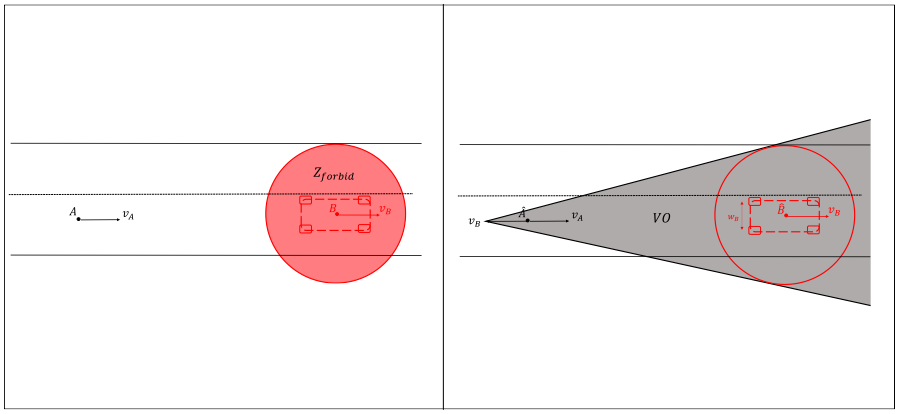

5-6: Illustration of big circle problem for obstacle avoidance. Left: Potential field. Right: Velocity obstacle

In velocity obstacle, the VO cone is so wide which cover all the road and no velocity vector can make vehicle A overtake vehicle B. In both cases overtaking maneuver is not possible but in reality road has two lanes and left one is free.

5.4.2 Better geometry definition

In order to avoid the problem stated before, a new circumscribed shape must be defined. Due to the general form of the most vehicles, a circumscribed rectangle is the most precise replacement for circle. Using rectangle instead of circle solves the previous problem and free space on the left lane can be used to overtake another vehicle. Rectangle shape to cover the obstacle increase the complexity of the problem as it has complex mathematical formulation. Another issue to consider is in the case of velocity obstacle strategy. Rectangle shape unlike circle shape that has only two tangential lines, require four tangential lines and two of them based on the situation with obstacle must be chosen to define the velocity obstacle cone. This last increases the complexity of approach as the calculation of these lines is time consuming.

Figure 5-7 left shows the definition of obstacle velocity cone when a rectangle shape is used. Black rectangle around obstacle B is its circumscribed rectangle. Velocity obstacle cone for two different positions are shown in this figure. Light gray cone is velocity

obstacle cone when the vehicle is behind the obstacle and black lines are tangential lines. Dark gray cone is velocity obstacle cone while overtaking and black dashed lines are tangential lines. As it is shown tangential lines for these two situations are defined based on different edges of the rectangle.

Using any other shape definition, such as ellipse or soft rectangle which will be explained later, does not decrease the complexity of the problem for velocity obstacle approach as in all of them four tangential lines must be calculated and based on two of them depends on the position of the obstacle with vehicle, velocity obstacle cone is defined. Due to the mathematical complexity of rectangle definition for forbidden zone,Z_{forbid} in potential field approach, an ellipse or a rectangle with soft edges, here called soft rectangle, can be used. Both of them have simpler formulation which reduce the complexity and both circumscribed cover the obstacle. Figure 5-7 right, illustrates forbidden zone, Z_{forbid} definition for circle, rectangle, soft rectangle and ellipse. As it is shown, except circle other shapes do not block the left lane and obstacle can be overtaken. As it is shown on the figure rectangle shape cover the most and ellipse the least and soft rectangle can be considered as between. For implementation, a security region must be added to these shapes both in width and length which can make ellipse circumscribed. As it is mentioned before, unlike circle shape, in other shapes distance from vehicle to the obstacle must be calculated based on the angle between them.

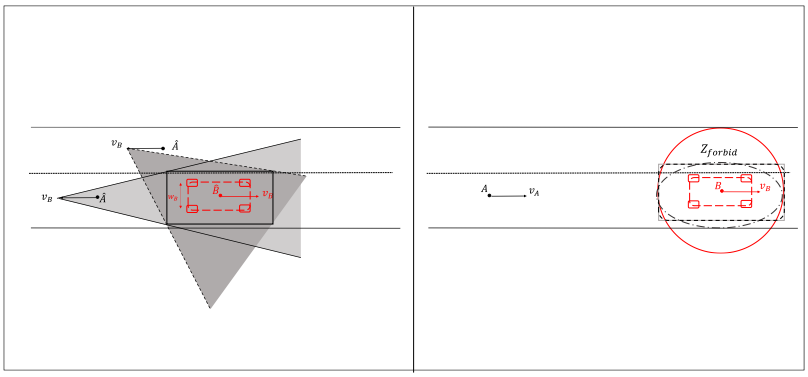

5-7: Obstacle avoidance strategy with rectangle shape. Left: Obstacle velocity strategy. Right: Potential field strategy

Hence using polar coordinate system simplify the problem in which first the angle between obstacle and vehicle is calculated and then based on this angle corresponding distance based on shape definition is found, figure 5-8 left. Based on this distance corresponding penalty function, figure 5-8 right, to maximize this distance is created and added to the objective function, equation 4-31.

Previous results show that velocity obstacle and potential field approach both can avoid static and dynamic obstacles. In order to choose one, based on a scenario explained in figure 5-4, they are compared to each other. In all of the experiments horizon τ, is $2s$ and increment is equal to $0.2s$ or 10% of horizon. The calculation time for all the experiments are shown in Table 5-1. In both strategies minimum of calculation time belongs to circle shape definition and maximum to rectangle. This calculation time difference is due to the complexity of using rectangle formulation in potential field strategy and necessity of calculating four tangential lines in velocity obstacle strategy. In potential field, ellipse calculation time is less than soft rectangle calculation time which is due to simplicity of ellipse mathematic formulation. Therefore using potential field strategy based on ellipse and soft rectangle are suitable and ellipse is chosen for rest of development, although all of eventual development can be implemented in others shape definition also.

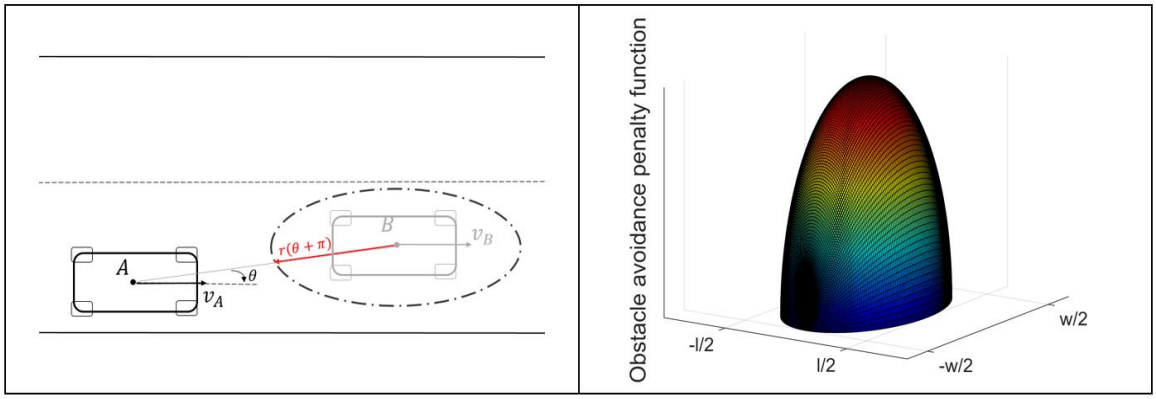

5-8: Left: Distance calculation for potential field strategy. Right: Potential field penalty function

#	Obstacle avoidance strategy	Circumscribed shape	τ in s	ξ % of τ	Relative $\sum t_{calc}$ in s
1	Velocity obstacle	Circle	2.0	10%	1.17
2	Velocity obstacle	Rectangle	2.0	10%	1.69
3	Potential field	Circle	2.0	10%	1.0
4	Potential field	Rectangle	2.0	10%	1.32
5	Potential field	Soft rectangle	2.0	10%	1.26
6	Potential field	Ellipse	2.0	10%	1.15

Table 5-1: Comparison between different avoidance strategy and different circumscribed shapes

5.5 Pedestrian and cyclist

Pedestrian and cyclist avoidance is more critical than vehicle or stationary obstacle due to the safety. In another hand there is no communication between the vehicle and pedestrian or cyclist which may exist between two vehicles such as Car2Car, therefore the information about obstacle must be captured by sensors. Detect pedestrian and cyclist mostly done by camera through some recognition algorithm [62] [63] [64] which is not the focus of this work. The main focus is on avoidance by having reliable knowledge of pedestrian and cyclist position and velocity. Avoiding pedestrian and cyclist by an overtake maneuver increase dramatically danger as in this case the human reaction is not predictable. Studies show that pre-crash reaction of pedestrian in most cases is to run, step-back or stop in fright in a dangerous situation [65]. Therefore when a pedestrian or cyclist is detected, due to safety is preferable to decrease the velocity or stop, let the pedestrian or cyclist pass and after continue the course. This last behavior can be reached by changing the ellipse size to the lane width. In this case when there is pedestrian or cyclist on the road, course is considered blocked and vehicle must reduce its velocity

instead of searching a new overtaking path. In figure **5-9** an urban scenario is simulated in which the vehicle drives with velocity of $8^{m}/_{s}$ and after $40m$ a pedestrian with velocity of $1.4^{m}/_{s}$ crosses the street. The blue line is vehicle trajectory and blue circle and red stars are vehicle and pedestrian trajectory sampled each one second. As it is shown when the vehicle faces pedestrian it reduces its velocity, pedestrian cross the street and vehicle accelerates again to its previous velocity.

In this case, as the ellipse size is considered big, the vehicle reduces its velocity instead of searching an overtake maneuver. Velocity of the vehicle for all course and given sampled time is shown in figure **5-9**.

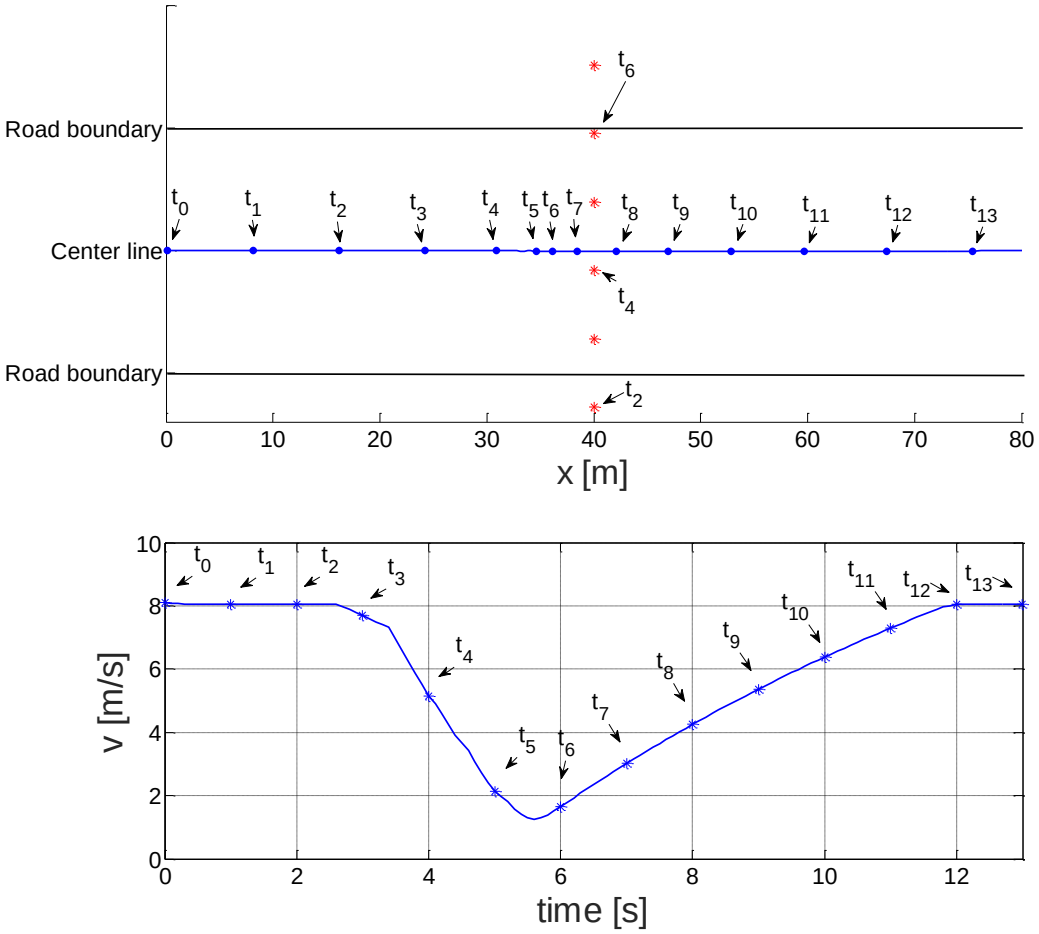

5-9: Pedestrian avoidance. Up: Vehicle and pedestrian position. Down: Vehicle velocity

Path planning level finds the shortest path from a start point to end point by taking into

5.6 Effect of initial solution on path optimization

In chapter 3 by using shortest path algorithm a rough initial solution for optimization problem is found. In previous works [66] [51] [50] , center line data was used as initial solution. In chapter 3 the initial solution is found by considering known stationary obstacles. This last does not guaranty collision free path as it is calculated based on geometry of the vehicle, road and obstacles and no dynamics is taken into consideration. But it can be considered as a better initial solution comparing to center line based initial solution especially when the obstacle is situated on the center line. For a given scenario similar to figure **3-5** chapter 3, optimal problem with initial solution based on center line and initial solution with path planning by considering static obstacles is solved. Figure 5-10 shows the result of this scenario for path planning initial solution and center line initial solution. Red dotted line is the path used to find initial solution and blue line is the vehicle trajectory and black rectangles are stationary obstacles. In both cases obstacles are avoided in a similar way as both have equal objective function. The only difference remain on initial solution. When the initial solution has collision with all the obstacles makes the optimal control problem more complicated and path optimization level needs more iteration in order to find optimal solution as the initial solution results in collision with obstacles which is not desirable and path optimization must find a collision free path. Comparing the number of iteration needed to find optimal solution as a reference of complexity of the problem shows that when path planning initial solution is used, reduces 28% complexity of the problem and gives 30% improvement on calculation time for the given case. In another hand result of center line initial solution shows that when a stationary obstacle in not considered in initial solution the path optimization level is able to find a collision free path but with more calculation time.

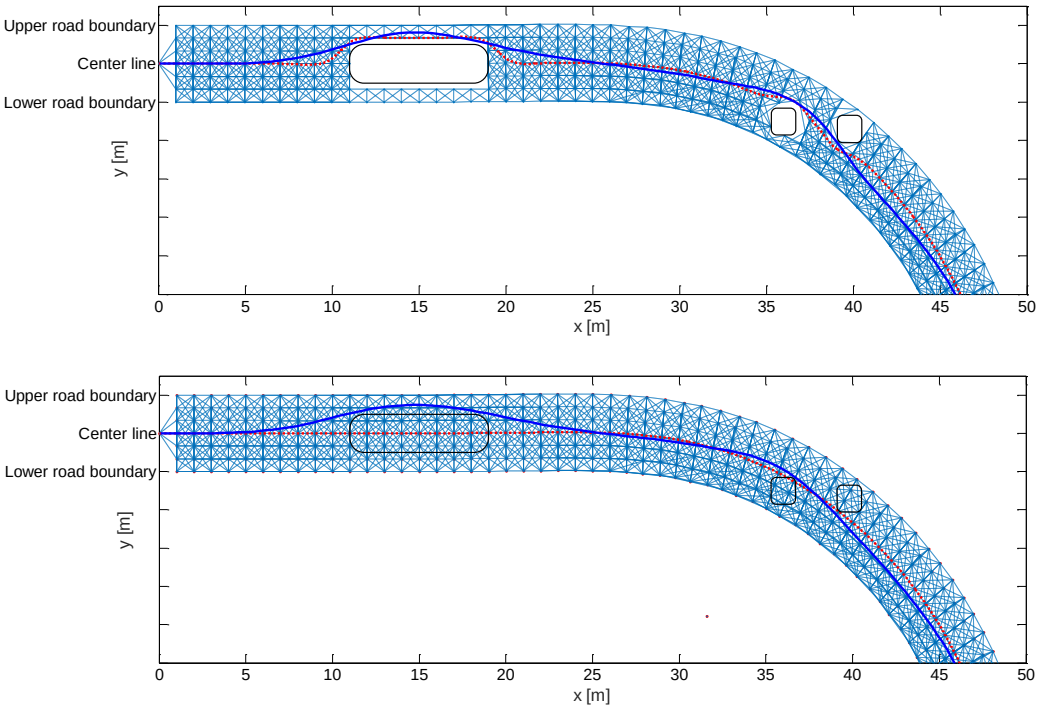

5-10: Stationary obstacle avoidance. Up: Path planning as initial solution. Down: Center line of track as initial solution

It can happen that in some cases taking a maneuver as it is found in path planning level is not possible. For example in scenario illustrated in figure 5-11, in order to avoid the stationary obstacle, shows with black rectangle, a left maneuver is chosen, gray dotted line, which is desirable. But in left lane there is a moving obstacle which makes the given maneuver impossible due to collision. In this case in order to avoid any collision with stationary and moving obstacle, right maneuver is done. In this case the path planning based initial solution is a bad initial solution and increase 60% complexity of the problem and 52% computational time for this example. In this figure blue circles on the left lane are the trajectory of the moving obstacle for sample time of one second. The same sampling is done with the trajectory of the vehicle, shown with blue and red circle on the right lane. Blue line is the trajectory of the vehicle using path planning as initial solution and red line is trajectory of the vehicle using center line as initial solution.

As the dynamic of road is unknown in path planning level this kind of situation might happen, but as the desired trajectory is defined to be on center line, see chapter 4, in most

cases vehicle before facing obstacle is on center line and left collision avoidance maneuver is preferred as it is also considered in path planning level. Therefore if the left side of the vehicle has enough room, the path planning reduce the complexity of the problem. If this last is not true, path optimization solution will be different form path planning and more deviation from initial solution results in more complexity of the problem. Proposed solution to benefit from the positive effect of path planning is to update path planning problem based on vehicle position in path optimization level. In this case when right maneuver for previous example is chosen to overtake the stationary obstacle by path optimization, path planning problem based on vehicle position, which is on the right side of the lane, is updated and new path from this position is found. In this case the new path to overtake the stationary obstacle is from right as the shortest path from the actual vehicle position is through right maneuver.

Road dynamics can also be considered in path planning level, which means not only considering the stationary obstacles but also moving obstacles. In this case path planning problem must be updated and new problem must be solved based on the last states of the path optimization problem by considering stationary and dynamics obstacles.

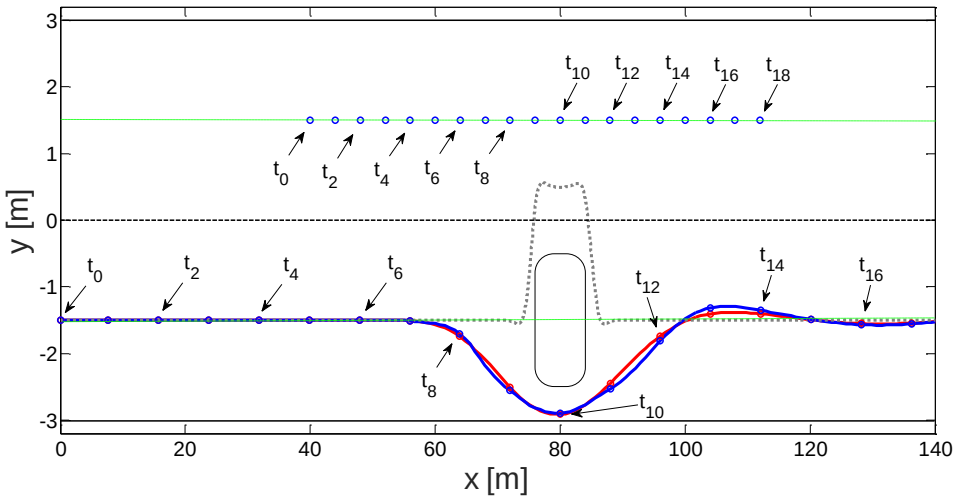

5-11: Obstacle avoidance maneuver for a stationary and moving obstacle.

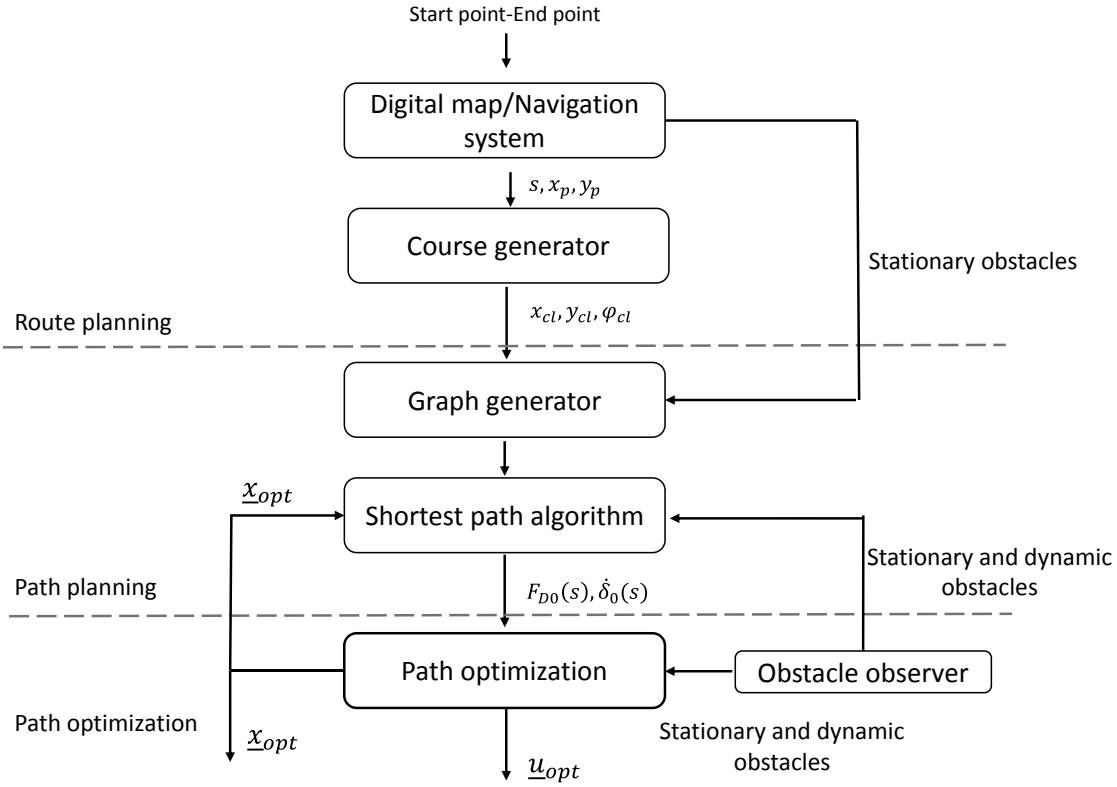

5-12: Path planning with update from path optimization states

In that event, first, initial solution for given course is generated in path planning level for a period of time t_p in which $t_p > \tau$. Then based on this initial solution an optimal path is found on path optimization level. Based on the position and velocity of the vehicle at the end of increment ξ, path planning is updated and a new path is found for new t_p and this new path is the initial solution for next horizon τ. Path planning with update from path optimization is illustrated in figure 5-12.

Figure 5-13 illustrates timing between different levels of hierarchical concept with update between path planning and path optimization. As it is shown at beginning, in path planning level a path for time interval of $[t_0, t_p]$ is found, then based on this path as initial solution an optimal path for a horizon τ is found for time interval of $[t_0 + \xi\ , t_0 + \xi + \tau]$ and a part of this solution, an increment ξ, is sent to control level. Path planning in this level cannot be updated, as at $t_0 + \xi$ there is no path optimization to be used to update path planning problem. Therefore, the initial path planning is used again to run the second

path optimization starts at $t_0 + 2\xi$ and one increment of this result is sent to control level. At time $t_0 + 2\xi$ based on the vehicle position found in first path optimization $[t_0 + \xi\,, t_0 + \xi + \tau]$ at time $t_0 + 3\xi$ a new path planning is run for time interval of $[t_0 + 2\xi, t_0 + 2\xi + t_p]$. Initial solution of this path planning is used for next path optimization problem. And this sequence continues.

Another important advantage of coupling between path planning and path optimization is the possibility to consider forehead road situation such as traffic light or a cross section in path planning level. In this case is not necessary to find optimal inputs of the system for these far forehead situations but they can be considered in path planning when $t_p \gg \tau$. In this case, when a change is needed on driving force or steering angle such as reducing velocity or changing a lane, they can be considered before in initial solution, which consequently results in a faster and more efficient optimal solution. This last probably increase safety also, as far forehead events are seen in path planning before being seen in path optimization level.

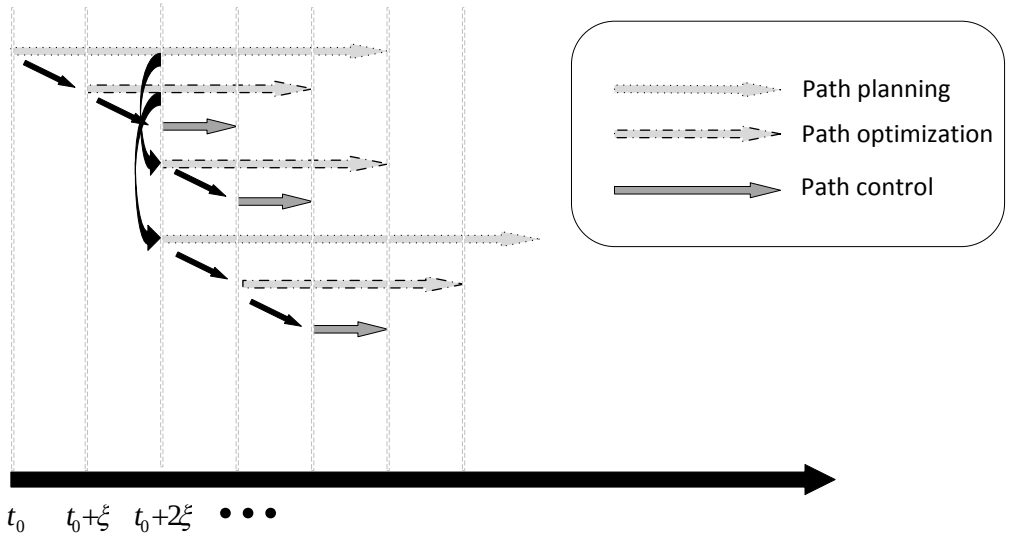

5-13: Timing between different levels of hierarchical concept

5.7 Conclusion

In this chapter two different strategies to avoid obstacles has been explained which are velocity obstacle and a simple form of potential field. Both approaches are added to the path optimization level with their penalty function and their functionality has been studied. To construct the penalty function different shapes to cover obstacle was tested and between them ellipse needed less calculation time due to its formulation simplicity. Comparison between both approaches to avoid the obstacle showed that potential field has les complexity compared to velocity obstacle approach. Hence the potential field approach with ellipse shape is preferred. Figure 5-14 illustrates main concept of path optimization level with obstacle avoidance. As it is shown when the optimal input $\underline{u}_{opt}$, is applied to the vehicle results in $\underline{x}_{act}$. Because of disturbances and model uncertainty there is difference between $\underline{x}_{act}$ and $\underline{x}_{opt}$. These difference, so called error, will be decompensate by adding new level called path control level which will be explained in next chapter.

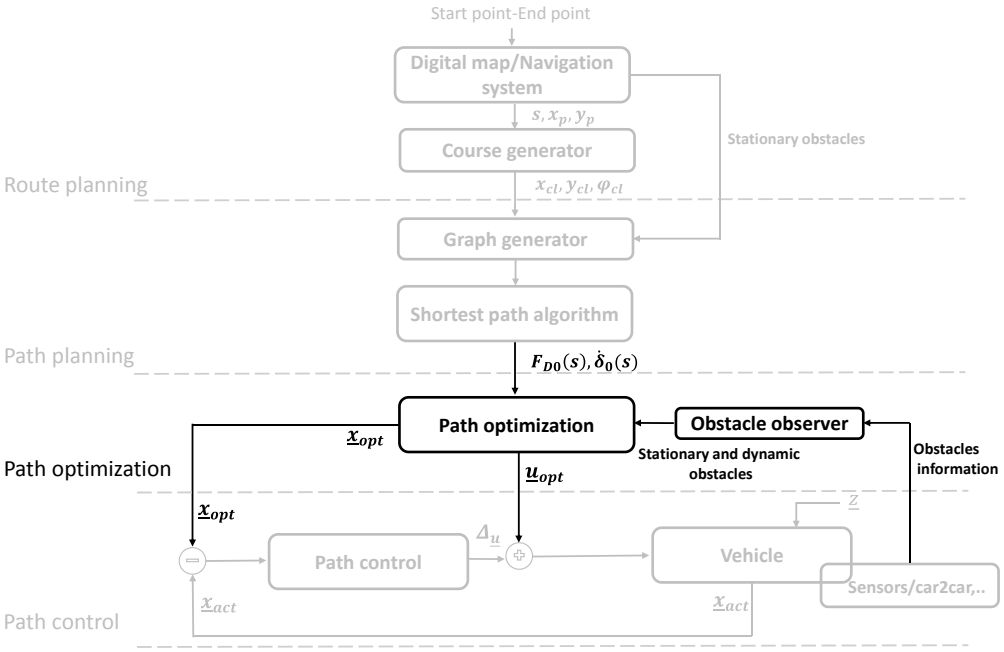

5-14: Path optimization level concept with obstacle avoidance in hierarchical concept

6 PATH CONTROL AND SIMULATION RESULTS

6.1 Introduction

In previous chapters generating optimal inputs of vehicle for a given objective function is explained. As these inputs are found based on a simple vehicle model, equation 2-31, which is simplified based on some assumption and also the model does not consider external disturbances such as friction or side wind, applying these inputs to the vehicle does not result equal to the optimal solution. In another hand considering all the external parameters in the model is impossible as our knowledge about them is limited through the course and it is shown before that using more complicated model increase the calculation time which is not desirable. Therefore, a path control level is added to the hierarchical concept of the work, see figure 6-1.

6.2 Control approach

It can be concluded that the external disturbances and uncertainty of the model result on error in position level which can be mapped on lateral and longitudinal directions. Longitudinal error caused by deviation in velocity and it can be compensated by additional driving force, Δ_{F_D} and lateral error caused mainly by failure in yaw angle and can be compensated by additional steering angle Δ_δ. Figure **6-2** illustrates actual vehicle position, dotted blue, and optimal vehicle position, solid black, and their related slip angle β, yaw angle ψ, and velocity vector v.

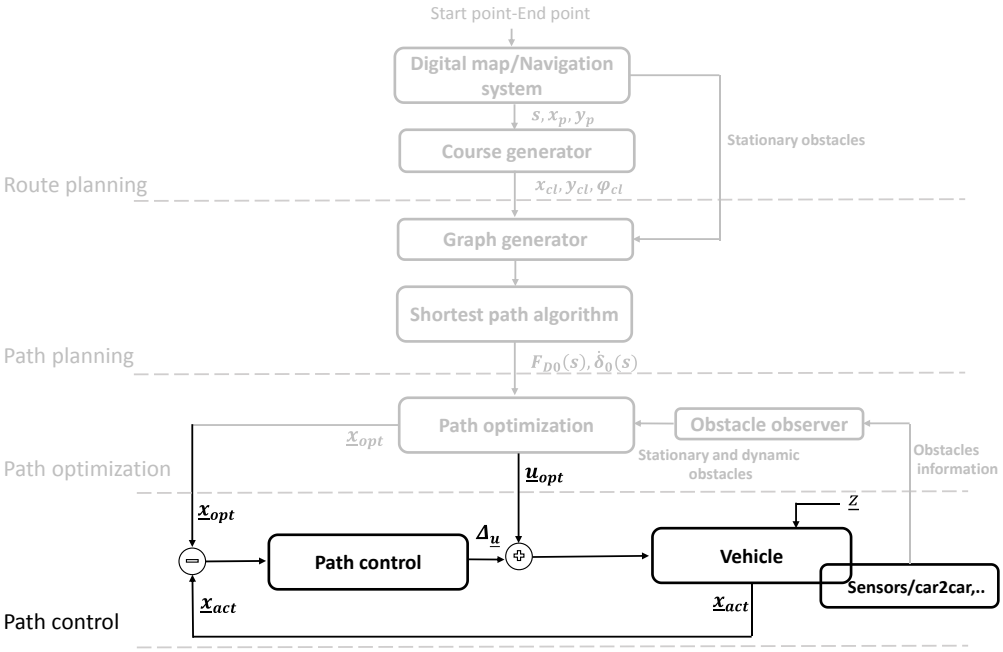

6-1: Path control level on hierarchical concept of autonomous driving

Lateral distance or side distance and longitudinal distance between actual vehicle position and optimal vehicle position are shown by d_s and d_l respectively. These two distances as representative values of errors are used to calculate additional force and steering angle. Lateral and longitudinal distances are calculated as follows:

$$\begin{bmatrix} d_l(\underline{x}_{opt}, \underline{x}_{act}) \\ d_s(\underline{x}_{opt}, \underline{x}_{act}) \end{bmatrix} = \begin{bmatrix} cos(\psi_{opt}) & sin(\psi_{opt}) \\ -sin(\psi_{opt}) & cos(\psi_{opt}) \end{bmatrix} \cdot \begin{bmatrix} x_{opt} - x_{act} \\ y_{opt} - y_{act} \end{bmatrix} \qquad 6\text{-}1$$

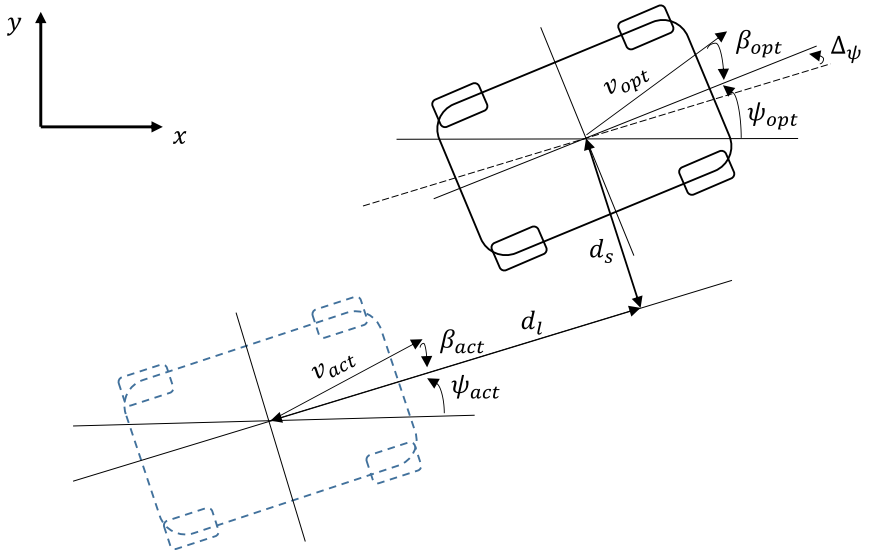

6-2: Longitudinal and lateral error between actual vehicle position and optimal position

As it is explained due to the model uncertainty and external disturbances vehicle behavior differs from optimal solution, therefore, path control level must be added to the hierarchical concept of autonomous driving. Figure 6-3 illustrates the main concept of path control level in which based on optimal states and vehicle states the error on longitudinal and lateral position is calculated. Then base on these errors corresponding additional driving force and steering angle is generated. At longitudinal level as it is shown, to reduce the longitudinal error first an additional velocity is generated and then this velocity is added to velocity controller loop to generate corresponding additional force. And to compensate lateral error, based on lateral error corresponding additional steering angle is generated.

Without losing generality, when relation between lateral-longitudinal error and corresponding inputs of the system is known, adaptive control can also be used. Schmidt [48] calculated transfer function between yaw angle deviation and corresponding steering angle and also side distance error and corresponding steering angle which can be used to develop an adaptive yaw controller and lateral controller. Calculated transfer function between velocity error and corresponding driving force and also longitudinal error and corresponding driving force can be used also to develop velocity and longitudinal controller by respecting presented concept, see [67].

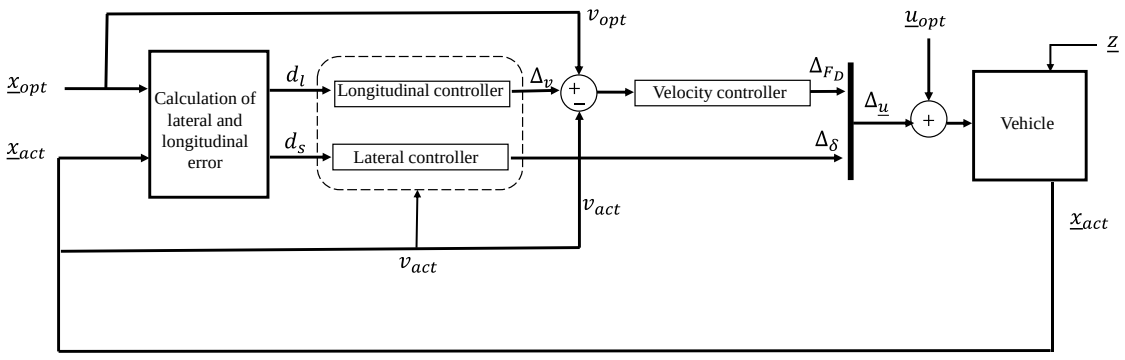

6-3: Path control concept

6.3 Simulation results

In order to check functionality of the path control level, IPG CarMaker as a simulation tool is chosen in which vehicle is modeled with 3D-double track model, and vehicle parameters such as vehicle body characteristics are chosen with respect to the experimental vehicle, BugEE, figure 1-4. The simulated vehicle powertrain is composed of four electric motors with respect to the wheel-hub motors characteristics used in the experimental vehicle. More information about the experimental vehicle can be found in next chapter. Simulation experiments offers the possibility to test our approach in different critical situations with high velocity. For example, an overtaking maneuver with high velocity is simulated in which the vehicle has velocity of 24 $^{m}/_{s}$ and 60 meter in front there is another vehicle with velocity of 13$^{m}/_{s}$ in the same lane. Aim is to overtake the vehicle and return back to initial lane. The road is asphalt and the wheel-road dry sliding friction coefficient is 0.8. Figure 6-4 shows the optimal position of the vehicle with blue line and vehicle position with red dotted line. Optimal position of the vehicle, actual position of the vehicle and obstacle position sampled each two seconds are shown with blue circle, red star and black diamond respectively. Figure 6-5 left shows the steering angle on optimization level and steering angle which is applied to the vehicle. As it is shown in order to complete the maneuver by keeping the lateral error small, additional steering angle is generated by controller which makes the steering angle applied to the vehicle bigger than the optimal steering angle. The main reason of this difference between optimal steering angle and applied steering angle to the vehicle is due to the simplification done on single track model on lateral dynamics and influence of external parameters such as friction. The same figure right shows the optimal velocity and vehicle velocity.

Figure 6-6 shows the lateral and longitudinal error. As it is shown, before and after overtaking maneuver lateral error is zero as the vehicle starts and the center line and the controller avoid any probable deviation especially after overtaking maneuver and while cornering, controller by generating additional steering angle, figure 6-5, keeps the lateral error small, see figure 6-6 left, here less than $30cm$ while maneuver which is an expectable value for this velocity.

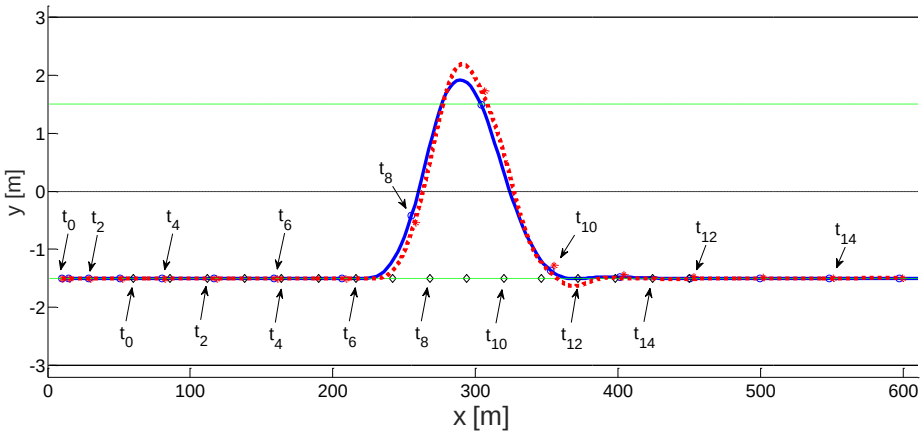

6-4: Overtaking maneuver: Optimal solution vs. Vehicle

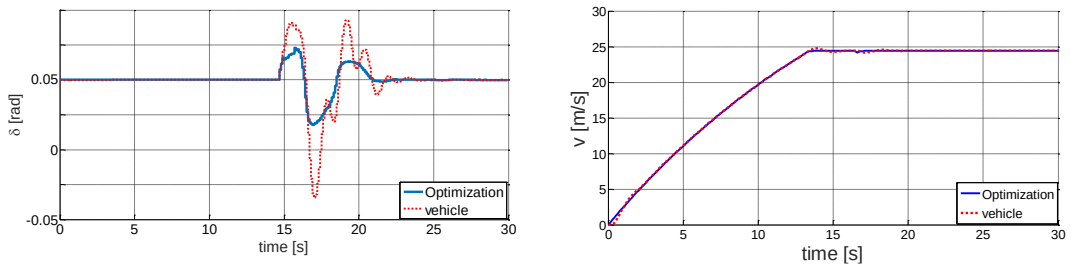

6-5: Left: Steering angle: Optimization vs. Vehicle. Right: Velocity: Optimization vs. Vehicle

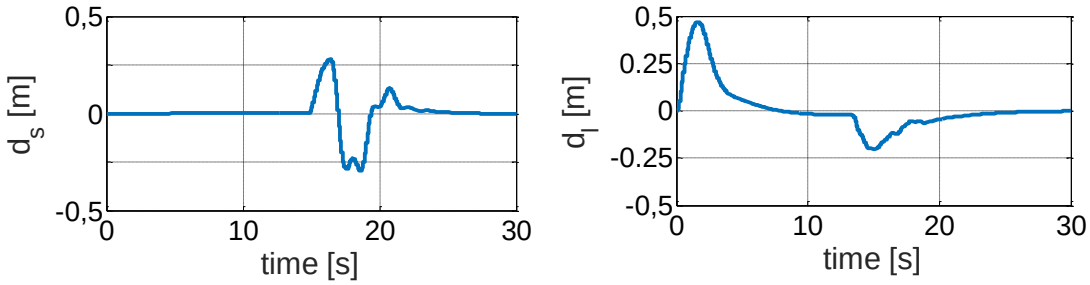

6-6: Lateral error (left) and longitudinal error (right)

In figure 6-6 right, longitudinal error is illustrated in which at beginning due to the different longitudinal dynamic there is an error less than $50cm$ which vanishes because of controller and while cornering due to the effect of side forces which are simplified in single track model there is negative value of longitudinal error which is kept small by longitudinal controller.

6.4 Conclusion

In this chapter is explained that due to model uncertainty and disturbances there is error between the optimal states and vehicle states after applying optimal inputs to the vehicle. Therefore, a path control level is added to the hierarchical concept of the autonomous driving in which first this error is mapped into longitudinal and lateral error and after by adding the related controllers, corresponding additional driving force and steering angle are generated to reduce these errors respectively.

7 EXPERIMENTAL SETUP AND RESULTS

7.1 Introduction

In order to go one step further than proving our approach functionality by simulation, some experiments are done. In that event a buggy car with mass of $750kg$,width of $1.80m$ and length of $2.6m$ is converted from combustion engine vehicle to electric vehicle, see figure 1-4. The combustion engine is replaced by four wheel hub motors. Motors on front axle have $6.5kw$ and maximum torque of $150\ Nm$ and on rear axle $8kw$ and $291\ Nm$. Steering system is replaced by active front steering, *AFS* consisting of steering wheel, steering column, intermediate shaft, a brushless DC motor with the maximum mechanical speed of $6000\ rpm$, which limits the steering angle rate to $0.4\ {}^{rad}/_{s}$, the rack , and gear assembly and steering linkages, figure **7-1** .

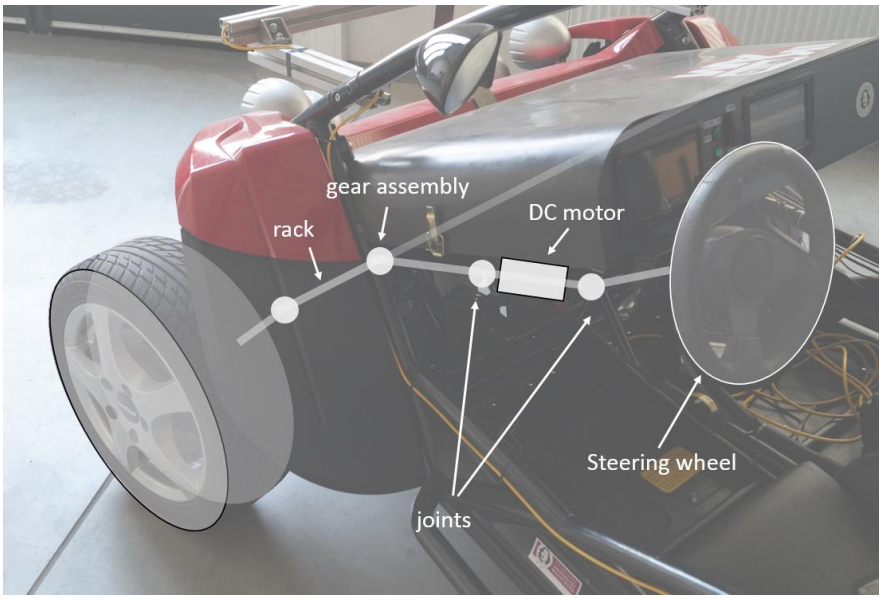

7-1: Active front steering system implemented on BugEE

Optimization problem is solved in Laptop PC in real-time and data via USB_CAN converter are sent to real-time prototyping unit. A differential GPS, *DGPS* is used to measure the position of the vehicle. In this system a ground-based antenna as reference is implemented to broadcast the difference between the positions indicated by GPS satellite system and the known fix position. This last improve precision of measurement, around $2cm$ precision. Data transmission between station and rover is done via radio communication. Difference between position measured with *DGPS* and optimal position is used to calculate longitudinal and lateral error which are inputs of controllers. A box with size of $0.6m * 0.4m$ is considered as an obstacle which has a rover *GPS* antenna which transmit position and velocity data of the box. The communication between obstacle and vehicle is done via radio communication. Using two antennas, one in front of the vehicle and one in rear offers the possibility to measure yaw angle of the vehicle. Figure 7-2 shows the setup used for experiments.

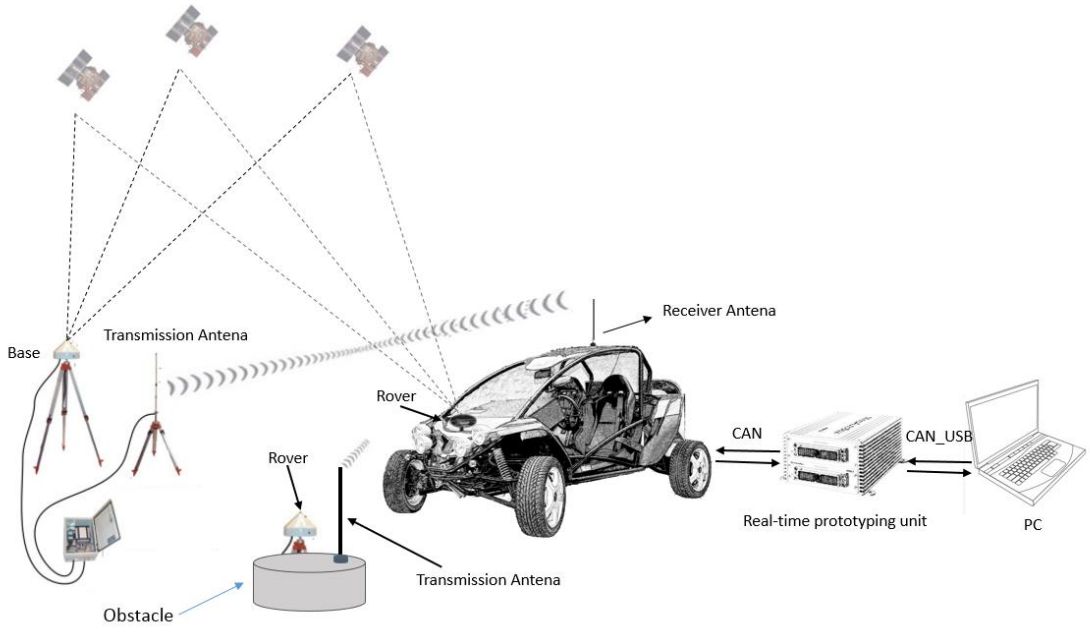

7-2: Experimental setup

7.2 Experimental results

Two different experiments are chosen for this chapter, first is an oval to shows the maneuverability and second one is an obstacle avoidance. Figure 7-3 shows the optimal position calculated in path optimization level for this experiments, blue line, and vehicle position measured by *DGPS* system, red dashed. Vehicle velocity for this experiment is 6 $^{m}/_{s}$. Figure 7-4 up, shows the optimal velocity versus reference velocity and vehicle velocity. Optimal velocity is the velocity calculated on path optimization level which is the result of optimal inputs on vehicle dynamic model. Reference velocity is the optimal velocity plus the additional velocity generated on longitudinal controller which is applied on velocity controller, see figure 6-3 and vehicle velocity is the velocity measure with sensors of the vehicle.

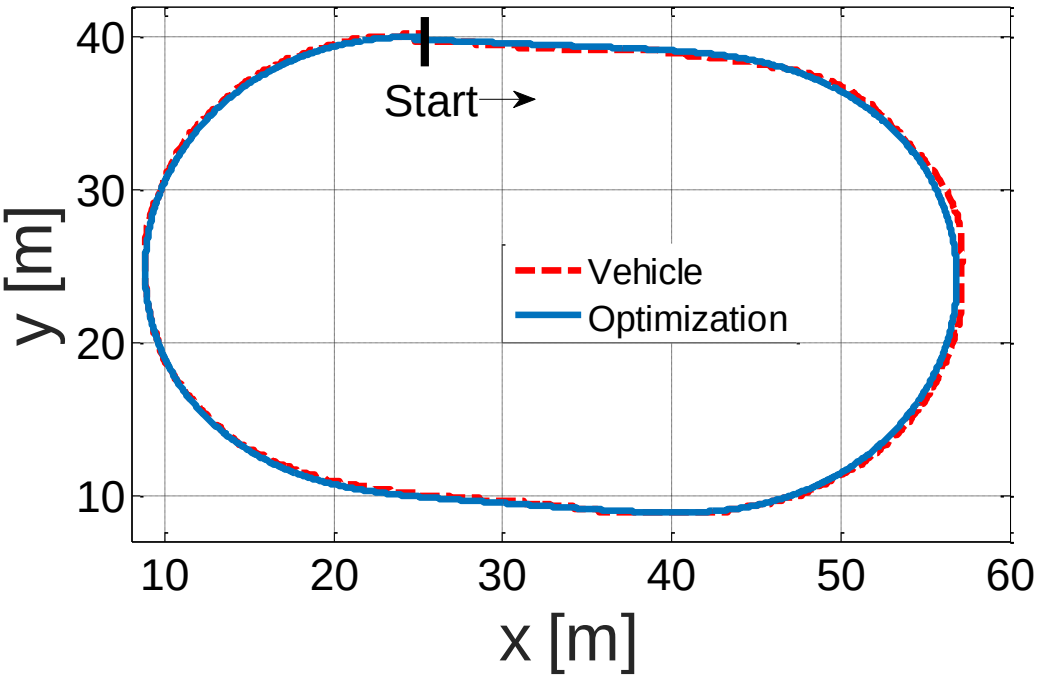

7-3: Oval experiment. Vehicle position vs. Optimal position

As it is shown in figure 7-4, vehicle velocity at beginning differs from optimization velocity due to external disturbances and dynamic difference of vehicle and vehicle model used in path optimization level therefore, longitudinal error has a positive value, reason why reference velocity is more than optimal velocity to compensate longitudinal error. When the vehicle velocity stabilized after transitionary part at beginning, longitudinal error vanishes also while curving. Figure 7-4 down right shows side error or lateral error, which has its maximum and minimum while entering and quitting the curve and during straight line it vanishes.

Second experiment is an obstacle avoidance in which aim is to avoid a fix obstacle with the size of $0.6m * 0.4m$ (obstacle box) which is situated $20m$ ahead from vehicle starting position. Vehicle has velocity of $5\,{}^{m}/_{s}$ and road is one lane unidirectional. In this case the obstacle is left overtaken and vehicle returns back to the center of the lane.

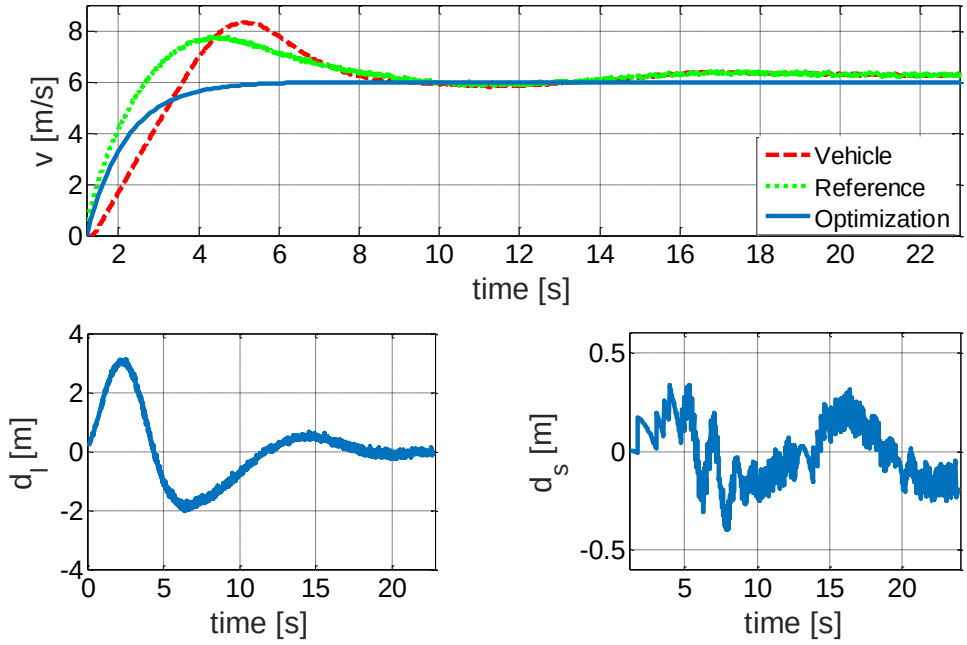

7-4: Experiment one. Up: vehicle velocity vs. optimal velocity. Down left: longitudinal error. Down right: lateral error

Figure 7-5 right shows the vehicle position, red dashed, versus optimal vehicle position calculated in path optimization level, blue. Figure 7-6 shows the vehicle velocity versus optimal velocity and reference velocity in which like previous example at beginning vehicle velocity is less than optimal velocity which results in longitudinal error which is reduced due to longitudinal controller effect by generating additional reference velocity.

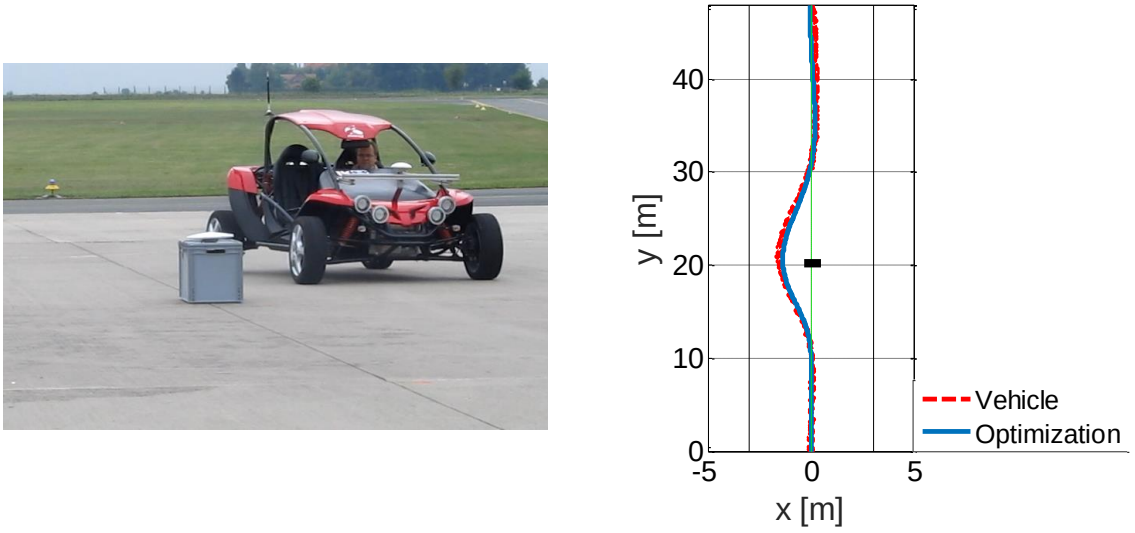

7-5: Left: Vehicle while avoidance. Right: Avoidance maneuver, vehicle position vs. optimal position

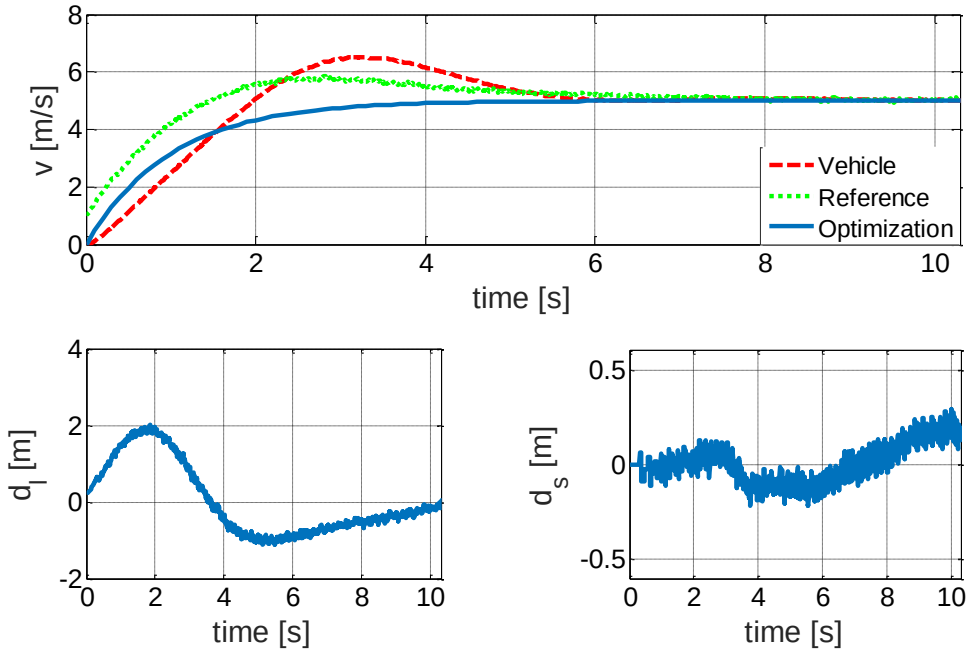

7-6: Experiment two. Up: vehicle velocity vs. optimal velocity. Down left: longitudinal error. Down right: lateral error

Figure 7-6 down right shows the lateral error which has very small value at beginning when vehicle drives straight line and while cornering increases a bit which is kept small, around $20cm$, while avoidance.

7.3 Conclusion

Despite simplification done on vehicle and tire model, neglecting external disturbances, and also difference of vehicle dynamic of BugEE and vehicle model used in path optimization level, experimental results show that by adding path control level, vehicle response to optimization inputs is similar to optimal states.

8 CONCLUSION AND OUTLOOK

In this dissertation a hierarchical concept for autonomous driving is developed and explained level by level. At the end, functionality of the approach is tested by simulations and experiments. At first vehicle dynamic model and tire model have been explained and further by implementing them, choice of vehicle model was justified on path optimization level. To drive autonomous from a given start point to end point, course and graph generation between these two points has been explained on route planning and path planning level and based on generated graphs by using a shortest path algorithm, a path connecting these two points by satisfying some criteria's has been found. Based on this path and a simple kinematic vehicle model initial inputs for path optimization level have been found. On path optimization level, unlike path planning level, dynamic of the vehicle has been considered to find an optimal path by respecting some criteria's such as road permissible width , energy efficiency and comfort. On this level has been shown that using single track model due to its simplicity satisfies better real-time criteria of autonomous driving.

As the length of course is big and optimal control problem complex a Moving-horizon approach as a solution has been proposed to partitioned big optimal control problem to sub local problems. To avoid any collision two different avoidance strategies have been presented, explained and compared. A simple form of potential field has been chosen to avoid any collision. Due to the external disturbances and simplification of vehicle model used on path optimization level, path control level has been added in which the error between vehicle response to the optimal inputs and optimal states on position level has been calculated and this error has been mapped on longitudinal and lateral direction in

order to generate corresponding inputs to reduce this error. Figure 8-1 illustrates hierarchical concept of autonomous driving.

Effect of initial solution on path optimization is shown and results show that better initial solution reduce the complexity of the problem and calculation time. But as the dynamic of the road is not consider in path planning level, in some cases path found on path planning level might differ from path found on path planning level. Proposed solution which can be implemented for further development of the project can be the possibility of updating the path planning problem based on the vehicle position found on path optimization level. An extension to this proposed solution can be dynamic path planning in which based on the vehicle position and velocity found on optimization level, path planning can be updated by considering stationary and dynamic obstacles. Dynamic path planning unlike static path planning has also time dimension which makes the problem more complicated but probably considering forehead dynamics in path planning when $tp \gg \tau$ increase safety and security.

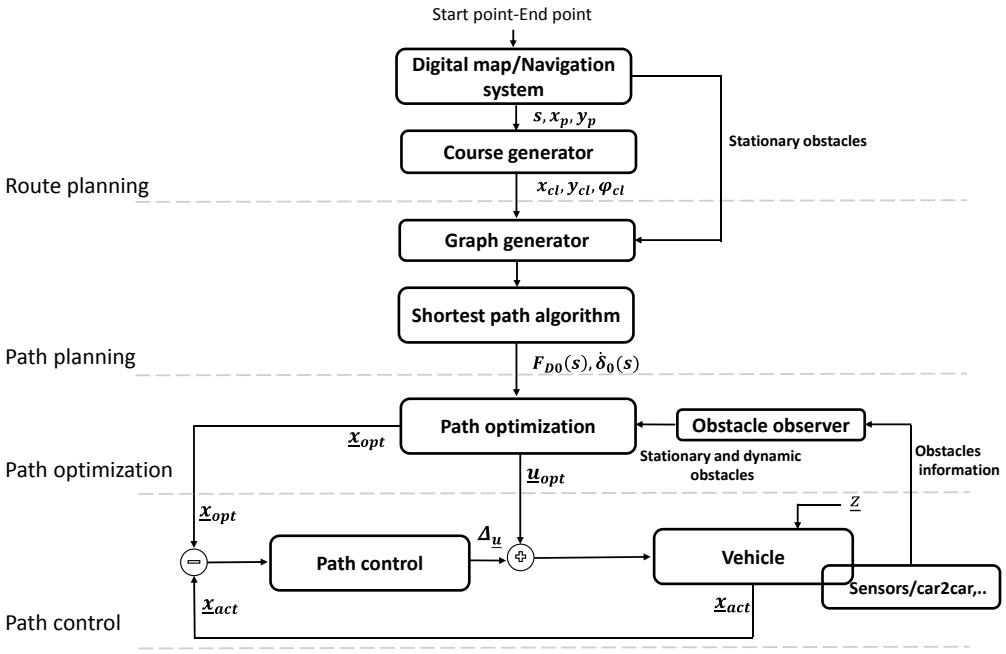

8-1: Complete hierarchical concept of autonomous driving

9 REFERENCES

[1] D. Howard and D. Dai, “Public perceptions of self-driving cars: The case of Berkeley, California,” Prepared for the 93rd Annual Meeting of the Transportation Research Board, Berkeley, CA, 2013.

[2] “Economic and enviromental impact of traffic congestion in europe and the US,” [Online]. Available: http://inrix.com/economic-environment-cost-congestion/.

[3] B. Mirbaha, M. Safarzadeh, S. E. S.Abrishami and A. Pirdavani, “Evaluating the willingness to pay for urban congestion priced zones (Case study of Tehran),” *International Journal of Transportation Engineering,* vol. Vol.1/ No.3/, Winter 2013.

[4] "Global status report on raod safety 2013. Supporting a decade of action," World health organization, 2013.

[5] “Glossary of transport statistics,” European communities-United nations, Luxembourg, 2003.

[6] “Centers for disease control and prevention, National center for injury prevention and control-web based injury statistics query and reporting system,” [Online]. Available: http://www.cdc.gov/injury/wisqars.

[7] “Global plan for the decade of action for road safety,2011-2012,” World health organization, Geneva, 2011.

[8] C. Liu, D. Utter and C.-L. Chen, “Characteristics of traffic crashes among young, middle-aged, and older drivers,” National highway traffic safety administration,NHTSA, Washington DC, November 2007.

[9] K. Reif, Brakes, brake control and driver assistance systems. Function, Regulation and Components, Springer Vieweg, 2014.

[10] “Toyota enhances pre-crash safety system with eye monitor,” 22 1 2008. [Online]. Available: http://www.toyota.co.jp/en/news/08/0122.html.

[11] G. Platzer, “The geometry of automotive rearview mirrors - Why blind zones exist and strategies to overcome them,” SAE International in United States, 1995.

[12] W. D. Jones, “Safer driving in the dead of night. Infrared vision systems are set to become standard in high-end cars,” IEEE spectrum, 1 March 2006.

[13] “Adaptive cruise control system overview,” 5th Meeting of the U.S. Software System Safety Working Group, Anaheim, California USA, April 12th-14th 2005.

[14] J. Pohl and J. Ekmark, “A lane keeping assist system for passenger cars. Design aspects of the user interface,” Volvo Car Corporation, Paper No.529, Gothenburg, Sweden.

[15] S. A. Kanarachos, “A new method for computing optimal obstacle avoidance steering manoeuvres of vehicles,” *Int. J. of Vehicle Autonomous Systems,* vol. 7, pp. 73-95, 2009.

[16] “ Electronic stability control could prevent nearly one-third of all fatal crashes and reduce rollover risk by as much as 80%; effect is found on single- and multiple-vehicle crashes,” IIHS News release, 2006.

[17] J. N.Dang, “Preliminary results analyzing the effectiveness of electronic stability control (ESC) systems,” US. Department of Transportation. National Highway Traffic, Safety Administration, September 2004.

[18] M. Weber, “Where to? A history of autonomous vehicles,” [Online]. Available: http://www.computerhistory.org/atchm/where-to-a-history-of-autonomous-vehicles/.

[19] C. Schwarz, G. Thomas, K. Nelson, M. McCrary, N. Schlarmann and M. Powell, “Towards autonomous vehicles,” Final Reports & Technical Briefs from Mid-America Transportation Center, 2013.

[20] “National highway traffic safety administration-Preliminary statement of policy concerning automated vehicles,” [Online]. Available: http://www.nhtsa.gov/Research/Crash+Avoidance/Automated+Vehicles.

[21] D. S. Zuby, “The promise and reality of crash avoidance technology,” in *Lifesavers National Conference*, Nashville, TN, 27 April 2014.

[22] J. M.Anderson, N. Kalra, K. D.Stanley, P. Sorensen, C. Samaras and O. A.Oluwataba, Autonomous vehicle Technology. A guide for policymakers, Santa Monica, California: RAND corporation.

[23] A. Kelly and A. Stentz, “Rough terrain autonomous mobility-Part 1: Tachnical analysis of requirements in autonomous robots,” pp. 129-161, 1998.

[24] K. Aström and B. Wittenmark, Computer controlled systems, Prentice Hall, 1997.

[25] R. N.Jazar, Vehicle dynamics. Theory and application, Springer Science+Business Media, LLC, 233 Spring Street, New York, NY 10013, USA.

[26] P. Rieckert and A. Schunk, “Zur Fahrdynamik des gummibereiften Kraftfahrzeuges, Ingenieur Archiv,” Germany, 1940, pp. 210-244.

[27] R. Mayr, “Verfahren zur Bahnfolgeregelung für ein automatisch geführtes Fahrzeug,” Universität Dortmund, 1991.

[28] M. Neculau, “Modellierung des Fahrverhaltens: Informationsaufnahme, Regel- und Steuerstrategien in Experiment und Simulation, PhD Thesis,” Fachbereich 12: Verkehrswesen, Technische Universität Berlin, 1992.

[29] T. Moder, “Optimale Steuerung eines KFZ im fahrdynamischen Grenzbereich. Master’s thesis,” Mathematisches Institut, Technische Universität München, 1994.

[30] H. B.Pacejka and I. Besselink, Tire and vehicle dynamics, SAE International, Third edition 2012.

[31] O. Reynolds, “On rolling friction,” Philosophical transactions, 1 January 1876.

[32] H. Pacejka and E. Bakker, The magic formula tyre model. Vehicle System Dynamics, vol.21, ISS.Sup001, 1992.

[33] M. Gisper, “DNS-Tire, ein dynamisches, räumliches nichtlineares Reifenmodell. In: Reifen,Fahrwerk, Fahrbahn,” In VDI Berichte 650, S 115-35. VDI-Verlag, Düsseldorf, 1987.

[34] S. Schmidt, M. Schunemann and R. Kasper, “Path planning for a four wheel driven electric vehicle,” in *Advanced Intelligent Mechatronics (AIM), 2011 IEEE/ASME International Conference*, 3-7 July 2011.

[35] P. Deb, N. Singh, S. Kumar and N. Rai, “Offline navigation system for mobile devices,” *International Journal of Software Engineering & Application,* vol. 1, April 2010.

[36] F. Chausee, J. Laneurit and R. Chapuis, “Vehicle localization on a digital map using particles filtering,” in *Intelligent Vehicle Symposium,2005. Proceedings. IEEE*, 6-8 June 2005.

[37] O. Khatib, “Real-time obstacle avoidance for manipulators and mobile robots,” *The international Journal of Robotics Research,* vol. 5, Spring 1986.

[38] D. Ferguson, M. Likhachev and A. Stentz, “A guide to Heuristic-based path planning,” in *American Association for Artificial Inteligence*, 2005.

[39] LaValle and Steven, “Rapidly-exploring random trees: A new tool for path planning,” Technical report (Computer science department , Iowa state university), October 1998.

[40] L. Kavarki and J. Latombe, “Randomized preprocessing of configuration space for fast path planning,” in *Proc.IEEE Int.Conf. on Robotics and Automation*, 1994.

[41] M. Overmars, “A random approach to motion planning,” Technical Report RUU-CS-92-32, Universiteit Utrecht, 1992.

[42] S. LaValle, “Planning algorithms,” Cambridge University Press, Newyork, 2006.

[43] L. Jaillet, A. Yershova, S. LaValle and T. Simeon, “Adaptive tunning of sampling domain for Dynamic-Domain RRTs,” in *Intelligent Robots and systems*, 2005.

[44] J. P. v. d. Berg, “Path planning in dynamic environments,” PhD Thesis, 2007.

[45] Z. Shiller and Y. Gwo, “Dynamic motion planning of autonomous vehicles: Robotics and Automation,” *IEEE Transactions on.In: Robotics and Automation,* pp. 241-249, 1991.

[46] J. Nocedal and S. J.Wright, Numerical optimization, Springer Verlag Newyork.

[47] K. Schittkowski, “NLPQLP: A Fortran implementation of a sequential quadratic programming algorithm with distributed and non-monotone line search - User’s guide,” 2010.

[48] S. Schmidt, “Ein optimales Steuerungs- und Regelungskonzept für autonome Elektrofahrzeuge,” Otto-von-Guericke-Universität Magdeburg, Magdeburg, 2013.

[49] M. Gerdts, “A moving horizon technique for the simulation of automobile test-drives,” *Journal of applied mathematics and mechanics,* vol. 83, no. 3, pp. 147-162, 25 February 2003.

[50] R. Dariani, S. Schmidt and R. Kasper, “Optimization based obstacle avoidance,” in *ICCSMIT: International Conference on Computer Science, Mechatronics and Information Technology*, Paris, 2014.

[51] S. Schmidt, R. Dariani and R. Kasper, “Echtzeitfähige Umsetzung eines Bahnplanungsverfahrens für autonome Fahrzeuge auf Basis der Optimalen Steuerung,” in *11.Magdeburger maschinenbau-Tage*, Magdeburg,Germany, 2013.

[52] T. Lozano-Perez, “Spatial planning: A configuration space approach,” *IEEE Transaction on Computers,* pp. 108-120, Feb.1983.

[53] J. Djugash and B. Hamner, “Neural Networks for obstacle avoidance”.

[54] S. X. Yang and M. Meng, “An efficient neural network approach to dynamic robot motion planning,” *Elsevier science- Neural networks 13,* pp. 143-148, 2000.

[55] P. Fiorini and Z. Shiller, “Motion planning in dynamic environments using velocity obstacles,” *The International Journal Of Robotics Research,* vol. 17, pp. 760-772, July 1998.

[56] “Layered object recognition system for pedestrian sensing,” U.S. department of transportation. Federal highway administration, October 2012.

[57] D. Gavrila and V. Philomin, “Real-time object detection for "smart" vehicles,” in *The proceedings of the Seventh IEEE International Conference on* , 1999.

[58] P. Fiorini and Z. Schiller, “Motion planning in dynamic environments using velocity obstacles,” in *The International Journal of Robotics Research*, 1998.

[59] S. Guy, J. Chhugani, C. Kim, N. Satish, M. Lin, D. Manocha and P. Dubey, “Highly parallel collision avoidance for multi-agent simulation,” *Eurographics symposium on computer animation,* pp. 177-187, 2009.

[60] O. Khatib, “Real-time obstacle avoidance for manipulators and mobile robots,” in *International conference on robotics and automation*, St. Louis, Missouri, 1985.

[61] Y. Koren and J. Borenstein, “Potential field methods and their inherent limitations for mobile robot navigation,” in *Robotics and Automation, 1991. Proceedings., 1991 IEEE International Conference on* , April 1991.

[62] D. Gray and H. Tao, “Viewpoint invariant pedestrain recognition with an ensemble of localized features,” in *Computer vision ECCV 2008*, pp. 262-275.

[63] C. Curio, J. Edelbrunner, T. Kalinke, C. Tzomakas and W. v. Seelen, “Walking pedestrain recognition,” *IEEE Transactions on Intelligent Transportation Systems,* Vols. 1, No 3, September 2000.

[64] B. Fardi, J. Dousa, G. Wanielik and B. Elias, “Obstacle detection and pedestrain recognition using a 3D PMD camera,” *Intelligent Vehicles symposium, IEEE,* pp. 225-230, 2006.

[65] A. Soni, T. Robert, F. Rongieras and P. Beillas, “Observation on pedestrain pre-crash reactions during simulated accidents,” *Stapp car crash journal,* Nov 2013.

[66] S. Schmidt and R. Kasper, “Bahnfolgeregelung für ein spurgeführtes Elektrofahrzeug,” in *6. Paderborner Workshop Entwurf mechatronischer Systeme*, Paderborn,Germany, 2009.

[67] R. Dariani, S. Schmidt and R. Kasper, “Hierarchical concept for optimization based path planning,” in *12. Magdeburger Maschinenbau Tage*, Magdeburg, 2015.